ANALYSIS OF THREE-DIMENSIONAL ORTHOTROPIC SANDWICH PLATE STRUCTURES BY FINITE ELEMENT METHOD

Huy Kinh Ha

A THESIS

in

The Faculty

of

Engineering

Presented in Partial Fulfillment of the Requirements for
the Degree of Doctor of Engineering at
Sir George Williams University
Montreal, Canada

September, 1972

kính dâng cậu mạ

in memory of my father

ANALYSIS OF THREE-DIMENSIONAL ORTHOTROPIC SANDWICH PLATE STRUCTURES BY FINITE ELEMENT METHOD

by

Huy Kinh Ha

ABSTRACT

Sandwich construction when subjected to bending experiences appreciable deflection due to transverse shear strains in the core. Using the assumed stress distribution approach, stiffness matrices for rectangular and triangular elements are derived taking into account these shear deformations. The elements are applicable to sandwich construction having both orthotropic core and facings, the latter may be of different materials and thickness. Solutions of several sandwich plate bending problems are compared with theoretical values. Membrane stiffness matrices are derived using the same formulation. Full compatibility of displacements along interelement boundaries are ensured even for cases when elements meet at an angle. Several three-dimensional sandwich plate structures are analyzed, results are compared with experimental data.

ACKNOWLEDGEMENTS

The investigation reported herein was supported by La Formation de Chercheurs et d'Action Concertée du Québec, the National Research Council (NRC) and the Aluminum Company of Canada (ALCAN). For their financial support the author is grateful.

The author wishes to express his gratitude and appreciation to his thesis supervisor, Dr. P.P. Fazio, Director of the Systems Building Center at Sir George Williams University, for providing encouragement and valuable advice throughout the course of research.

The author also wishes to thank the following groups or individuals:

To all members of the Building System Group for their work on the experimental part which was performed in the Structures Laboratory at Sir George Williams University, and assistance in the typing and drafting;

To his parents, brothers and sisters for their understanding and encouragement;

And finally, to his yet unknown wife, without her absence this work would have been more difficult.

TABLE OF CONTENTS

LIST OF TABLES

LIST OF FIGURES

NOTATIONS

x,y,z	Cartesian coordinates, z-axis normal to plane of plate
a,b	Dimensions of plate or elements
d	Distance between the middle planes of two facings
h	Thickness of core layer
q	Intensity of transverse loading
s,c	Sine and cosine of angle θ
t_1,t_2,t	Thickness of facings
u,v,w	Displacements in x,y,z directions
$\bar{x},\bar{y}$	Dimensionless ratios x/a,y/b respectively
B_x,B_y,B	Flexural rigidities of sandwich plates
D_x,D_y,D	Flexural rigidities of sandwich plates
E_x,E_y,E	Modulii of elasticity of facing material
F_x,F_y,F_z	Nodal forces in x,y,z directions
G_{xy},G_{yx},G	Shear modulii of facing material
$G_{xz},G_{yz},$ G_c	Shear modulii of core materials
M_x,M_y,M_{xy}	Bending and twisting moments per unit length of plate
M_x,M_y,M_z	Nodal moments in x,y,z directions
Q_x,Q_y	Transverse shear forces per unit length of plate
S_x,S_y,S	Shearing rigidities of sandwich plates
T	Total thickness of plate
U	Strain energy in plate or element
W	Work done by edge forces
α,β,γ	Dimensionless coefficients representing the deflection and resultant stresses

$\varepsilon_x, \varepsilon_y, \gamma_{xy}$	Strains in the facings
γ_{xz}, γ_{yz}	Shear strains in the core
$\sigma_x, \sigma_y, \tau_{xy}$	Stresses in the facings
τ_{xz}, τ_{yz}	Shear stresses in the core
θ	Angle between x-axis and the hypotenuse of the triangular element
θ_x, θ_y	Rotations of the cross-section about x and y-axis
θ_z	In-plane rotation (about z-axis)
ν_{xy}, ν_{yx}, ν	Poisson's ratios of facing material
ν_x, ν_y	Poisson's ratios defined in terms of curvatures
η	Dimensionless ratio a/b
Π_c	Total complementary energy in the plate or element
[L]	Transformation matrix, and used also in the relation $\{u\} = [L]\{q\}$
[H]	Matrix expressing the strain energy, defined in the text
[K]	Stiffness matrix of element or structure
[N]	Matrix defined by $\{\varepsilon\} = [N]\{\sigma\}$
[R]	Matrix defined by $\{S\} = [R]\{\beta\}$
[T]	Matrix defined by $W = \{\beta\}^T [T]\{q\}$
{Q},{q}	Vectors of generalized element forces and displacements respectively
{R},{r}	Vector of generalized forces and displacements of the whole structure
{u},{S}	Vector of generalized displacements and forces of the element edges
$\{\beta\}$	Vector of parameters in assumed stress functions
$\{\varepsilon\}$	Vector of strain components

$\{\sigma\}$	Vector of stress components
f,c	Subscripts denoting the facings and core respectively
m,b	Subscripts denoting the membrane and bending actions respectively

CHAPTER I

INTRODUCTION

1.1 STRUCTURAL SANDWICH CONSTRUCTION

Recently, there has been a growing interest in many applications of multilayer construction in building industry. By "sandwiching" several layers of different materials, it is possible to satisfy certain requirements as to mechanical and physical properties that are not yet available in any material. Through optimum structural design each material layer can be stressed to its maximum practical limit; this efficient use of material allows appreciable reduction in weight of the structure without loss in structural strength.

In the building industry, panels of multilayer construction have been used for partitions, curtain-walls, flooring or roofing, etc..., they are now being used more and more as main load-carrying components. These panels can be assembled to form a three-dimensionally rigid structure which does not require any supporting framework. High torsional stiffness is achieved in this type of structure by having stiffening walls spanning in two directions. Because of its many advantages, multilayer construction holds great promise in the field of panelization.

In general, multilayer construction may be classified into two broad divisions:

- "Laminates", in which the layers are of similar mechanical strength and when subjected to bending, the usual hypothesis that lines initially normal to the middle plane remain so after deformation is still valid.

- "Sandwiches", in which the inner layers are much less stiff than the outer ones. Under bending, the deflection due to transverse shear strains is significant compared to the total deflection. Consequently, the theory of sandwich structures must take into account these shear deformations which are often neglected in laminate or homogeneous systems.

The most common form of sandwich construction composes of two thin outer layers of strong, stiff material, between which there is a thick layer of soft, light material. All three layers are bonded together to form a light-weight composite much stronger and stiffer than the sum of the individual layer stiffness and strength.

Action of a sandwich member subjected to bending is similar to that of an I-beam, large moment of inertia of the cross-section is achieved by placing far apart the main stress-carrying elements. The faces act as the flanges in an I-beam to create an internal resisting couple, the core supplies the necessary moment-arm and sets up transverse shear stresses to resist the shear forces; besides these functions the core also offers lateral support for the faces. This stabilizing effect of the core against face buckling

and wrinkling requires that the core be sufficiently stiff to resist transverse tension and compression created by the facings as they try to wrinkle. Obviously, the bond between facings and core is of critical importance, it must be strong so that substantial relative movements of the faces and the core are prevented.

1.2 LITERATURE REVIEW OF SANDWICH PLATE ANALYSIS

The theory of stress analysis of the laminate structures has been fully developed; however, theories of various degrees of refinement that include the effect of transverse shear strains are limited mostly to the local or overall stability of sandwich plates. There have been few solutions available on the bending of sandwich plates having boundary conditions other than simply-supported. Applications of this type of construction in civil engineering require a better understanding of the bending behaviour, unlike the aerospace industry which is primarily interested in the stability aspect.

The early theories of Williams et al [1], Leggett and Hopkins [2], Hopkins and Pearson [3] account for the transverse shear effect in the core by assuming that the initial straight line normal to the middle plane of the core remains straight after deformation but not necessarily perpendicular to the middle plane. This method was further extended by March [4] and Ericksen and March [5]. The later

theories of Libove and Batdorf [6] and Reissner [7] assumed that the core resists no face-parallel stresses, along this line Goodier and Hsu [8] have developed a set of equations for the displacements and stresses in the plate. Eringen [9] and Hoff [10] used the energy approach to treat the problem, the theory took into account the flexural rigidities of the core and also of the faces about their own middle planes. A comprehensive treatment of the theory of sandwich plates may be found in the books by Plantema [11] and Allen [12].

The above-mentioned papers describe various approaches to the mathematical formulation of the sandwich plate problems. As to practical applications, their use is limited because of the complexity of the governing equations, analytical solutions are possible only for simple structures with simple boundary conditions. For complex problems, closed form solutions do not exist and consequently, numerical methods must be resorted to. In this class, the finite element method emerges as an elegant, simple and extremely powerful method which virtually removes all mentioned limitations. During the last decade this new method has been extensively developed and now reserved a unique position in the field of structural analysis.

Only recently, finite element method was used to solve sandwich plate problems. Monforton and Schmit [13] developed an 80-degree of freedom rectangular element using Hermite polynomials for the assumed displacements; Abel and

Popov [14] used Yu's sandwich beam theory [15] to develop a one-dimensional element. Pryor's rectangular element [16] is applicable to the general class of anisotropic multilayer plate; more recently, Ahmed [38] introduced another element for sandwich material. All of the above-mentioned elements were based on the displacement formulation approach; and in order to take into account the effect of transverse shear deformation, additional degrees of freedom such as shear angles, curvatures, rate of twist and even higher order derivatives have been used. Because of these non-geometrical degrees of freedom, the elements developed are not suitable for general three-dimensional analysis. Using an alternative approach, namely, the assumed stress distribution approach pioneered by Pian [18], Lundgren [17] has developed a rectangular sandwich bending element having only three degrees of freedom per node. Unfortunately, the shear deformation was not taken into account correctly and the results obtained by this element do not converge [19].

It is the purpose of this investigation to adapt the finite element method to the analysis of general three-dimensional orthotropic sandwich plate structures. Stiffness matrices for bending and membrane actions of rectangular and triangular elements are developed. Convergence of solutions is shown by numerical examples; the method is then applied to three-dimensional plate structures and results are compared to experimental data. Because of the size and the modularity of the structures to be analysed, a special purpose

large-capacity program is developed to take full advantage of the characteristics of the structures.

CHAPTER II

GOVERNING EQUATIONS AND STIFFNESS OF SANDWICH PLATES

2.1 STRAIN ENERGY IN SANDWICH PLATES

Consider a rectangular sandwich plate of dimensions a,b consisting of a core of thickness h and two facings of thickness t_1 and t_2 (Fig. 2.1). Let the plate be subjected to transverse load q(x,y) and the origin of the coordinate axes at the plate center.

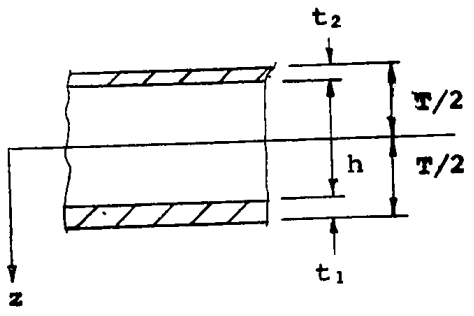

FIG. 2.1 CROSS-SECTION OF SANDWICH PLATE

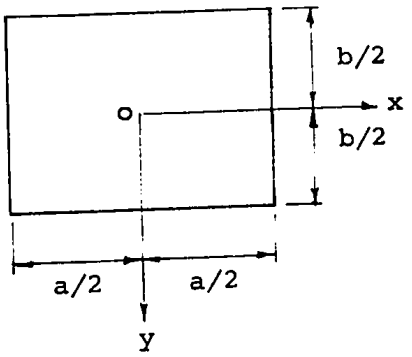

FIG. 2.2 PLATE GEOMETRY

The facings and the core of the sandwich plate to be treated here may be of orthotropic materials, the principal axes of orthotropy coincide with the coordinate axes.

The assumptions used in the present analysis are:

1. Displacements and strains are small and the

materials obey Hook's law.

2. Perfect bonding occurs between layers of the structure.

3. The transverse displacement of all points on a line normal to the middle surface is the same (Fig. 2.3).

4. Bending stiffness of the facings can be ignored and transverse shear stresses in the facings are neglected. This means that the faces behave as solid membrane.

5. The core resists only transverse shear stresses, normal stresses in directions parallel to the faces are neglected.

The last two assumptions have been verified experimentally [35,36] and proved to be reliable for most types of sandwich construction. Adopting these assumptions the non-zero stress components in the faces are $\sigma_x, \sigma_y, \tau_{xy}$ and in the core τ_{xz}, τ_{yz} (Fig. 2.4).

The strain energy in a sandwich plate is equal to the strain energy in the two faces plus that in the core.

$$U = \tfrac{1}{2} \int_f \sum_{i=1}^{2} \left[t_i \left(\frac{\sigma^2_{xi}}{E_{xi}} + \frac{\sigma^2_{yi}}{E_{yi}} - \frac{2\nu_{xyi}}{E_{xi}} \sigma_{xi}\, \sigma_{yi} \right) + \right.$$

$$\left. + \frac{t_i}{G_i} \tau^2_{xyi} \right] dA + \tfrac{1}{2} \int_c \left(\frac{\tau^2_{xz}}{G_{xz}} + \frac{\tau^2_{yz}}{G_{yz}} \right) dV \qquad (2.1)$$

where f and c refer to the facing and core respectively; ν_{xy} = Poisson's ratio; E = Young modulus; G = shear modulus; and the subscripts 1,2 refer to faces 1 and 2.

Because the stresses in the facings are uniform across the thickness, the resultant moments per unit length may be expressed in terms of these stresses as

$$M_x = t_1 d\sigma_{x_1} = - t_2 d\sigma_{x_2} \tag{2.2a}$$

$$M_y = t_1 d\sigma_{y_1} = - t_2 d\sigma_{y_2} \tag{2.2b}$$

$$M_{xy} = t_1 d\tau_{xy_1} = - t_2 d\tau_{xy_2} \tag{2.2c}$$

where

$$d = h + (t_1 + t_2)/2$$

As $\sigma_x, \sigma_y, \tau_{xy}$ are assumed to be zero in the core, it follows from the differential equilibrium equations that the transverse shear stresses do not vary across the core thickness; hence the relations between transverse shearing stresses τ and shearing forces per unit length Q, are:

$$Q_x = h\ \tau_{xz} \tag{2.3a}$$

$$Q_y = h\ \tau_{yz} \tag{2.3b}$$

Fig.2.5 shows the positive directions of moments M_x, M_y, M_{xy} and shearing forces Q_x and Q_y.

Substitution of eqns. (2.2) and (2.3) into eq. (2.1) yields

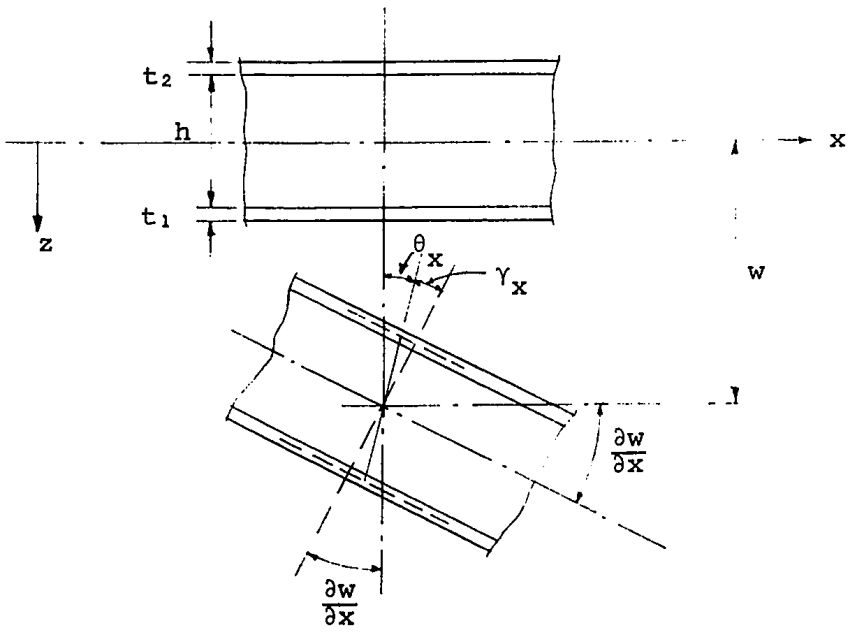

FIG. 2.3 DEFORMED PLATE SECTION

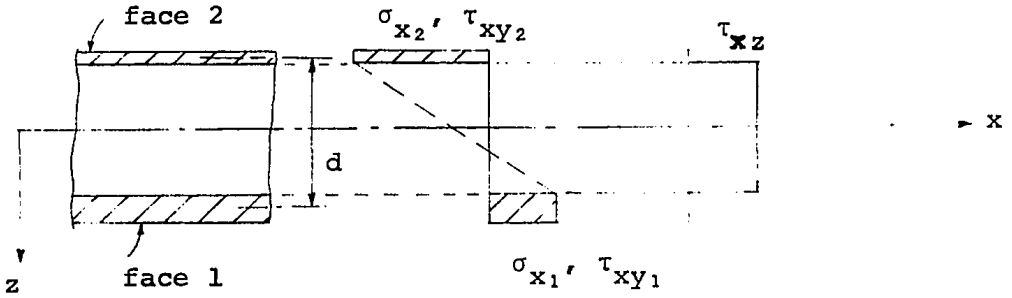

FIG. 2.4 STRESS DISTRIBUTION OVER SANDWICH PLATE SECTION

$$U = \tfrac{1}{2} \int_A \{\frac{1}{d^2} [(\frac{1}{t_1 E_{x_1}} + \frac{1}{t_2 E_{x_2}}) M^2_x + (\frac{1}{t_1 E_{y_1}} + \frac{1}{t_2 E_{y_2}}) M^2_y - 2 (\frac{\nu_{xy_1}}{t_1 E_{x_1}} + \frac{\nu_{xy_2}}{t_2 E_{x_2}}) M_x M_y + (\frac{1}{t_1 G_{xy_1}} + \frac{1}{t_2 G_{xy_2}}) M^2_{xy}] + \frac{1}{h} [\frac{Q^2_x}{G_{xz}} + \frac{Q^2_y}{G_{yz}}]\} dA \qquad (2.4)$$

This expression gives the strain energy in an orthotropic sandwich plate having facings of different thickness and materials.

Introducing the following notations:

$$B_x = d^2/(\frac{1}{t_1 E_{x_1}} + \frac{1}{t_2 E_{x_2}}) \qquad (2.5a)$$

$$B_y = d^2/(\frac{1}{t_1 E_{y_1}} + \frac{1}{t_2 E_{y_2}}) \qquad (2.5b)$$

$$B_G = d^2/(\frac{1}{t_1 G_{xy_1}} + \frac{1}{t_2 G_{xy_2}}) \qquad (2.5c)$$

$$B_\nu = d^2/(\frac{\nu_{xy_1}}{t_1 E_{x_1}} + \frac{\nu_{xy_2}}{t_2 E_{x_2}}) \qquad (2.5d)$$

$$S_x = G_{xz}\, d^2/h \qquad (2.5e)$$

$$S_y = G_{yz}\, d^2/h \qquad (2.5f)$$

the eq. (2.4) may be rewritten more compactly as:

$$U = \tfrac{1}{2}\int_A [\,(\frac{M^2_x}{B_x} + \frac{M^2_y}{B_y} - 2\,\frac{M_x M_y}{B_\nu} + \frac{M^2_{xy}}{B_G}) + \\ + \frac{d^2}{h^2}\,(\frac{Q^2_x}{S_x} + \frac{Q^2_y}{S_y})\,]\,dA \qquad (2.6)$$

2.2 EQUILIBRIUM EQUATIONS

The equilibrium equations for a sandwich plate are identical to those for an ordinary thin plate as stresses in both are expressed in terms of the same set of stress resultants. The equations are obtained by consideration of force and moment equilibrium of a differential element of the plate (Fig. 2.5).

$$\frac{\partial M_x}{\partial x} + \frac{\partial M_{xy}}{\partial y} - Q_x = 0 \qquad (2.7a)$$

$$\frac{\partial M_y}{\partial y} + \frac{\partial M_{xy}}{\partial x} - Q_y = 0 \qquad (2.7b)$$

$$\frac{\partial Q_x}{\partial x} + \frac{\partial Q_y}{\partial y} + q = 0 \qquad (2.7c)$$

where q is the intensity of the transverse loading.

2.3 GOVERNING EQUATIONS BY COMPLEMENTARY ENERGY THEOREM

For a material obeying Hook's law, and for given stresses or displacements, the complementary energy is equal to the difference of the strain energy U and of the work W which the surface stresses do over the boundary where

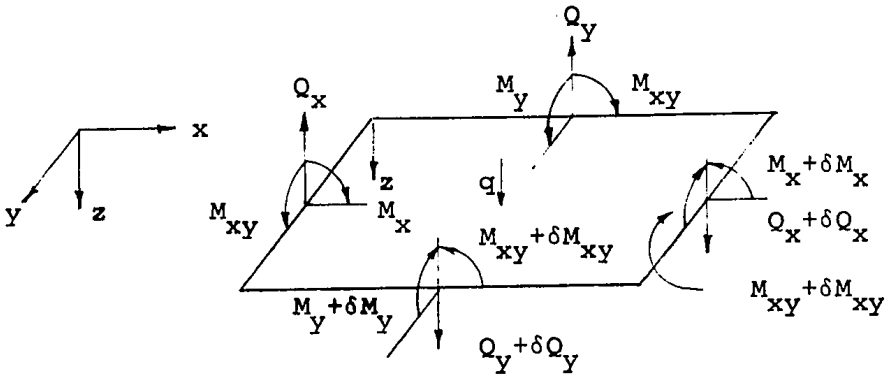

FIG. 2.5 EDGE FORCES ON DIFFERENTIAL ELEMENT

displacements are prescribed. Strain energy U is given by eq. (2.6) and W is

$$W = \int_{-b/2}^{b/2} (wQ_x + \theta_y M_x + \theta_x M_{xy})_{\substack{x=-a/2 \\ x=\ a/2}} dy +$$

$$+ \int_{-a/2}^{a/2} (wQ_y + \theta_x M_y + \theta_y M_{xy})_{\substack{y=-b/2 \\ y=\ b/2}} dx \qquad (2.8)$$

where w, θ_x, θ_y represent the generalized displacements.

In order that the system be in equilibrium, the complementary energy (U-W) must be minimized subject to the equilibrium conditions expressed by eqns. (2.7). By so doing, Ueng and Lin [20] have arrived at the governing equation, eq. (2.9), for an orthotropic sandwich plate having isotropic facings of different material and thickness. ($E_x=E_y=E$, $\nu_{xy}=\nu_{yx}=\nu$, $B_x=B_y=B$).

$$(1 - A_y\frac{\partial^2}{\partial x^2} - A_x\frac{\partial^2}{\partial y^2})\nabla^2\nabla^2 w = \frac{1}{B^*}[1 - (A^*_x + A_y)\frac{\partial^2}{\partial x^2} -$$

$$(A^*_y + A_x)\frac{\partial^2}{\partial y^2} + (A^*_x A_y\frac{\partial^2}{\partial x^2} + A^*_y A_x\frac{\partial^2}{\partial y^2})\nabla^2]q \qquad (2.9)$$

where $\nabla = \frac{\partial^2}{\partial x^2} + \frac{\partial^2}{\partial y^2}$: Laplacian operator

$$\frac{1}{B^*} = \frac{(1/B)}{(1/B)^2 - (1/B_\nu)^2}$$

$$(A_x, A^*_x) = (B_G, B^*)/hG_{xz}$$

$$(A_y, A^*_y) = (B_G, B^*)/hG_{yz}$$

The problem of bending of a sandwich plate reduces to solving the governing eq. (2.9) subject to the boundary conditions. Once w is found, the shear forces Q_x, Q_y may be obtained from the equations

$$A_x \nabla^2 \nabla^2 Q_x + (A_y - A_x)\frac{\partial^2}{\partial x^2}\nabla^2 Q_x - \nabla^2 Q_x = \frac{\partial}{\partial x}(q - A_y\nabla^2 q)$$

$$A_y \nabla^2 \nabla^2 Q_y + (A_x - A_y)\frac{\partial^2}{\partial y^2}\nabla^2 Q_y - \nabla^2 Q_y = \frac{\partial}{\partial y}(q - A_x\nabla^2 q)$$

Moments M_x, M_y, M_{xy} and θ_x, θ_y are found using the following expressions:

$$\theta_x = -\frac{Q_x}{hG_{xz}} + \frac{\partial w}{\partial x}$$

$$\theta_y = -\frac{Q_y}{hG_{yz}} + \frac{\partial w}{\partial y}$$

$$M_x = -\frac{B\,B_\nu}{B^2_\nu - B^2}(B_\nu\frac{\partial\theta_x}{\partial x} + B\frac{\partial\theta_y}{\partial y})$$

$$M_y = -\frac{B\,B_\nu}{B^2_\nu - B^2}\left(B_\nu \frac{\partial \theta_y}{\partial y} + B\frac{\partial \theta_x}{\partial x}\right)$$

$$M_{xy} = B_G\left(\frac{\partial \theta_y}{\partial x} + \frac{\partial \theta_x}{\partial y}\right)$$

It is interesting to note that when $G_{xz} = G_{yz} \to \infty$ eqn. (2.9) can be reduced to the classical thin plate equation $\nabla^2\nabla^2 w = q/D$.

2.4 BOUNDARY CONDITIONS FOR COMMON EDGES

The governing equation is a sixth order differential equation in w, which admits three boundary conditions at each edge, unlike the fourth order equation in classical thin plate theory which admits only two of such conditions. Boundary conditions for various types of edge supports commonly found in practice are given below, assuming the edge considered is parallel to the y-axis (Fig. 2.3).

1. Free Edge

$$M_x = 0; \quad M_{xy} = 0; \quad Q_x = 0$$

2. Simply-Supported Edge

$$w = 0; \quad M_x = 0$$

If the edge is stiffened so that shear strains are prevented then the additional condition is $\gamma_y = 0$. If no forces parallel to the y-axis are applied to prevent shear strains then the third condition is $M_{xy} = 0$.

3. Clamped Edge

$$w = 0; \quad \gamma_y = 0$$

the third boundary condition is that the cross-section along the edge does not rotate

$$\frac{\partial w}{\partial x} - \gamma_x = 0$$

A theoretical possibility exists, where $\gamma_y \neq 0$ but $M_{xy} = 0$, however this case does not occur in practice.

2.5 STIFFNESS OF SANDWICH PLATES

The bending stiffness properties of an orthotropic sandwich plate can be described by means of seven physical constants, of which only six are independent. They are the two flexural rigidities D_x, D_y; the two Poisson's ratio ν_x, ν_y defined in terms of curvatures; the torsional rigidity D_{xy} and the two transverse shearing rigidities S_x, S_y. (By reciprocal theorem it can be proved that $D_x\nu_y = D_y\nu_x$). The constants D_x, D_y and D_{xy} are related to the constants in eqns. (2.5) by the expressions:

$$D_x = \frac{B_x}{(1-\nu_x\nu_y)} \; ; \; D_y = \frac{B_y}{(1-\nu_x\nu_y)} \; ; \; D_{xy} = 2B_G \qquad (2.10)$$

It can be shown that the curvatures and rate of twist of the plate are given [11,12] by the equations

$$\frac{\partial^2 w}{\partial x^2} = -\frac{M_x}{B_x} + \nu_y \frac{M_y}{B_y} + \frac{1}{S_x}\frac{\partial Q_x}{\partial x} \qquad (2.11a)$$

$$\frac{\partial^2 w}{\partial y^2} = -\frac{M_y}{B_y} + \nu_x \frac{M_x}{B_x} + \frac{1}{S_y}\frac{\partial Q_y}{\partial y} \qquad (2.11b)$$

$$\frac{\partial^2 w}{\partial x \partial y} = -\frac{M_{xy}}{2B_G} + \frac{1}{2S_x}\frac{\partial Q_x}{\partial y} + \frac{1}{2S_y}\frac{\partial Q_y}{\partial x} \qquad (2.11c)$$

These are the fundamental equations which define the stiffness of the plate in bending and shear.

The stiffness constants of an orthotropic sandwich plate may then be determined experimentally making use of eqns. (2.11) or theoretically from eqns. (2.5). Simplified expressions for the stiffness constants are given below for special cases.

1. Isotropic faces and core; faces of equal thickness and material. Since $B_x = B_y = B$ and $\nu_{xy} = \nu_{yx} = \nu$, eqns. (2.10) reduce to:

$$D_x = D_y = D = \frac{B}{1 - \nu^2} = \frac{Etd^2}{2(1-\nu^2)}$$

$$D_{xy} = \frac{Etd^2}{2(1+\nu)}$$

and for the shear stiffness $G_{xz} = G_{yz} = G_c$ hence $S_x = S_y = S = \frac{G_c d^2}{h}$.

2. Orthotropic faces and core; faces of equal thickness and similar material:

$$D_x = \frac{E_x td^2}{2(1-\nu_{xy}\nu_{yx})} \; ; \quad D_y = \frac{E_y td^2}{2(1-\nu_{xy}\nu_{yx})}$$

$$D_{xy} = G_{xy} td^2 \; ; \quad \nu_{yx} E_x = \nu_{xy} E_y$$

$$S_x = \frac{G_{xz} d^2}{h} \; ; \quad S_y = \frac{G_{yz} d^2}{h}$$

CHAPTER III

IMPLEMENTATION OF THE FINITE ELEMENT METHOD FOR SANDWICH CONSTRUCTION

3.1 STIFFNESS MATRIX BY ASSUMED STRESS DISTRIBUTION APPROACH

Pian [18] has first used the assumed stress distribution approach to derive the stiffness matrix for a rectangular plane stress element. Pian [22] and subsequently Severn and Taylor [23] applied the technique to bending of rectangular isotropic plate. The procedure, which is fully detailed in the above papers, may be summarized as follows:

1. Assume stress distributions in the element

$$\{\sigma\} = [P]\{\beta\} \tag{3.1}$$

where $\{\sigma\}$: generalized stress vector, must satisfy the equilibrium conditions.

$\{\beta\}$: undetermined stress parameters.

$[P]$: functions of the coordinates.

2. Evaluate the strain energy in terms of stress parameters

$$U = \tfrac{1}{2}\{\beta\}^T[H]\{\beta\} \tag{3.2}$$

The matrix $[H]$ may be determined directly from the strain energy expression or as follows:

Stress-Strain Relation $\{\varepsilon\} = [N]\{\sigma\}$

Strain Energy $U = \frac{1}{2} \int_V \{\sigma\}^T \{\varepsilon\} dV$ (3.3)

Substitution of $\{\varepsilon\}$ from eqn. (3.3) and $\{\sigma\}$ from eqn. (3.1) into the above equation yields:

$$U = \frac{1}{2} \int_V \{\beta\}^T [P]^T [N][P]\{\beta\} dV$$

$$= \frac{1}{2} \{\beta\}^T \int_V [P]^T [N][P] dV \{\beta\}$$

Then

$$[H] = \int_V [P]^T [N][P] dV \quad (3.4)$$

Matrix [H] is positive, definite and symmetric.

3. Introduce the generalized edge displacements

$$\{u\} = [L]\{q\} \quad (3.5)$$

where

$\{q\}$: generalized nodal displacements.

$[L]$: functions of the coordinates.

By choosing suitable interpolation functions for [L] the displacement compatibility along the element boundaries can be achieved.

4. Form the generalized edge forces $\{S\}$ in terms of $\{\beta\}$ by using eqn. (3.1).

$$\{S\} = [R]\{\beta\}$$

The coefficients in $\{S\}$ should correspond to those in $\{u\}$ so that the work done by the edge forces is given by the expression

$$W = \oint \{S\}^T\{u\}ds$$

$$= \oint \{\beta\}^T[R]^T[L]\{q\}ds$$

$$= \{\beta\}^T[T]\{q\} \qquad (3.6)$$

where

$$[T] = \oint [R]^T[L]ds$$

The vector $\{Q\}$ of nodal generalized forces is defined by

$$\{Q\}^T\{q\} = W = \{\beta\}^T[T]\{q\}$$

or

$$\{Q\} = [T]^T\{\beta\} \qquad (3.7)$$

5. Form the total complementary energy

$$\Pi_C = U - W = \tfrac{1}{2}\{\beta\}^T[H]\{\beta\} - \{\beta\}^T[T]\{q\}$$

The principle of stationary complementary energy requires that

$$\frac{\partial \Pi_C}{\partial \{\beta\}} = [H]\{\beta\} - [T]\{q\} = 0$$

Hence

$$\{\beta\} = [H]^{-1}[T]\{q\} \qquad (3.8)$$

6. The stiffness matrix [K] is given by

$$\{Q\} = [K]\{q\} \tag{3.9}$$

using eqns. (3.7) and (3.8)

$$[K]\{q\} = [T]^T[H]^{-1}[T]\{q\}$$

Then

$$[K] = [T]^T[H]^{-1}[T] \tag{3.10}$$

This expression for the stiffness matrix may also be derived from the principle of virtual forces [24]. The described procedure is based on a variational principle in which stresses are assumed within the elements and displacements along the boundaries of the elements. Convergence proof is given by Pin Tong and Pian [31]; briefly the admissibility requirements for the assumed functions are:

1. Internal stresses must satisfy the equilibrium equations within the elements.

2. Boundary displacements must satisfy interelement compatibility conditions.

3. The total number of degrees of freedom in stresses must be greater than or equal to that of the displacements.

If these conditions are satisfied explicitly then it can be shown that the remaining conditions:

4. Compatibility within the elements, and

5. Equilibrium along element boundaries are satisfied implicitly through the process of extremization.

Pian and Tong [19] have also shown that the solution obtained by the assumed stress distribution model may be either an upper or lower bound. However, the solution will always be bounded by that of a compatible model using the same type of interelement boundary displacements and that of an equilibrium model using the same type of interior stresses.

3.2 RECTANGULAR ELEMENT - BENDING STIFFNESS MATRIX

A rectangular finite element of a sandwich panel is shown in Fig. 3.1, it consists of a core, thickness h, sandwiched between two faces, same thickness t. A right-handed coordinate system x,y,z is chosen such that the middle plane of the plate is the plane xoy. The dimensions of the element along the x and y directions are a and b respectively.

The first step in the derivation of the stiffness matrix using the assumed stress approach is to choose the expressions for the stress variations ir the element.

According to the assumptions described in Chapter II, the face stresses σ_x, σ_y and τ_{xy} are uniform across the face thickness. In the core, there are only the transverse shear

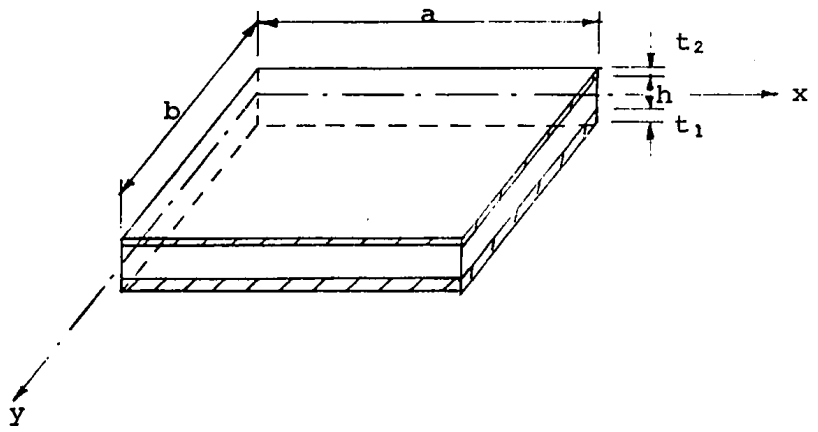

FIG. 3.1 RECTANGULAR SANDWICH ELEMENT

stresses, τ_{xz} and τ_{yz}, which are also uniform across the thickness of the core section. These assumptions enable the resultant moments and shear forces to be expressed simply by eqns. (2.2) and (2.3). The stress variations in the x and y directions may be approximated by polynomial expressions, the degree of these polynomials are rather arbitrary. However, results for isotropic plate analysis reported by Pian [19] support the use of quadratic variation for σ_x, σ_y τ_{xy} and linear for τ_{xz}, τ_{yz}.

Inspection of eqns. (2.2) and (2.3) shows that the shear forces and moments are directly related to the stresses. Their distribution may be assumed as follows:

$$\left.\begin{aligned} M_x &= \beta_1+\beta_2\bar{x}+\beta_3\bar{y}+\beta_4\bar{x}^2+\beta_5\bar{x}\bar{y}+\beta_6\bar{y}^2 \\ M_y &= \beta_7+\beta_8\bar{x}+\beta_9\bar{y}+\beta_{10}\bar{x}^2+\beta_{11}\bar{x}\bar{y}+\beta_{12}\bar{y}^2 \\ M_{xy} &= \beta_{13}+\beta_{14}\bar{x}+\beta_{15}\bar{y}+\beta_{16}\bar{x}^2+\beta_{17}\bar{x}\bar{y}+\beta_{18}\bar{y}^2 \\ Q_x &= \beta_{19}+\beta_{20}\bar{x}+\beta_{21}\bar{y} \\ Q_y &= \beta_{22}+\beta_{23}\bar{x}+\beta_{24}\bar{y} \end{aligned}\right\} \quad (3.11)$$

where

$$\bar{x} = \frac{x}{a}$$

$$\bar{y} = \frac{y}{b}$$

The stress parameters $\{\beta\}$ are not all independent because they are subject to the equilibrium conditions, substitution of eqn. (3.11) into eqn. (2.7) allows the elimination of seven of the β's:

$$\beta_{17} = -\frac{b}{a}\beta_4 - \frac{a}{b}\beta_{12}$$

$$\beta_{19} = \frac{\beta_2}{a} + \frac{\beta_{15}}{b}$$

$$\beta_{20} = \frac{\beta_4}{a} - \frac{a}{b^2}\beta_{12}$$

$$\beta_{21} = \frac{\beta_5}{a} + \frac{2\beta_{18}}{b}$$

$$\beta_{22} = \frac{\beta_9}{b} + \frac{\beta_{14}}{a}$$

$$\beta_{23} = \frac{\beta_{11}}{b} + \frac{2\beta_{16}}{a}$$

$$\beta_{24} = \frac{\beta_{12}}{b} - \frac{b}{a^2}\beta_4$$

Eqn. (3.11) may be rewritten using only the independent parameters:

$$\left.\begin{aligned}
M_x &= \beta_1+\beta_2\bar{x}+\beta_3\bar{y}+\beta_4\bar{x}^2+\beta_5\overline{xy}+\beta_6\bar{y}^2 \\
M_y &= \beta_7+\beta_8\bar{x}+\beta_9\bar{y}+\beta_{10}\bar{x}^2+\beta_{11}\overline{xy}+\beta_{12}\bar{y}^2 \\
M_{xy} &= -\frac{b}{a}\beta_4\ \overline{xy}-\frac{a}{b}\beta_{12}\ \overline{xy}\ +\beta_{13}+\beta_{14}\bar{x}+\beta_{15}\bar{y}+\beta_{16}\bar{x}^2+\beta_{18}\bar{y}^2 \\
Q_x &= \frac{1}{a}\beta_2+\frac{\beta_4}{a}\bar{x}+\frac{\beta_5}{a}\bar{y}-\frac{a}{b^2}\beta_{12}\bar{x}+\frac{\beta_{15}}{b}+\frac{2}{b}\beta_{18}\bar{y} \\
Q_y &= -\frac{b}{a^2}\beta_4\bar{y}+\frac{\beta_9}{b}+\frac{\beta_{11}}{b}\bar{x}+\frac{\beta_{12}}{b}\bar{y}+\frac{\beta_{14}}{a}+\frac{2}{a}\beta_{16}\ \bar{x}
\end{aligned}\right\} \quad (3.12)$$

Substituting eqn. (3.12) into the strain energy expression eqn. (2.6) and integrating over the element area, the strain energy U may be put in matrix form

$$U = \tfrac{1}{2}\ \{\beta\}^T[H]\ \{\beta\}$$

where

$$\{\beta\}^T = [\beta_1\ \beta_2\ \beta_3\ \beta_4\ \beta_5\ \beta_6\ \beta_7\ \beta_8\ \beta_9\ \beta_{10}\ \beta_{11}\ \beta_{12}\ \beta_{13}\ \beta_{14}\ \beta_{15}\ \beta_{16}\ \beta_{18}]$$

The square matrix [H] is symmetric, positive definite and of order 17. Let

$$[H] = \sum_{i=1}^{6} [H_i] \qquad (3.13)$$

the component matrices $[H_i]$ are given in compact form below. The correct position of each element in the matrix $[H_i]$ is indicated by the numbers along the sides and only terms in the upper triangle of the matrix $[H]$ are given.

$$[H_1] = \frac{ab}{B_x}\begin{bmatrix} \overset{1}{1} & \overset{2}{\frac{1}{2}} & \overset{3}{\frac{1}{2}} & \overset{4}{\frac{1}{3}} & \overset{5}{\frac{1}{4}} & \overset{6}{\frac{1}{3}} & 1 \\ & \frac{1}{3} & \frac{1}{4} & \frac{1}{4} & \frac{1}{6} & \frac{1}{6} & 2 \\ & & \frac{1}{3} & \frac{1}{6} & \frac{1}{6} & \frac{1}{4} & 3 \\ & & & \frac{1}{5} & \frac{1}{8} & \frac{1}{9} & 4 \\ \text{Symmetric} & & & & \frac{1}{9} & \frac{1}{8} & 5 \\ & & & & & \frac{1}{5} & 6 \end{bmatrix} \tag{3.14}$$

$$[H_2] = \frac{ab}{B_y}\begin{bmatrix} \overset{7}{1} & \overset{8}{\frac{1}{2}} & \overset{9}{\frac{1}{2}} & \overset{10}{\frac{1}{3}} & \overset{11}{\frac{1}{4}} & \overset{12}{\frac{1}{3}} & 7 \\ & \frac{1}{3} & \frac{1}{4} & \frac{1}{4} & \frac{1}{6} & \frac{1}{6} & 8 \\ & & \frac{1}{3} & \frac{1}{6} & \frac{1}{6} & \frac{1}{4} & 9 \\ \text{Symmetric} & & & \frac{1}{5} & \frac{1}{8} & \frac{1}{9} & 10 \\ & & & & \frac{1}{9} & \frac{1}{8} & 11 \\ & & & & & \frac{1}{5} & 12 \end{bmatrix} \tag{3.15}$$

$$[H_3] = -\frac{ab}{B_\nu}\begin{bmatrix} \overset{7}{1} & \overset{8}{\frac{1}{2}} & \overset{9}{\frac{1}{2}} & \overset{10}{\frac{1}{3}} & \overset{11}{\frac{1}{4}} & \overset{12}{\frac{1}{3}} \\ \frac{1}{2} & \frac{1}{3} & \frac{1}{4} & \frac{1}{4} & \frac{1}{6} & \frac{1}{6} \\ \frac{1}{2} & \frac{1}{4} & \frac{1}{3} & \frac{1}{6} & \frac{1}{6} & \frac{1}{4} \\ \frac{1}{3} & \frac{1}{4} & \frac{1}{6} & \frac{1}{5} & \frac{1}{8} & \frac{1}{9} \\ \frac{1}{4} & \frac{1}{6} & \frac{1}{6} & \frac{1}{8} & \frac{1}{9} & \frac{1}{8} \\ \frac{1}{3} & \frac{1}{6} & \frac{1}{4} & \frac{1}{9} & \frac{1}{8} & \frac{1}{5} \end{bmatrix}\begin{matrix} 1 \\ 2 \\ 3 \\ 4 \\ 5 \\ 6 \end{matrix} \qquad (3.16)$$

$$[H_4] = \frac{ab}{B_G}\begin{bmatrix} \overset{4}{\frac{1}{9\eta^2}} & \overset{12}{\frac{1}{9}} & \overset{13}{-\frac{1}{4\eta}} & \overset{14}{-\frac{1}{6\eta}} & \overset{15}{-\frac{1}{6\eta}} & \overset{16}{-\frac{1}{8\eta}} & \overset{17}{-\frac{1}{8\eta}} \\ & \frac{\eta^2}{9} & -\frac{\eta}{4} & -\frac{\eta}{6} & -\frac{\eta}{6} & -\frac{\eta}{8} & -\frac{\eta}{8} \\ & & 1 & \frac{1}{2} & \frac{1}{2} & \frac{1}{3} & \frac{1}{3} \\ & & & \frac{1}{3} & \frac{1}{4} & \frac{1}{4} & \frac{1}{6} \\ \text{Symmetric} & & & & \frac{1}{3} & \frac{1}{6} & \frac{1}{4} \\ \eta = \frac{a}{b} & & & & & \frac{1}{5} & \frac{1}{9} \\ & & & & & & \frac{1}{5} \end{bmatrix}\begin{matrix} 4 \\ 12 \\ 13 \\ 14 \\ 15 \\ 16 \\ 17 \end{matrix} \qquad (3.17)$$

$$[H_5] = \frac{abd^2}{h^2 S_x}$$

$$\begin{array}{c} \\ 2 \\ 4 \\ 5 \\ 12 \\ 15 \\ 17 \end{array}
\begin{bmatrix}
\overset{2}{\frac{1}{a^2}} & \overset{4}{\frac{1}{2a^2}} & \overset{5}{\frac{1}{2a^2}} & \overset{12}{-\frac{1}{2b^2}} & \overset{15}{\frac{1}{ab}} & \overset{17}{\frac{1}{ab}} \\
 & \frac{1}{3a^2} & \frac{1}{4a^2} & -\frac{1}{3b^2} & \frac{1}{2ab} & \frac{1}{2ab} \\
 & & \frac{1}{3a^2} & -\frac{1}{4b^2} & \frac{1}{2ab} & \frac{2}{3ab} \\
 & \text{Symmetric} & & \frac{\eta^2}{3b^2} & \frac{-\eta}{2b^2} & \frac{-\eta}{2b^2} \\
 & \eta = \frac{a}{b} & & & \frac{1}{b^2} & \frac{1}{b^2} \\
 & & & & & \frac{4}{3b^2}
\end{bmatrix}$$

(3.18)

$$[H_6] = \frac{abd^2}{h^2 S_y}$$

$$\begin{array}{c} \\ 4 \\ 9 \\ 11 \\ 12 \\ 14 \\ 16 \end{array}
\begin{bmatrix}
\overset{4}{\frac{1}{3\eta^2 a^2}} & \overset{9}{-\frac{1}{2a^2}} & \overset{11}{-\frac{1}{4a^2}} & \overset{12}{-\frac{1}{3a^2}} & \overset{14}{-\frac{1}{2\eta a^2}} & \overset{16}{-\frac{1}{2\eta a^2}} \\
 & \frac{1}{b^2} & \frac{1}{2b^2} & \frac{1}{2b^2} & \frac{1}{ab} & \frac{1}{ab} \\
 & & \frac{1}{3b^2} & \frac{1}{4b^2} & \frac{1}{2ab} & \frac{2}{3ab} \\
 & \text{Symmetric} & & \frac{1}{3b^2} & \frac{1}{2ab} & \frac{1}{2ab} \\
 & \eta = \frac{a}{b} & & & \frac{1}{a^2} & \frac{1}{a^2} \\
 & & & & & \frac{4}{3a^2}
\end{bmatrix}$$

(3.19)

So far, the strain energy for the element which is subjected to the stress field specified by eqn. (3.12) has been derived. Next, the work done by the edge forces is to be found.

Three generalized displacements are given at each corner of the element: a transverse deflection and two rotations (Fig. 3.2). In terms of these nodal displacements, the deflections and rotations along the edge are approximated using interpolation functions.

One may assume that the displacements vary linearly along the edges, although higher degree of variation is possible. The combination of quadratic stress modes and linear displacement modes seems to give very reasonable results as reported by Pian [19]. In sandwich construction, transverse shear deformations are significant, therefore the edge rotations are not exclusively dependent on the deflection.

The positive forces and displacements along the edges are shown in Fig. 2.5 and Fig. 3.2, respectively. Referring to Fig. 3.2, along the edge (1-2) the displacements are assumed as:

$$w = w_1(1 - \bar{x}) + w_2\bar{x}$$

$$\theta_x = \theta_{x1}(1 - \bar{x}) + \theta_{x2}\,\bar{x}$$

$$\theta_y = \theta_{y1}(1 - \bar{x}) + \theta_{y2}\,\bar{x}$$

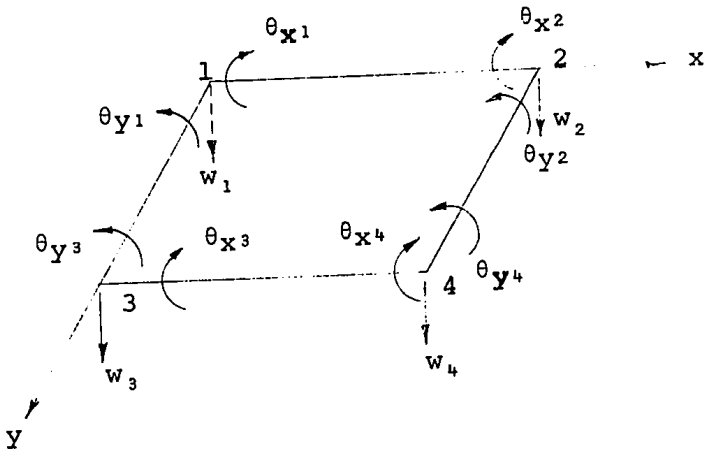

FIG. 3.2 NODAL DISPLACEMENTS FOR BENDING ACTION

Similar equations are written for the other three edges:

$$\{u\} = [L]\{q\} \tag{3.20}$$

where

$$\{q\}^T = [\theta_{x1}\ \theta_{y1}\ w_1\ \theta_{x2}\ \theta_{y2}\ w_2\ \theta_{x3}\ \theta_{y3}\ w_3\ \theta_{x4}\ \theta_{y4}\ w_4]$$

Explicit form of eqn. (3.20) is given in Appendix A.

The linearity of the above equations shows that complete compatibility of deflections and rotations at the element boundaries are ensured. Now if the inplane deformations

along the element edges are also assumed to be linear then compatibility still persists when the elements meet at an angle.

The moments and shear forces acting on the edges are evaluated using eqn. (3.12).

$$S_1 = M_{y12} = -(M_y)_{\bar{y}=o} = -\beta_7 - \beta_8\bar{x} - \beta_{10}\bar{x}^2$$

$$S_2 = M_{xy12} = -(M_{xy})_{\bar{y}=o} = -\beta_{13} - \beta_{14}\bar{x} - \beta_{16}\bar{x}^2$$

$$S_3 = Q_{y12} = -(Q_y)_{\bar{y}=o} = -\frac{\beta_9}{b} - \frac{\bar{x}}{b}\beta_{11} - \frac{\beta_{14}}{a} - \frac{2\bar{x}}{a}\beta_{16}$$

$$S_4 = M_{y34} = (M_y)_{\bar{y}=1} = ...$$

$$S_5 = M_{xy34} = (M_{xy})_{\bar{y}=1} = ...$$

$$S_6 = Q_{y34} = (Q_y)_{\bar{y}=1}$$

$$S_7 = M_{xy13} = -(M_{xy})_{\bar{x}=o}$$

$$S_8 = M_{x13} = -(M_x)_{\bar{x}=o}$$

$$S_9 = Q_{x13} = -(Q_x)_{\bar{x}=o}$$

$$S_{10} = M_{xy24} = (M_{xy})_{\bar{x}=1}$$

$$S_{11} = M_{x24} = (M_x)_{\bar{x}=1}$$

$$S_{12} = Q_{x24} = (Q_x)_{\bar{x}=1}$$

In matrix form

$$\{S\} = [R]\{\beta\} \qquad (3.20a)$$

the matrix $[R]$ is shown in Appendix A.

The work, W, done by the edge forces is given by eqn. (3.6)

$$W = \{\beta\}^T[T]\{q\}$$

where $$[T] = \oint [R]^T[L]\, ds$$

The line integral is evaluated along the boundaries of the element. The matrix $[T]$ is shown in eqn. (3.21).

Having obtained the matrices $[H]$ and $[T]$ the stiffness matrix is found by eqn. (3.10).

$$[K_b] = [T]^T[H]^{-1}[T]$$

The nodal displacements are the same as in eqn. (3.20).

3.3 RECTANGULAR ELEMENT - MEMBRANE STIFFNESS MATRIX

The membrane stiffness matrix also will be derived by using the assumed stress distribution approach. The procedure is similar to that used by Pian [18] for isotropic plate but modified to take into account the orthotropic properties of the layered construction.

Consider the sandwich element shown in Fig. (3.1), the core is assumed to resist only transverse shear stresses;

$$
\begin{bmatrix}
0 & -\frac{b}{2} & 0 & 0 & \frac{b}{2} & 0 & 0 & -\frac{b}{2} & 0 & 0 & \frac{b}{2} & 0 \\
0 & 0 & -\frac{b}{2a} & 0 & \frac{b}{2} & \frac{b}{2a} & 0 & 0 & -\frac{b}{2a} & 0 & \frac{b}{2} & \frac{b}{2a} \\
0 & -\frac{b}{6} & 0 & 0 & \frac{b}{6} & 0 & 0 & -\frac{b}{3} & 0 & 0 & \frac{b}{3} & 0 \\
0 & 0 & 0 & -\frac{b^2}{6a} & \frac{b}{2} & \frac{b}{2a} & 0 & -\frac{b}{6} & -\frac{b}{2a} & -\frac{b^2}{3a} & \frac{b}{6} & 0 \\
0 & 0 & -\frac{b}{6a} & 0 & \frac{b}{6} & \frac{b}{6a} & 0 & 0 & -\frac{b}{3a} & 0 & \frac{b}{3} & \frac{b}{3a} \\
0 & -\frac{b}{12} & 0 & 0 & \frac{b}{12} & 0 & 0 & -\frac{b}{4} & 0 & 0 & \frac{b}{4} & 0 \\
-\frac{a}{2} & 0 & 0 & -\frac{a}{2} & 0 & 0 & \frac{a}{2} & 0 & 0 & \frac{a}{2} & 0 & 0 \\
-\frac{a}{6} & 0 & 0 & -\frac{a}{3} & 0 & 0 & \frac{a}{6} & 0 & 0 & \frac{a}{3} & 0 & 0 \\
0 & 0 & -\frac{a}{2b} & 0 & 0 & -\frac{a}{ab} & \frac{a}{2} & 0 & \frac{a}{2b} & \frac{a}{2} & 0 & \frac{a}{2b} \\
-\frac{a}{12} & 0 & 0 & -\frac{a}{4} & 0 & 0 & \frac{a}{12} & 0 & 0 & \frac{a}{4} & 0 & 0 \\
0 & 0 & -\frac{a}{6b} & 0 & 0 & -\frac{a}{3b} & \frac{a}{6} & 0 & \frac{a}{6b} & \frac{a}{3} & 0 & \frac{a}{3b} \\
0 & 0 & 0 & -\frac{a}{6} & 0 & -\frac{a}{2b} & \frac{a}{2} & -\frac{a^2}{6b} & \frac{a}{2b} & \frac{a}{6} & -\frac{a^2}{3b} & 0 \\
-\frac{b}{2} & -\frac{a}{2} & 0 & \frac{b}{2} & -\frac{a}{2} & 0 & -\frac{b}{2} & \frac{a}{2} & 0 & \frac{b}{2} & \frac{a}{2} & 0 \\
0 & -\frac{a}{6} & -\frac{1}{2} & \frac{b}{2} & -\frac{a}{3} & -\frac{1}{2} & 0 & \frac{a}{6} & \frac{1}{2} & \frac{b}{2} & \frac{a}{3} & \frac{1}{2} \\
-\frac{b}{6} & 0 & -\frac{1}{2} & \frac{b}{6} & 0 & \frac{1}{2} & -\frac{b}{3} & \frac{a}{2} & -\frac{1}{2} & \frac{b}{3} & \frac{a}{2} & \frac{1}{2} \\
0 & -\frac{a}{12} & -\frac{1}{3} & \frac{b}{2} & -\frac{a}{4} & -\frac{2}{3} & 0 & \frac{a}{12} & \frac{1}{3} & \frac{b}{2} & \frac{a}{4} & \frac{2}{3} \\
-\frac{b}{12} & 0 & -\frac{1}{3} & \frac{b}{12} & 0 & \frac{1}{3} & -\frac{b}{4} & \frac{a}{2} & -\frac{2}{3} & \frac{b}{4} & \frac{a}{2} & \frac{2}{3}
\end{bmatrix}
$$

$$\text{Matrix } [T] = \oint [R]^T [L] \, ds \qquad (3.21)$$

consequently, the strain energy in the element due to in-plane deformation is that done by stresses in the faces. For the general case of facings having different thickness and materials, there is certain amount of coupling between in-plane and transverse deformations, but this coupling effect has always been neglected in small-deflection theory of sandwich plates. However, when the extensional stiffness of the two facings are the same (i.e. $E_1t_1 = E_2t_2$) the coupling ceases to exist. To simplify the analysis it is assumed that there is no coupling between bending and membrane actions in the sandwich plates.

With the above assumptions, the membrane stiffness of the sandwich plate is equal to the sum of the stiffness of the two faces. Strain energy in an orthotropic face of thickness t is given as

$$U_m = \frac{t}{2} \int_A \{\sigma\}^T \{\varepsilon\} \, dA \tag{3.22}$$

where

$$\{\sigma\} = \begin{Bmatrix} \sigma_x \\ \sigma_y \\ \tau_{xy} \end{Bmatrix} \quad \text{and} \quad \{\varepsilon\} = \begin{Bmatrix} \varepsilon_x \\ \varepsilon_y \\ \gamma_{xy} \end{Bmatrix}$$

The stress-strain relation is

$$\{\varepsilon\} = [N] \{\sigma\} \tag{3.23}$$

in which

$$[N] = \begin{bmatrix} \frac{1}{E_x} & -\frac{\nu_{yx}}{E_y} & 0 \\ -\frac{\nu_{xy}}{E_x} & \frac{1}{E_y} & 0 \\ 0 & 0 & G_{xy} \end{bmatrix}$$

Substituting this equation into the strain energy expression, eqn. (3.22) gives

$$U_m = \frac{t}{2} \int_A \{\sigma\}^T [N] \{\sigma\} \, dA \qquad (3.24)$$

The stresses in the faces are assumed to vary quadratically in x and y directions:

$$\sigma_x = \beta_1+\beta_2\bar{x}+\beta_3\bar{y}+\beta_4\bar{x}^2+\beta_5\bar{x}\bar{y}+\beta_6\bar{y}^2$$

$$\sigma_y = \beta_7+\beta_8\bar{x}+\beta_9\bar{y}+\beta_{10}\bar{x}^2+\beta_{11}\bar{x}\bar{y}+\beta_{12}\bar{y}^2$$

$$\tau_{xy} = \beta_{13}+\beta_{14}\bar{x}+\beta_{15}\bar{y}+\beta_{16}\bar{x}^2+\beta_{17}\bar{x}\bar{y}+\beta_{18}\bar{y}^2$$

Six of the above eighteen stress parameters can be eliminated by using the equilibrium conditions:

$$\frac{\partial \sigma_x}{\partial x} + \frac{\partial \tau_{xy}}{\partial y} = 0$$

$$\frac{\partial \sigma_y}{\partial y} + \frac{\partial \tau_{xy}}{\partial x} = 0$$

The resulting stresses are in equilibrium

$$\sigma_x = \beta_1+\beta_2\bar{x}+\beta_3\bar{y}+\beta_4\bar{x}^2+\beta_5\bar{x}\bar{y}+\beta_6\bar{y}^2$$

$$\sigma_y = \frac{b^2}{a^2}y^2\beta_4+\beta_7+\beta_8\bar{x}+\beta_9\bar{y}+\beta_{10}\bar{x}^2+\beta_{11}\bar{x}\bar{y}$$

$$\tau_{xy} = -\frac{b}{a^2}\bar{y}\beta_2-\frac{2b\bar{x}\bar{y}}{a}\beta_4-\frac{b}{2a^2}\bar{y}^2\beta_5-\frac{a\bar{x}}{b}\beta_9-\frac{a\bar{x}^2}{2b}\beta_{11}+\beta_{13}$$

or

$$\{\sigma\} = [P]\{\beta\} \qquad (3.25)$$

Substituting this equation into eqn. (3.24) yields

$$U = \frac{t}{2}\int_A\{\beta\}^T[P]^T[N][P]\{\beta\}\,dA$$

From this equation the matrix $[H]_m$ is found as

$$[H]_m = t\int_A[P]^T[N][P]\,dA \qquad (3.26)$$

and its explicit form is given in eqn. (3.26a).

Define the nodal displacement vector $\{q\}$ (Fig.3.3).

$$\{q\}^T = [u_1\ v_1\ u_2\ v_2\ u_3\ v_3\ u_4\ v_4]$$

Along the edges, linear deformations are assumed

$$\{u\} = [L]\{q\}$$

where

$$\{u\}^T = [u_{12}\ v_{12}\ u_{24}\ v_{24}\ u_{34}\ v_{34}\ u_{13}\ v_{13}]$$

and $[L]$ is given in Appendix A.

Corresponding to the edge displacements, the edge forces are evaluated from eqn. (3.25).

$$
\begin{array}{c}
\begin{array}{cccccccccccc}
1 & 2 & 3 & 4 & 5 & 6 & 7 & 8 & 9 & 10 & 11 & 12
\end{array} \\
\left[\begin{array}{cccccccccccc}
d & \frac{d}{2} & \frac{d}{2} & \frac{d}{3}-\frac{f}{3\eta^2} & \frac{d}{4} & \frac{d}{3} & -f & -\frac{f}{2} & -\frac{f}{2} & -\frac{f}{3} & -\frac{f}{4} & 0 \\
 & \frac{d}{3}+\frac{g}{3\eta^2} & \frac{d}{4} & \frac{d}{4}-\frac{f}{6\eta^2}+\frac{g}{3\eta^2} & \frac{d}{6}+\frac{g}{8\eta^2} & \frac{d}{6} & -\frac{f}{2} & -\frac{f}{3} & -\frac{f}{4}+\frac{g}{4} & -\frac{f}{4} & -\frac{f}{6}+\frac{g}{12} & -\frac{g}{2\eta} \\
 & & \frac{d}{3} & \frac{d}{6}-\frac{f}{4\eta^2} & \frac{d}{6} & \frac{d}{4} & -\frac{f}{2} & -\frac{f}{4} & -\frac{f}{3} & -\frac{f}{6} & -\frac{f}{6} & 0 \\
 & & & \frac{d}{5}-\frac{2f}{9\eta^2}+\frac{e}{5\eta^4}+\frac{4g}{9\eta^2} & \frac{d}{8}-\frac{f}{8\eta^2}+\frac{g}{8\eta^2} & \frac{d}{9}-\frac{f}{5\eta^2} & -\frac{f}{3}+\frac{e}{3\eta^2} & -\frac{f}{4}+\frac{e}{6\eta^2} & -\frac{f}{6}+\frac{e}{4\eta^2}+\frac{g}{3} & -\frac{f}{5}+\frac{e}{9\eta^2} & -\frac{f}{8}+\frac{e}{8\eta^2}+\frac{g}{8} & -\frac{g}{2\eta} \\
 & & & & \frac{d}{9}+\frac{g}{20\eta^2} & \frac{d}{8} & -\frac{f}{4} & -\frac{f}{6} & -\frac{f}{6}+\frac{g}{12} & -\frac{f}{8} & -\frac{f}{9}+\frac{g}{36} & -\frac{g}{6\eta} \\
\eta = \frac{a}{b} & & & & & \frac{d}{5} & -\frac{f}{3} & -\frac{f}{6} & -\frac{f}{4} & -\frac{f}{9} & -\frac{f}{8} & 0 \\
d = \frac{t_i}{E_{xi}}ab & & & & & & e & \frac{e}{2} & \frac{e}{2} & \frac{e}{3} & \frac{e}{4} & 0 \\
 & & & & & & & \frac{e}{3} & \frac{e}{4} & \frac{e}{4} & \frac{e}{6} & 0 \\
e = \frac{t_i}{E_{yi}}ab & & & & & & & & \frac{e}{3}+\frac{g\eta^2}{3} & \frac{e}{6} & \frac{e}{6}+\frac{g\eta^2}{8} & -\frac{g\eta}{2} \\
f = \frac{\nu_{xyi}\ t_i}{E_{xi}}ab & & & & & & & & & \frac{e}{5} & \frac{e}{8} & 0 \\
g = \frac{t_i}{G_{xyi}}ab & & & & & \text{Symmetric} & & & & & \frac{e}{9}+\frac{g\eta^2}{20} & -\frac{g\eta}{6} \\
 & & & & & & & & & & & g
\end{array}\right]
\begin{array}{c}
1 \\ 2 \\ 3 \\ 4 \\ 5 \\ 6 \\ 7 \\ 8 \\ 9 \\ 10 \\ 11 \\ 12
\end{array}
\end{array}
$$

$$
\text{MATRIX } [H]_m = \int_A [P]^T [N]\,[P]\,dA \qquad (3.26a)
$$

$$\{S\} = \begin{Bmatrix} S_1 \\ S_2 \\ S_3 \\ S_4 \\ S_5 \\ S_6 \\ S_7 \\ S_8 \end{Bmatrix} = 2t \begin{Bmatrix} -(\tau_{xy})\bar{y} = 0 \\ -(\sigma_y)\bar{y} = 0 \\ (\sigma_x)\bar{x} = 1 \\ (\tau_{xy})\bar{x} = 1 \\ (\tau_{xy})\bar{y} = 1 \\ (\sigma_y)\bar{y} = 1 \\ -(\sigma_x)\bar{x} = 0 \\ -(\tau_{xy})\bar{x} = 0 \end{Bmatrix} = [R]\{\beta\} \qquad (3.27)$$

where [R] is given in Appendix A.

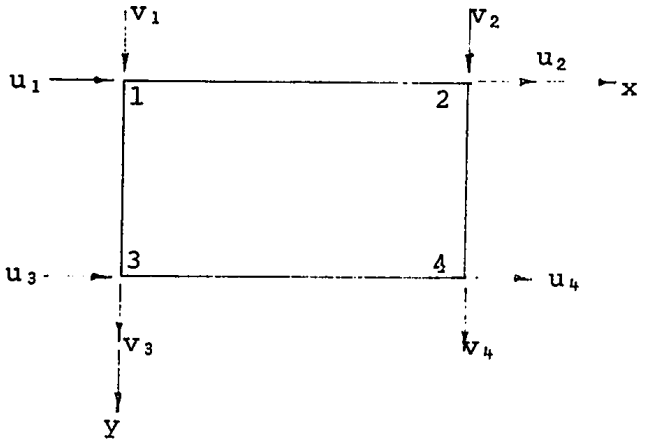

FIG. 3.3 NODAL DISPLACEMENTS FOR MEMBRANE ACTION

The matrix $[T] = \oint [R]^T [L]\, ds$ is found and shown in eqn. (3.28). Finally, the stiffness matrix is obtained by summing the contribution of each face

$$[K]_m = \sum_{i=1}^{2} [T]_m^T [H]_m^{-1} [T]_m$$

$$[T]_m = t_i \begin{bmatrix}
-\frac{b}{2} & 0 & \frac{b}{2} & 0 & -\frac{b}{2} & 0 & \frac{b}{2} & 0 \\
0 & \frac{b^2}{6a} & \frac{b}{2} & -\frac{b^2}{6a} & -\frac{b}{2} & \frac{b^2}{3a} & 0 & -\frac{b^2}{3a} \\
-\frac{b}{6} & 0 & \frac{b}{6} & 0 & -\frac{b}{3} & 0 & \frac{b}{3} & 0 \\
0 & 0 & \frac{b}{2} & -\frac{b^2}{3a} & -\frac{b}{3} & \frac{b^2}{2a} & -\frac{b}{6} & -\frac{b^2}{6a} \\
0 & \frac{b^2}{24a} & \frac{b}{6} & -\frac{b^2}{24a} & -\frac{b}{4} & \frac{b^2}{8a} & \frac{b}{12} & -\frac{b^2}{8a} \\
-\frac{b}{12} & 0 & \frac{b}{12} & 0 & -\frac{b}{4} & 0 & \frac{b}{4} & 0 \\
0 & -\frac{a}{2} & 0 & -\frac{a}{2} & 0 & \frac{a}{2} & 0 & \frac{a}{2} \\
0 & -\frac{a}{6} & 0 & -\frac{a}{3} & 0 & \frac{a}{6} & 0 & \frac{a}{3} \\
\frac{a^2}{6b} & 0 & \frac{a^2}{3b} & -\frac{a}{2} & -\frac{a^2}{6b} & \frac{a}{2} & -\frac{a^2}{3b} & 0 \\
0 & -\frac{a}{12} & 0 & -\frac{a}{4} & 0 & \frac{a}{12} & 0 & \frac{a}{4} \\
\frac{a^2}{24b} & 0 & \frac{a^2}{8b} & -\frac{a}{4} & -\frac{a^2}{24b} & \frac{a}{6} & -\frac{a^2}{8b} & \frac{a}{12} \\
-\frac{a}{2} & -\frac{b}{2} & -\frac{a}{2} & \frac{b}{2} & \frac{a}{2} & -\frac{b}{2} & \frac{a}{2} & \frac{b}{2}
\end{bmatrix} \qquad (3.28)$$

3.4 RIGHT-ANGLED TRIANGULAR ELEMENT BENDING STIFFNESS MATRIX

Triangular elements have a distinct advantage over rectangular elements in that they may be used to idealize structures having non-rectangular panels or cut-outs. For

shell structures the use of triangular elements is necessary to provide a close approximation of the shell geometry.

Consider the right-angled triangular element shown in Fig. 3.4, the geometry of the triangle is specified by the lengths a and b of the two sides parallel to x and y axes respectively.

Let

$$\bar{x} = \frac{x}{a}$$

$$\bar{y} = \frac{y}{b}$$

The variations of the stresses and edge displacements in the element are assumed to be the same as in the rectangular element case. The matrix [H] is obtained from the strain energy expression, (eqn.2.6), using the moments and shear forces in egn. (3.12).

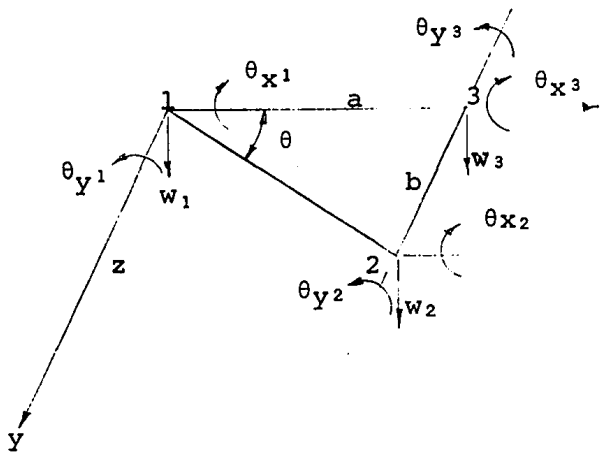

FIG. 3.4 NODAL DISPLACEMENTS FOR BENDING ACTION

The integration is performed over the area of the triangle. The resulting matrix [H] may be split up into six component matrices as before

$$[H] = \sum_{i=1}^{6} [H_i]$$

where $[H_i]$ is given below in compact form:

$$[H_1] = \frac{ab}{B_x}$$

1	2	3	4	5	6	
$\frac{1}{2}$	$\frac{1}{3}$	$\frac{1}{6}$	$\frac{1}{4}$	$\frac{1}{8}$	$\frac{1}{12}$	1
	$\frac{1}{4}$	$\frac{1}{8}$	$\frac{1}{5}$	$\frac{1}{10}$	$\frac{1}{15}$	2
		$\frac{1}{12}$	$\frac{1}{10}$	$\frac{1}{15}$	$\frac{1}{20}$	3
			$\frac{1}{6}$	$\frac{1}{12}$	$\frac{1}{18}$	4
Symmetric				$\frac{1}{18}$	$\frac{1}{24}$	5
					$\frac{1}{30}$	6

$$[H_2] = \frac{ab}{B_y}$$

7	8	9	10	11	12	
$\frac{1}{2}$	$\frac{1}{3}$	$\frac{1}{6}$	$\frac{1}{4}$	$\frac{1}{8}$	$\frac{1}{12}$	7
	$\frac{1}{4}$	$\frac{1}{8}$	$\frac{1}{5}$	$\frac{1}{10}$	$\frac{1}{15}$	8
		$\frac{1}{12}$	$\frac{1}{10}$	$\frac{1}{15}$	$\frac{1}{20}$	9
			$\frac{1}{6}$	$\frac{1}{12}$	$\frac{1}{18}$	10
Symmetric				$\frac{1}{18}$	$\frac{1}{24}$	11
					$\frac{1}{30}$	12

$$[H_3] = \frac{-ab}{B_\nu}$$

7	8	9	10	11	12	
$\frac{1}{2}$	$\frac{1}{3}$	$\frac{1}{6}$	$\frac{1}{4}$	$\frac{1}{8}$	$\frac{1}{12}$	1
$\frac{1}{3}$	$\frac{1}{4}$	$\frac{1}{8}$	$\frac{1}{5}$	$\frac{1}{10}$	$\frac{1}{15}$	2
$\frac{1}{6}$	$\frac{1}{8}$	$\frac{1}{12}$	$\frac{1}{10}$	$\frac{1}{15}$	$\frac{1}{20}$	3
$\frac{1}{4}$	$\frac{1}{5}$	$\frac{1}{10}$	$\frac{1}{6}$	$\frac{1}{12}$	$\frac{1}{18}$	4
$\frac{1}{8}$	$\frac{1}{10}$	$\frac{1}{15}$	$\frac{1}{12}$	$\frac{1}{18}$	$\frac{1}{24}$	5
$\frac{1}{12}$	$\frac{1}{15}$	$\frac{1}{20}$	$\frac{1}{18}$	$\frac{1}{24}$	$\frac{1}{30}$	6

$$[H_4] = \frac{ab}{B_G}$$

4	12	13	14	15	16	17	
$\frac{1}{18\eta^2}$	$\frac{1}{18}$	$\frac{-1}{8\eta}$	$\frac{-1}{10\eta}$	$\frac{-1}{15\eta}$	$\frac{-1}{12\eta}$	$\frac{-1}{24\eta}$	4
	$\frac{\eta^2}{18}$	$\frac{-\eta}{8}$	$\frac{-\eta}{10}$	$\frac{-\eta}{15}$	$\frac{-\eta}{12}$	$\frac{-\eta}{24}$	12
		$\frac{1}{2}$	$\frac{1}{3}$	$\frac{1}{6}$	$\frac{1}{4}$	$\frac{1}{12}$	13
			$\frac{1}{4}$	$\frac{1}{8}$	$\frac{1}{5}$	$\frac{1}{15}$	14
Symmetric				$\frac{1}{12}$	$\frac{1}{10}$	$\frac{1}{20}$	15
$\eta = \frac{a}{b}$					$\frac{1}{6}$	$\frac{1}{18}$	16
						$\frac{1}{30}$	17

$$[H_5] = \frac{ab\ d^2}{h^2 S_x}$$

	2	4	5	12	15	17	
	$\frac{1}{2a^2}$	$\frac{1}{3a^2}$	$\frac{1}{6a^2}$	$\frac{-1}{3b^2}$	$\frac{1}{2ab}$	$\frac{1}{3ab}$	2
		$\frac{1}{4a^2}$	$\frac{1}{8a^2}$	$\frac{-1}{4b^2}$	$\frac{1}{3ab}$	$\frac{1}{4ab}$	4
			$\frac{1}{12a^2}$	$\frac{-1}{8b^2}$	$\frac{1}{6ab}$	$\frac{1}{6ab}$	5
				$\frac{\eta^2}{4b^2}$	$\frac{-\eta}{3b^2}$	$\frac{-\eta}{4b^2}$	12
	Symmetric				$\frac{1}{2b^2}$	$\frac{1}{3b^2}$	15
						$\frac{1}{3b^2}$	17

$$[H_6] = \frac{ab\ d^2}{h^2 S_y}$$

	4	9	11	12	14	16	
	$\frac{1}{12a^2\eta^2}$	$\frac{-1}{6a^2}$	$\frac{-1}{8a^2}$	$\frac{-1}{12a^2}$	$\frac{-1}{6\eta a^2}$	$\frac{-1}{4\eta a^2}$	4
		$\frac{1}{2b^2}$	$\frac{1}{3b^2}$	$\frac{1}{6b^2}$	$\frac{1}{2ab}$	$\frac{2}{3ab}$	9
			$\frac{1}{4b^2}$	$\frac{1}{8b^2}$	$\frac{1}{3ab}$	$\frac{1}{2ab}$	11
	Symmetric			$\frac{1}{12b^2}$	$\frac{1}{6ab}$	$\frac{1}{4ab}$	12
	$\eta = \frac{a}{b}$				$\frac{1}{2a^2}$	$\frac{2}{3a^2}$	14
						$\frac{1}{a^2}$	16

The procedure for establishing matrix [T] is similar to that used in the case of rectangular elements, however, the contour integration must be performed along the

triangular boundary. The generalized forces on the sloping edge may be found by consideration of equilibrium of a plate element shown in Fig. 3.5.

$$\left.\begin{aligned} M_n &= M_x \sin^2\theta + M_y \cos^2\theta - 2M_{xy} \sin\theta \cos\theta \\ M_{nt} &= (M_y - M_x) \cos\theta \sin\theta + (\cos^2\theta - \sin^2\theta) M_{xy} \\ Q_n &= Q_y \cos\theta - Q_x \sin\theta \end{aligned}\right\} \quad (3.29)$$

Using eqn. (3.29) in conjunction with eqn. (3.12), the matrix [R] in

$$\{S\} = [R]\{\beta\} \quad (3.30)$$

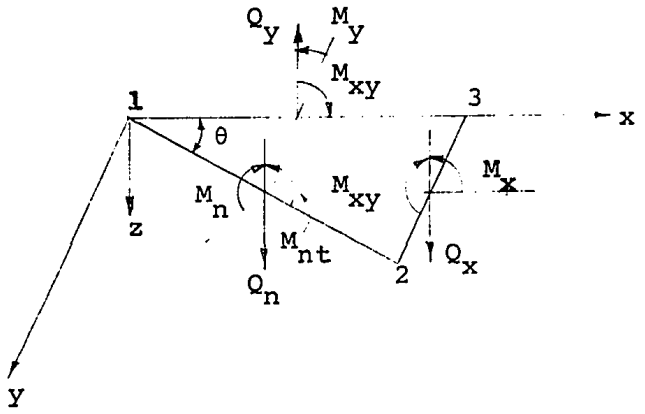

FIG. 3.5 STRESS RESULTANTS ON EDGES OF THE TRIANGULAR ELEMENT

is found and shown in Appendix B. Vectors $\{S\}$ and $\{\beta\}$ are defined as follows:

$$\{S\}^T = [(M_{nt})_{\bar{y}=\bar{x}}, (M_n)_{\bar{y}=\bar{x}}, (Q_n)_{\bar{y}=\bar{x}}, (M_{xy})_{\bar{x}=1},$$

$$(M_x)_{\bar{x}=1}, (Q_x)_{\bar{x}=1}, (-M_y)_{\bar{y}=o}, (-M_{xy})_{\bar{y}=o},$$

$$(-Q_y)_{\bar{y}=o}]$$

$$\{\beta\}^T = [\beta_1\ \beta_2\ \beta_3\ \beta_4\ \beta_5\ \beta_6\ \beta_7\ \beta_8\ \beta_9\ \beta_{10}\ \beta_{11}\ \beta_{12}\ \beta_{13}$$

$$\beta_{14}\ \beta_{15}\ \beta_{16}\ \beta_{18}]$$

The generalized displacements of edge (1-2) may be expressed in terms of displacements of nodes 1 and 2:

$$w_{12} = (1-\bar{x})w_1 + \bar{x}w_2$$

$$\theta_{n12} = (1-\bar{x})(\theta_{x_1} \sin\theta + \theta_{y_1} \cos\theta) + \bar{x}(\theta_{x_2} \sin\theta + \theta_{y_2} \cos\theta)$$

$$\theta_{t12} = (1-\bar{x})(\theta_{x_1} \cos\theta - \theta_{y_1} \sin\theta) + \bar{x}(\theta_{x_2} \cos\theta - \theta_{y_2} \sin\theta)$$

where θ_n and θ_t are the rotations about the axes normal and tangential to the sloping edge respectively.

Collectively for all edges

$$\{u\} = [L]\{q\} \tag{3.31}$$

where

$$\{u\}^T = [\theta_{n12}\ \theta_{t12}\ w_{12}\ \theta_{x23}\ \theta_{y23}\ w_{23}\ \theta_{x31}\ \theta_{y31}\ w_{31}]$$

$$\{q\}^T = [\theta_{x_1}\ \theta_{y_1}\ w_1\ \theta_{x_2}\ \theta_{y_2}\ w_2\ \theta_{x_3}\ \theta_{y_3}\ w_3]$$

$$
[T] = \begin{bmatrix}
0 & -\frac{b}{2} & 0 & 0 & 0 & 0 & 0 & \frac{b}{2} & 0 \\
0 & -\frac{b}{6} & \frac{-b}{2a} & 0 & \frac{b}{6} & 0 & 0 & \frac{b}{2} & \frac{b}{2a} \\
0 & -\frac{b}{6} & 0 & 0 & 0 & 0 & 0 & \frac{b}{6} & 0 \\
\frac{b^2}{12a} & -\frac{b}{6} & \frac{-b}{3a} & \frac{-b^2}{12a} & 0 & \frac{-b}{6a} & \frac{-b^2}{6a} & \frac{b}{2} & \frac{b}{2a} \\
0 & \frac{-b}{12} & \frac{-b}{6a} & 0 & \frac{b}{12} & 0 & 0 & \frac{b}{6} & \frac{b}{6a} \\
0 & \frac{-b}{12} & 0 & 0 & 0 & 0 & 0 & \frac{b}{12} & 0 \\
0 & 0 & 0 & \frac{a}{2} & 0 & 0 & \frac{-a}{2} & 0 & 0 \\
0 & 0 & 0 & \frac{a}{3} & 0 & 0 & \frac{-a}{3} & 0 & 0 \\
\frac{a}{6} & 0 & 0 & \frac{a}{3} & 0 & \frac{a}{2b} & 0 & 0 & \frac{-a}{2b} \\
0 & 0 & 0 & \frac{a}{4} & 0 & 0 & \frac{-a}{4} & 0 & 0 \\
\frac{a}{12} & 0 & 0 & \frac{a}{4} & 0 & \frac{a}{3b} & 0 & 0 & \frac{-a}{3b} \\
\frac{a}{6} & \frac{-a^2}{12b} & \frac{a}{3b} & \frac{a}{6} & \frac{-a^2}{4b} & \frac{a}{6b} & \frac{-a}{6} & 0 & \frac{-a}{2b} \\
-\frac{b}{2} & 0 & 0 & 0 & \frac{a}{2} & 0 & \frac{b}{2} & -\frac{a}{2} & 0 \\
-\frac{b}{6} & 0 & 0 & \frac{b}{6} & \frac{a}{3} & \frac{1}{2} & \frac{b}{2} & -\frac{a}{3} & -\frac{1}{2} \\
-\frac{b}{6} & \frac{a}{6} & -\frac{1}{2} & 0 & \frac{a}{3} & 0 & \frac{b}{6} & 0 & \frac{1}{2} \\
\frac{-b}{12} & 0 & 0 & \frac{b}{4} & \frac{a}{4} & \frac{2}{3} & \frac{b}{2} & \frac{-a}{4} & \frac{-2}{3} \\
\frac{-b}{12} & \frac{a}{12} & -\frac{1}{3} & 0 & \frac{a}{4} & 0 & \frac{b}{12} & 0 & \frac{1}{3}
\end{bmatrix}
$$

(3.32)

and [L] is given in Appendix B.

Now [T] can be evaluated by performing the integration

$$[T] = \oint [R]^T [L] \, ds$$

the result is shown in eqn. (3.32), and the stiffness matrix is given by eqn. (3.10).

3.5 RIGHT-ANGLED TRIANGULAR ELEMENT MEMBRANE STIFFNESS MATRIX

For membrane action the face stresses σ_x, σ_y and τ_{xy} are again assumed as in eqn. (3.25). By substituting these equations into eqn. (2.26) and integrating over the area of the triangle, the matrix [H] is found and shown in eqn. (3.33).

The matrix [R] is defined by equation

$$\{S\} = [R] \{\beta\} \tag{3.34}$$

where

$$\{\beta\}^T = [\beta_1 \ \beta_2 \ \beta_3 \ \beta_4 \ \beta_5 \ \beta_6 \ \beta_7 \ \beta_8 \ \beta_9 \ \beta_{10} \ \beta_{11} \ \beta_{13}]$$

and

$$\{S\} = \begin{bmatrix} (\sigma_n)_{\bar{y}=\bar{x}} \\ (\tau_t)_{\bar{y}=\bar{x}} \\ (\sigma_x)_{\bar{x}=1} \\ (\tau_{xy})_{\bar{x}=1} \\ (-\tau_{xy})_{\bar{y}=0} \\ (-\sigma_y)_{\bar{y}=0} \end{bmatrix}$$

$$
[H]_m = \begin{array}{c}
\begin{array}{cccccccccccc}
1 & 2 & 3 & 4 & 5 & 6 & 7 & 8 & 9 & 10 & 11 & 12
\end{array} \\
\left[\begin{array}{cccccccccccc}
\frac{d}{2} & \frac{d}{3} & \frac{d}{6} & \frac{d}{4}\frac{f}{12\eta^2} & \frac{d}{8} & \frac{d}{12} & -\frac{f}{2} & -\frac{f}{3} & -\frac{f}{6} & -\frac{f}{4} & -\frac{f}{8} & 0 \\
 & \frac{d}{4}+\frac{g}{12\eta^2} & \frac{d}{8} & \frac{d}{5}-\frac{f}{15\eta^2}+\frac{2g}{15\eta^2} & \frac{d}{10}+\frac{g}{40\eta^2} & \frac{d}{15} & -\frac{f}{3} & -\frac{f}{4} & -\frac{f}{8}+\frac{g}{8} & -\frac{f}{5} & -\frac{f}{10}+\frac{g}{20} & -\frac{g}{6\eta} \\
 & & \frac{d}{12} & \frac{d}{10}-\frac{f}{20\eta^2} & \frac{d}{15} & \frac{d}{20} & -\frac{f}{6} & -\frac{f}{8} & -\frac{f}{12} & -\frac{f}{10} & -\frac{f}{15} & 0 \\
 & & & \frac{d}{6}+\frac{e}{30\eta^4}-\frac{f}{9\eta^2}+\frac{2g}{9\eta^2} & \frac{d}{12}+\frac{g}{24\eta^2}-\frac{f}{24\eta^2} & \frac{d}{18}-\frac{f}{30\eta^2} & \frac{e}{12\eta^2}-\frac{f}{4} & \frac{e}{15\eta^2}-\frac{f}{5} & \frac{e}{20\eta^2}-\frac{f}{10}+\frac{g}{5} & \frac{e}{18\eta^2}-\frac{f}{6} & \frac{e}{24\eta^2}-\frac{f}{12}+\frac{g}{12} & -\frac{g}{4\eta} \\
 & & & & \frac{d}{18}+\frac{g}{120\eta^2} & \frac{d}{24} & -\frac{f}{8} & -\frac{f}{10} & -\frac{f}{15}+\frac{g}{30} & -\frac{f}{12} & -\frac{f}{18}+\frac{g}{72} & -\frac{g}{24\eta} \\
 & & & & & \frac{d}{30} & -\frac{f}{12} & -\frac{f}{15} & -\frac{f}{20} & -\frac{f}{18} & -\frac{f}{24} & 0 \\
 & & & & & & \frac{e}{2} & \frac{e}{3} & \frac{e}{6} & \frac{e}{4} & \frac{e}{8} & 0 \\
 & & & & & & & \frac{e}{4} & \frac{e}{8} & \frac{e}{5} & \frac{e}{10} & 0 \\
 & & & & & & & & \frac{e}{12}+\frac{\eta^2 g}{4} & \frac{e}{10} & \frac{e}{15}+\frac{\eta^2 g}{10} & -\frac{g\eta}{3} \\
 & & & & & & & & & \frac{e}{6} & \frac{e}{12} & 0 \\
 & & & & & & & & & & \frac{e}{18}+\frac{\eta^2 g}{24} & -\frac{g\eta}{8} \\
 & & & & & & & & & & & \frac{g}{2}
\end{array}\right]
\end{array}
\begin{array}{c}
1 \\ 2 \\ 3 \\ 4 \\ 5 \\ 6 \\ 7 \\ 8 \\ 9 \\ 10 \\ 11 \\ 12
\end{array}
\qquad (3.33)
$$

Symmetric

$\eta = \frac{a}{b}$

$d = \frac{t_i ab}{E_{xi}}$

$e = \frac{t_i ab}{E_{yi}}$

$f = \frac{\nu_{xyi}\, t_i\, ab}{E_{xi}}$ $\qquad g = \frac{t_i ab}{G_{xyi}}$

The stresses σ_n, τ_t on the sloping side are found from the equilibrium conditions

$$\sigma_n = \sigma_x \sin^2\theta+\sigma_y\cos^2\theta-2\tau_{xy} \sin\theta \cos\theta$$

$$\tau_t = (\sigma_y-\sigma_x)\sin\theta \cos\theta+(\sin^2\theta-\cos^2\theta)\tau_{xy}$$

The corresponding edge displacements are

$$\delta_t = (1-\bar{x})(u_1\cos\theta+v_1\sin\theta)+ \bar{x}(u_2\cos\theta+v_2\sin\theta)$$

$$\delta_n = (1-\bar{x})(-u_1\sin\theta+v_1\cos\theta)+ \bar{x}(-u_2\sin\theta+v_2\cos\theta)$$

Displacements along all edges

$$\{u\} = [L]\{q\} \tag{3.35}$$

where

$$\{u\}^T = [\delta_n \ \delta_t \ u_{23} \ v_{23} \ u_{13} \ v_{13}]$$

$$\{q\}^T = [u_1 \ v_1 \ u_2 \ v_2 \ u_3 \ v_3]$$

Matrices [R] and [L] are given in Appendix B.

Matrix [T] is found by equation

$$[T] = \oint [R]^T[L] \ ds$$

The result is given as in Eqn. (3.36). The stiffness matrix is again found as

$$[K] = \sum_{i=1}^{2} [T]^T[H]^{-1}[T]$$

$$[T]_m = t_i \begin{bmatrix}
-\frac{b}{2} & 0 & 0 & 0 & \frac{b}{2} & 0 \\
-\frac{b}{3} & \frac{b^2}{6a} & -\frac{b}{6} & 0 & \frac{b}{2} & -\frac{b^2}{6a} \\
-\frac{b}{6} & 0 & 0 & 0 & \frac{b}{6} & 0 \\
-\frac{b}{4} & \frac{b^2}{4a} & -\frac{b}{4} & \frac{b^2}{12a} & \frac{b}{2} & -\frac{b^2}{3a} \\
-\frac{b}{8} & \frac{b^2}{24a} & -\frac{b}{24} & 0 & \frac{b}{6} & -\frac{b^2}{24a} \\
-\frac{b}{12} & 0 & 0 & 0 & \frac{b}{12} & 0 \\
0 & 0 & 0 & \frac{a}{2} & 0 & -\frac{a}{2} \\
0 & 0 & 0 & \frac{a}{3} & 0 & -\frac{a}{3} \\
0 & \frac{a}{3} & -\frac{a^2}{3b} & \frac{a}{6} & \frac{a^2}{3b} & -\frac{a}{2} \\
0 & 0 & 0 & \frac{a}{4} & 0 & -\frac{a}{4} \\
0 & \frac{a}{8} & -\frac{a^2}{8b} & \frac{a}{8} & \frac{a^2}{8b} & -\frac{a}{4} \\
0 & -\frac{b}{2} & \frac{a}{2} & 0 & -\frac{a}{2} & \frac{b}{2}
\end{bmatrix} \qquad (3.36)$$

3.6 INCLUSION OF STRESS-BOUNDARY CONDITIONS INTO ELEMENT STIFFNESS MATRIX

Using the assumed stress distribution approach it is possible to prescribe boundary stresses. This can be done only in the element-analysis stage by modifying the assumed stress functions.

The work done by the edge forces is given by eqn. (3.6).

$$W = \oint \{S\}^T \{u\}\, ds$$

$$= \{\beta\}^T [T]\, \{q\}$$

where $\{S\}$ is the vector of edge forces, which may include any prescribed boundary stresses. The matrix $[T]$ is then derived in the usual manner. Thus, a variety of stiffness matrices may be derived to take into account the stress boundary conditions of various types of edge supports.

The inclusion of stress boundary conditions at the element level improves the accuracy of the results as shown by studies done on isotropic plates [19,22]; however, the additional accuracy gained is diminishingly small when more elements are used in the analysis. To reduce programming effort, it is decided to use only those previously derived stiffness matrices in all numerical examples presented in the later Chapters.

3.7 ELEMENT STRESS RESULTANTS

Stress resultants in element may be expressed in terms of the nodal displacements by substituting eqn. (3.2) into eqn. (3.1).

$$\{\sigma\} = [P]\{\beta\}$$

$$\{\sigma\} = [P][H]^{-1}[T]\{q\} \qquad (3.37)$$

The coefficients of $[P]$ are functions of the coordinates, hence by substituting appropriate values of $\bar{x}$ and $\bar{y}$ the stresses at any point of the element may be found. Usually, stresses are evaluated at the corners of the element and at the centroid. When many elements meet at a joint, the stresses at the joint calculated on the basis of nodal displacements of the related elements are not identical; this stress discontinuity also exists along the interelement boundaries. The representative stresses are then taken to be the average of all correspondent stresses.

CHAPTER IV

STATIC ANALYSIS OF THREE-DIMENSIONAL PLATE STRUCTURES BY FINITE ELEMENT METHOD

4.1 INTRODUCTION

Three-dimensional plate or shell structures may be idealized as an assembly of flat rectangular or triangular elements. This approach has been used and reported by many authors.[25,26,27,28] One of the difficulties involved is the requirement to maintain compatibility of displacements and normal slope along the interelement boundaries. One solution to this problem has been proposed in Ref. [29]. Here, the authors use linear functions for displacements and rotations in the element, and the bending and "shear" stiffness matrices are derived using displacement formulation. All of these applications of finite element method to three-dimensional structures are limited to the types of material which exhibit insignificant transverse shear deformation.

The elements described in the previous Chapter takes into account the transverse shear deformation without introducing any more degrees of freedom other than the actual geometrical displacements and rotations of the nodes. The imposition of linear displacements and rotations along the element edges ensures complete compatibility, however, the stresses in the element are not constant since they are assumed independently of the displacements; this is a signi-

ficant difference between the displacement formulation and assumed stress formulation of finite element theory.

4.2 ANALYSIS PROCEDURE

The arbitrary surface of the structure is idealized by an assemblage of flat rectangular or triangular elements or combinations of both shapes. These elements are connected together only at the node points which lie on the mid-surface of the real structure. The purpose of the analysis is to determine the nodal displacements and the distribution of stresses and strains throughout the structure. The direct stiffness method [30] is used to obtain the solutions, the procedure is summarized below.

1. Determination of the stiffness matrices of typical elements, forces and displacements are directed along the element (local) axes.

2. Transformation of element nodal forces into an axis-system common to the adjacent elements so that nodal forces can be added up algebraically.

3. Assembly of the structure stiffness matrix $[K]$ which relates the applied nodal forces $\{R\}$ to the resulting nodal displacements $\{r\}$

$$\{R\} = [K]\{r\}$$

$[K]$ is found by direct addition of the transformed element stiffness matrices.

4. Introduction of displacement boundary conditions and external forces into the above equation system. The unknown nodal displacements are found

$$\{r\} = [K]^{-1}\{R\} \tag{4.1}$$

5. Transformation of the element nodal displacements into element axes. They are subsequently used in conjunction with the stress matrix of each individual element to yield stresses and strains at the desired points.

Each of the above steps is described below, particular attention is given to the programming aspects.

4.3 ELEMENT STIFFNESS MATRIX IN LOCAL AXES

In the previous Chapter, the element stiffness matrices have been found separately for bending and membrane actions. In this Section, a combined stiffness matrix which includes both types of action is described.

The membrane and bending actions of an element are characterized by the stiffness equations

$$\{Q_m\} = [K_m]\{q_m\}$$
$$\{Q_b\} = [K_b]\{q_b\}$$

where m and b denote membrane and bending actions respectively. Combining the two equations yields

$$\begin{Bmatrix} Q_m \\ Q_b \end{Bmatrix} = \begin{bmatrix} K_m & 0 \\ 0 & K_b \end{bmatrix} \begin{Bmatrix} q_m \\ q_b \end{Bmatrix} \tag{4.2}$$

From this equation it can be seen that the in-plane and bending actions are assumed to be uncoupled within an element. This assumption is valid if the deformations of the element are small.

In the derivation of $[K_b]$ and $[K_m]$, three and two degrees of freedom per node are associated with bending and membrane actions respectively; a total of five degrees of freedom for each node. To facilitate the transformation of forces and displacements in three-dimensional space, another degree of freedom is introduced at each element node. This additional one is the in-plane rotation θ_z, its corresponding fictitious force is M_z(Fig. 4.1).

Designate the stiffness coefficients corresponding to $\{\theta_z\}$ as $[K_z]$, then

$$\{Q_z\} = [K_z]\{q_z\} \tag{4.3}$$

with

$$\{Q_z\}^T = [M_{z1}, M_{z2}, \ \ldots\ldots\ M_{zn}]$$

$$\{q_z\}^T = [\theta_{z1}, \theta_{z2}, \ \ldots\ldots\ \theta_{zn}]$$

where n is the number of nodes in the element.

Eqn. (4.2) may now be expanded to include eqn. (4.3).

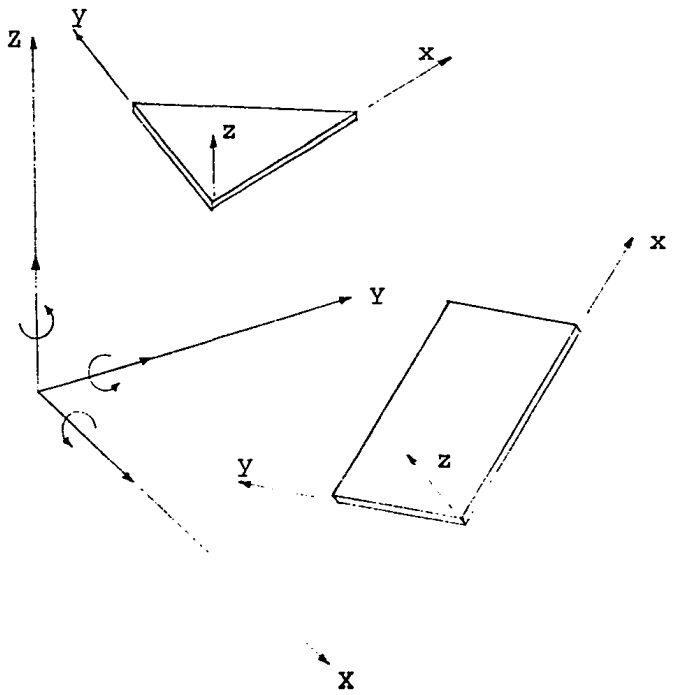

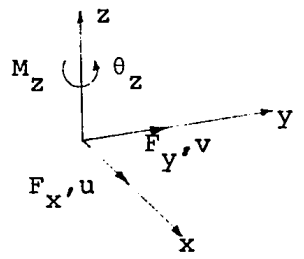

Membrane Action

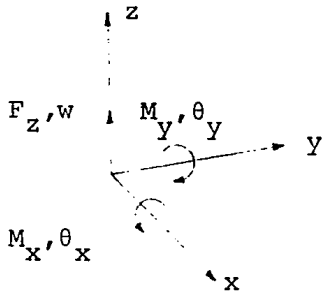

Bending Action

FIGURE 4.1 STRUCTURE AND ELEMENT AXIS-SYSTEMS

$$\begin{Bmatrix} Q_m \\ Q_b \\ Q_z \end{Bmatrix} = \begin{bmatrix} K_m & 0 & 0 \\ 0 & K_b & 0 \\ 0 & 0 & K_z \end{bmatrix} \begin{Bmatrix} q_m \\ q_b \\ q_z \end{Bmatrix} \qquad (4.4)$$

Because $\{q_z\}$ does not affect the strain energy in an element subjected to bending and membrane actions, the stiffness $[K_z]$ should be a null-matrix. However, zero stiffness may render the structure stiffness matrix ill-conditioned. This will happen when all elements connected to a node are coplanar because among the six equilibrium equations at this node only five are independent. A common practice to correct this situation is to assign small but arbitrary values to $[K_z]$. For a triangular element

$$\begin{Bmatrix} M_{z_1} \\ M_{z_2} \\ M_{z_3} \end{Bmatrix} = \gamma E(t_1+t_2)\frac{ab}{2} \begin{bmatrix} 1 & -0.5 & -0.5 \\ & 1 & -0.5 \\ \text{Sym.} & & 1 \end{bmatrix} \begin{Bmatrix} \theta_{z_1} \\ \theta_{z_2} \\ \theta_{z_3} \end{Bmatrix}$$

For a rectangular one

$$\begin{Bmatrix} M_{z_1} \\ M_{z_2} \\ M_{z_3} \\ M_{z_4} \end{Bmatrix} = \gamma E(t_1+t_2)ab \begin{bmatrix} 1 & -\frac{1}{3} & -\frac{1}{3} & -\frac{1}{3} \\ & 1 & -\frac{1}{3} & -\frac{1}{3} \\ & \text{Sym.} & 1 & -\frac{1}{3} \\ & & & 1 \end{bmatrix} \begin{Bmatrix} \theta_{z_1} \\ \theta_{z_2} \\ \theta_{z_3} \\ \theta_{z_4} \end{Bmatrix}$$

where γ is an arbitrary numerical constant. Studies made by several authors [29,30] have shown that the smaller γ gives better results but the effect is very small. γ was chosen to be 3×10^{-6} for all problems solved in the later Chapters.

An alternative way to avoid the ill-condition problem because of zero stiffness is to assemble the equilibrium equations in local coordinates at those nodes where the difficulty arises and then suppress the degrees of freedom corresponding to the in-plane rotations. Both approaches are incorporated in the computer program which will be described subsequently.

For programming purposes, the eqn. (4.4) is rearranged in the form

$$\begin{Bmatrix} Q^1 \\ Q^2 \\ \cdot \\ Q^n \end{Bmatrix} = \begin{bmatrix} K_{11} & K_{12} \cdots K_{1n} \\ K_{21} & K_{22} \cdots K_{2n} \\ \cdot & \cdot \quad \cdot \\ K_{n_1} & K_{n_2} \cdots K_{nn} \end{bmatrix} \begin{Bmatrix} q^1 \\ q^2 \\ \cdot \\ q^n \end{Bmatrix} \tag{4.5}$$

where $\{Q^i\}$ and $\{q^i\}$ are respectively the generalized forces and displacements at node i.

$$\begin{aligned} \{Q^i\}^T &= [F_{xi} \quad F_{yi} \quad F_{zi} \quad M_{xi} \quad M_{yi} \quad M_{zi}] \\ \{q^i\}^T &= [u_i \quad v_i \quad w_i \quad \theta_{xi} \quad \theta_{yi} \quad \theta_{zi}] \end{aligned} \tag{4.6}$$

4.4 TRANSFORMATION MATRIX

For the complete structure assembled from the individual elements, six equilibrium equations at each joint must be established in a common axis system. Let this new coordinate axes at node i be labelled $x_i^*\ y_i^*\ z_i^*$, the generalized forces $\{Q^i\}$ and displacements $\{q^i\}$ are related to those in the new system by a transformation as

$$\{Q^i\} = [L^i]\ \{Q_*^i\}$$
$$\{q^i\} = [L^i]\ \{q_*^i\}$$

in which

$$[L^i] = \begin{bmatrix} \lambda^i & 0 \\ 0 & \lambda^i \end{bmatrix}$$

with

$$[\lambda^i] = \begin{bmatrix} \cos(x_i, x_i^*) & \cos(x_i, y_i^*) & \cos(x_i, z_i^*) \\ \cos(y_i, x_i^*) & \cos(y_i, y_i^*) & \cos(y_i, z_i^*) \\ \cos(z_i, x_i^*) & \cos(z_i, y_i^*) & \cos(z_i, z_i^*) \end{bmatrix}$$

Complete transformation of the generalized forces at all nodes of the element is

$$\begin{Bmatrix} Q^1 \\ Q^2 \\ \vdots \\ Q^n \end{Bmatrix} = \begin{bmatrix} L^1 & 0 \cdots 0 \\ 0 & L^2 \cdots 0 \\ \vdots & \vdots \quad \vdots \\ 0 & 0 \cdots L^n \end{bmatrix} \begin{Bmatrix} Q_*^1 \\ Q_*^2 \\ \vdots \\ Q_*^n \end{Bmatrix}$$

or

$$\{Q\} = [L]\ \{Q_*\} \tag{4.7}$$

Similarly for the generalized displacements

$$\{q\} = [L]\{q_*\} \tag{4.8}$$

Substitution of eqns. (4.7) and (4.8) into eqn.(4.5)

$$[L]\{Q_*\} = [K][L]\{q_*\}$$

or

$$\{Q_*\} = [L]^{-1}[K][L]\{q_*\}$$

Since this is an orthogonal transformation $[L]^{-1} = [L]^T$, hence

$$\{Q_*\} = [L]^T[K][L]\{q_*\} \tag{4.9}$$

Thus, the transformed stiffness matrix which gives nodal forces in the new coordinate system is

$$[K_*] = [L]^T[K][L]$$

Expressing eqn. (4.9) in the same form as in eqn.(4.5) it can be seen that

$$[K^*_{ij}] = [L^i]^T[K_{ij}][L^j] \tag{4.10}$$

this form is efficient for programming.

In panelized structures many panels are of the same size and orientation, consequently, a large number of elements which idealize these panels possess identical transformed stiffness matrices. It is then necessary to generate stiffness matrices only for dissimilar elements, by this way substantial saving of computer time is achieved.

4.10 ASSEMBLY OF STRUCTURE STIFFNESS MATRIX

Once the stiffness matrices of all individual elements are calculated in the common coordinate system, the structure stiffness matrix is assembled by direct summation of the stiffness contributions of all elements, considering one element at a time. At this stage, zero-displacement boundary conditions may be introduced by not setting up those equations corresponding to the restrained directions. This allows saving of computer storage and solution time.

The structure stiffness matrix thus formed is symmetric and banded, it is necessary to store only the coefficients within the band of one triangle of the matrix.

4.11 BOUNDARY CONDITIONS AND SOLUTIONS

Zero-displacement boundary conditions may be conveniently treated as mentioned above, alternatively they may be handled in the same manner as for prescribed non-zero displacements. The method is described in Ref. [30]. It consists of multiplying the corresponding diagonal term in [K] by a large number, and replacing the load coefficients by the previous product multiplied by the prescribed displacement value. The modified system of equation still remains well-conditioned.

The introduction of external nodal forces presents no particular difficulty, the resulting set of equations is solved for the displacements using Gauss' elimination technique.

4.12 DETERMINATION OF STRESSES AND STRAINS

The element nodal displacements $\{q_*\}$ may be extracted from the structure nodal displacements $\{r\}$, they are further transformed into element axis-system using eqn. (4.8).

$$\{q\} = [L]\{q_*\} \quad \text{or} \quad \{q^i\} = [L^i]\{q_*^i\}$$

Rearranging $\{q\}$ into displacements corresponding to membrane and bending actions, and applying eqn. (3.37) to obtain the resultant moments, shearing forces and membrane stresses at all desired points. Stresses due to bending action are calculated from eqns. (2.2), they are superimposed with those due to in-plane deformations to obtain the final stresses. Strains in the faces are given by eqn. (3.23).

Stresses and strains thus obtained refer to the directions in local axes, principal stresses and strains are easily calculated from them.

4.13 COMPUTER PROGRAM

A large-capacity computer program was written using the matrix stiffness method incorporating the ideas explained in the previous sections. The program was divided into three links, the output of each link being stored in auxiliary storage and used as input for the next one.

The first link of the program generates the transformed element stiffness matrices. The second link assembles the structure stiffness matrix and solves for the unknown

displacements using Gauss' elimination technique. The third link calculates stresses and strains in all specified elements. Theoretically the program can solve an unlimited number of equations regardless of the size of the minimum half bandwidth.

The program was written in FØRTRAN and run on a CDC 6600 computer. All necessary arrays are allocated compactly and dynamically at execution stage, hence storage space is efficiently used. Listing of the programs is not given here for brevity. Several important features of the program are listed below:

1. The idealized structure may consist of rectangular or triangular elements or combination of both. Line elements may be introduced to simulate edge beams.

2. The joints may be rigid or hinged. Rigid body movement of a certain portion of the structure may be imposed.

3. Plate bending or plane stress problems for both isotropic and sandwich materials are analyzed efficiently in terms of input data, as well as computations.

4. The size of the structure and number of load cases are not restricted, however the total amount of data that can be efficiently handled is limited.

5. Regular mesh of rectangular or triangular elements is

automatically generated.

6 Output consists of displacements at the mesh points, moment resultants and stresses and strains in both faces of the sandwich material.

7 The organization of the program is in modular form. Introduction of new elements or modification of the program can be done with relative ease.

CHAPTER V

APPLICATION TO THE BENDING OF SANDWICH PLATES

5.1 CONVERGENCE OF THE SOLUTIONS OBTAINED BY THE RECTANGULAR SANDWICH PLATE ELEMENT

In this Chapter, the proposed finite element models are applied to selected sandwich plate bending problems. Results are compared to theoretical solutions to test the applicability of the models in predicting the behaviour of sandwich plates, which are largely characterized by the shear deformations. It is convenient when investigating the bending of sandwich plates to introduce dimensionless parameter Sa^2/D, which will be referred to as the shear parameter. For a sandwich plate with infinite shear parameter, it is expected that the solutions will correspond to solutions obtained from thin plate theory. On the other hand, for a plate with flexible core, the shear parameter normally varies between 100 and 10.

The first sandwich plate problem considered is that of a simply supported square plate subjected to a uniform transverse load, the edges of the plate are stiffened so that no shear strains can occur. Series solution for this problem is given by Plantema. [11]

Because of the symmetry of the geometry and loading, only one quadrant of the plate needs to be analyzed. In the finite element idealization, the boundary conditions are approximated by the vanishing of the deflections and torsional rotations of points along the edges. The analysis is

commenced with 1 x 1 square mesh and increased to 6 x 6. Loads are lumped together at the node points according to the element tributary areas.

For comparison with the theoretical solutions as given in Ref. [11], non-dimensional parameters are calculated for the maximum deflection and bending moments, which occur at the plate center. The results are tabulated in Table 5.1 and shown graphically in Fig. 5.1. Rapid convergence of both deflection and stresses to the exact values are observed.

The percentage error of the calculated value given in Table 5.1 is computed as

$$\% \text{ error} = \frac{|\text{Calculated value}| - |\text{Theoretical value}|}{|\text{Theoretical value}|} \times 100$$

For the 1 x 1 mesh the percentage errors of the deflection and bending moments are respectively 18 and 12, the errors decrease sharply as finer meshes are used and reach 2 and 0.8% for a 6 x 6 mesh. From Fig. 5.1 and 5.2 the finite element solutions are seen to converge to the exact values from above. This means that the idealized structure is too flexible in this case.

The second example problem is a square clamped sandwich plate subjected to uniform pressure. Ref. [11] gives numerical results for a particular shear parameter $Sa^2/D = 4\pi^2$. The theoretical analysis assumes that the edge sections are free to deform in shear, this assumption

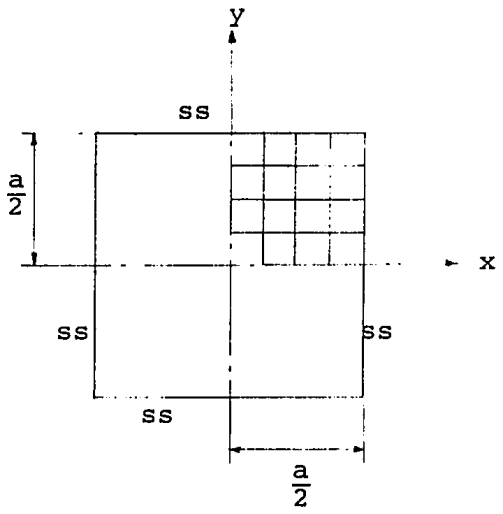

q = 1 lb/in^2

a = 120 in

t = 0.025 in

h = 1.975 in

E = 10^7 psi

G_c = 189 psi

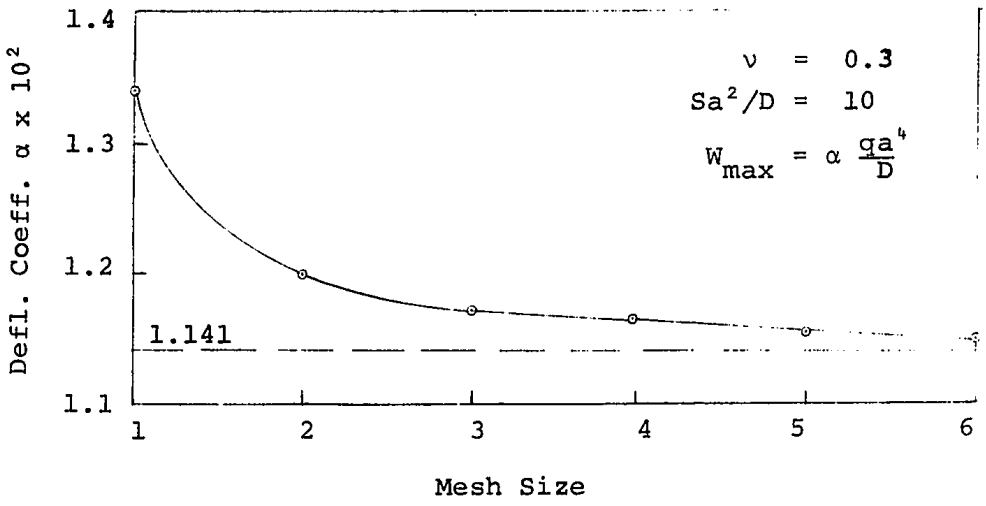

FIG. 5.1 CONVERGENCE OF MAXIMUM DEFLECTION. SIMPLY SUPPORTED SQUARE PLATE SUBJECTED TO UNIFORM LOAD

TABLE 5.1

SQUARE SIMPLY-SUPPORTED ISOTROPIC SANDWICH PLATE.SIMILAR FACES, UNIFORM LOAD.

$Sa^2/D = 10$ $\nu = 0.3$

Mesh Size	Deflection at Center		Moments at Center	
	F.E.	% Error	F.E.	% Error
1 x 1	1.340	18	5.58	12
2 x 2	1.203	5.3	5.11	6.5
3 x 3	1.178	3.2	4.94	2.9
4 x 4	1.170	2.6	4.87	1.7
5 x 5	1.166	2.2	4.84	1.0
6 x 6	1.164	2.0	4.83	0.8
Exact(11)	1.141	-	4.79	-
Multi-plier	$10^{-2}\ \frac{qa^4}{D}$		$10^{-2}\ qa^2$	

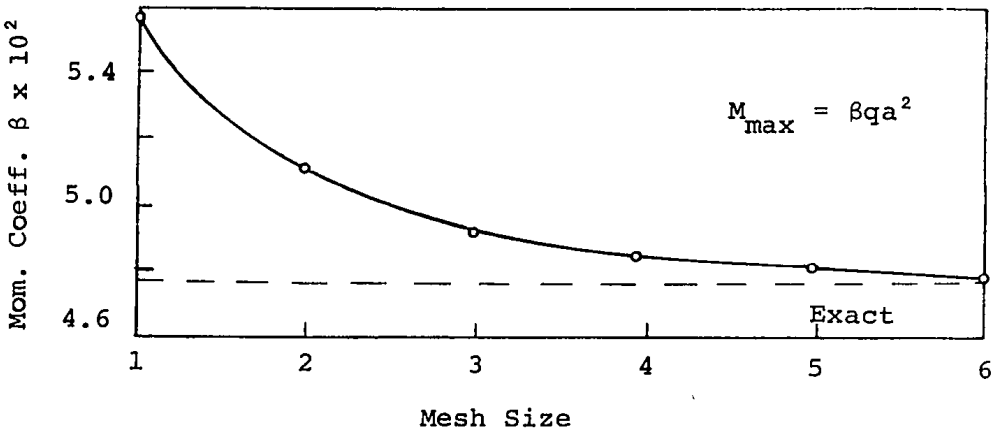

FIG. 5.2 CONVERGENCE OF MAXIMUM MOMENT. SIMPLY SUPPORTED SQUARE PLATE SUBJECTED TO UNIFORM LOAD

is not realistic, however it is claimed [11] that the more realistic one of zero shear strain along the edges would give substantially the same results. In the finite element analysis, the deflection and normal rotation of points along the clamped edges are taken to be zero.

In Fig. 5.3 the central deflection obtained by finite element method is plotted against the number of elements used per half span. For the 1 x 1 mesh the error is 12%, which is then reduced to 2.1 with the finest mesh used. The maximum bending moment occurs at the middle of the edges. Convergence of the finite element results can be seen in Fig. 5.4. Table 5.2 gives numerical values.

5.2 INFLUENCE OF TRANSVERSE SHEAR DEFORMATION

In the classical thin-plate theory, the effect of transverse shear deformation is neglected; however, for sandwich construction, appreciable deflection may result due to transverse shear stresses in the weak core. Moreover, because of this additional deformation, the magnitude and distribution of the stresses in the plate will in general be different from those predicted by the customary thin-plate theory.

To study the influence of the transverse shears in sandwich construction, two sandwich plate problems are considered. Both plates are of rectangular shape, uniformly loaded, but one with simply-supported edges and the other

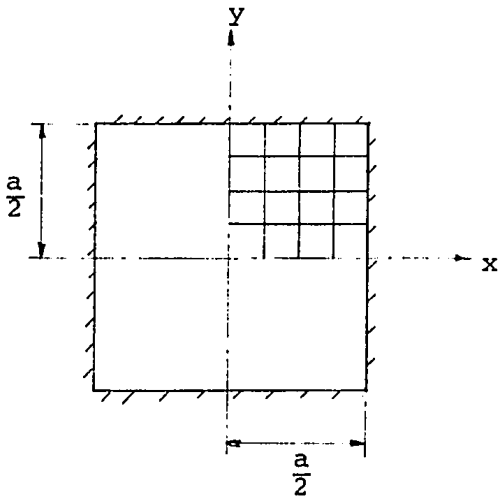

$q = 1\ lb/in^2$

$a = 120$ in

$t = 0.025$ in

$h = 1.975$ in

$E = 10^7$ psi

$\nu = 0.3$

$G_c = 744.$ psi

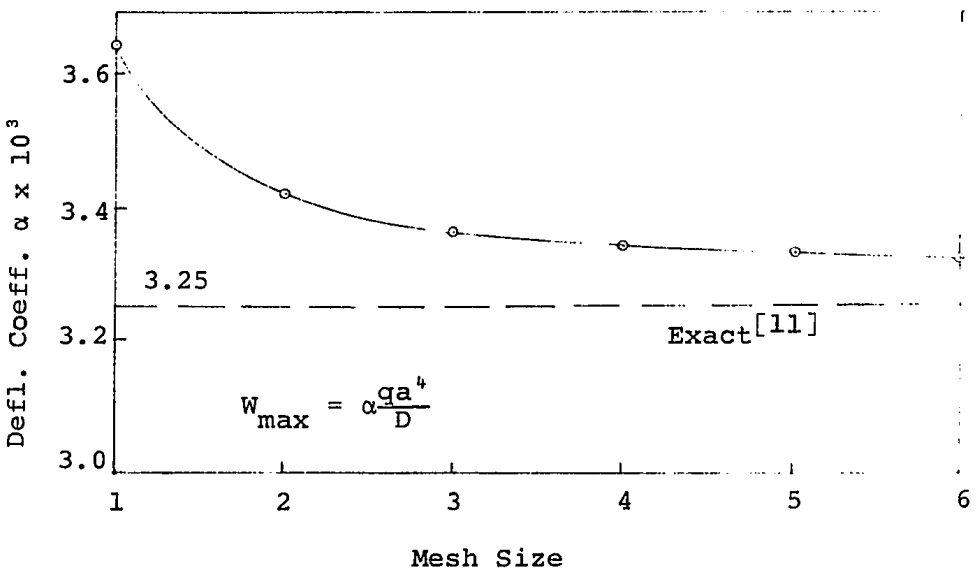

FIG. 5.3 CONVERGENCE OF MAXIMUM DEFLECTION. CLAMPED SQUARE PLATE SUBJECTED TO UNIFORM LOAD

TABLE 5.2

SQUARE CLAMPED ISOTROPIC SANDWICH PLATE
UNIFORM LOAD, SIMILAR FACES.

$Sa^2/D = 4\pi^2 \qquad \nu = 0.3$

Mesh Size	Deflection at Center		Maximum Negative Moments	
	F.E.	% Error	F.E.	% Error
1 x 1	3.64	12	2.34	-43
2 x 2	3.42	5.2	3.64	-11
3 x 3	3.36	3.4	3.94	-3.9
4 x 4	3.34	2.8	4.09	-0.2
5 x 5	3.33	2.5	4.18	2.0
6 x 6	3.32	2.1	4.20	2.4
Exact[11]	3.25	-	4.10	-
Multi-plier	10^{-3} qa^4		10^{-2} qa^2	

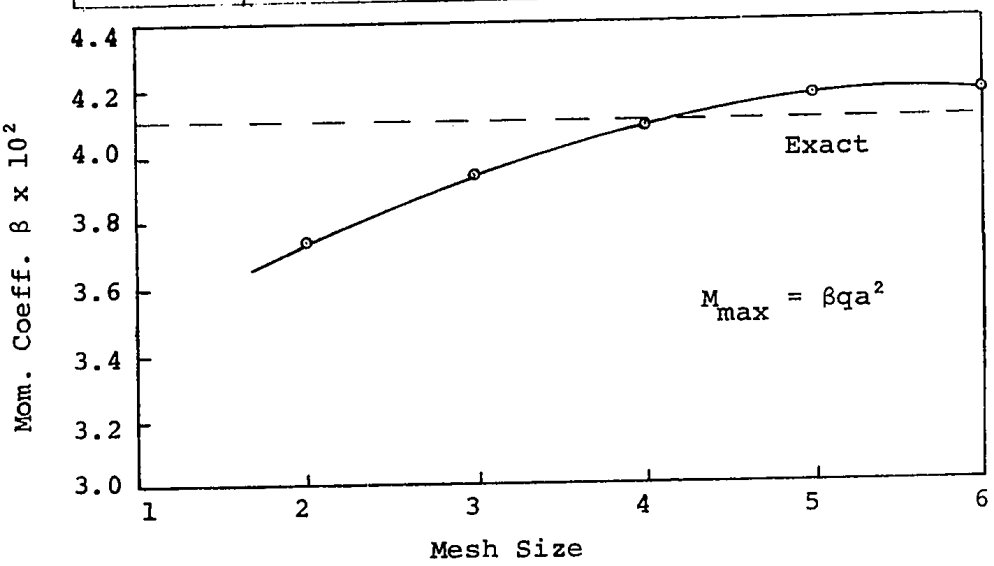

FIG. 5.4 CONVERGENCE OF MAXIMUM MOMENT.
CLAMPED SQUARE PLATE. UNIFORM LOAD

with edges clamped; edge shear strains are prevented in the former but not in the latter.

Plantema [11] showed that, in a simply-supported plate subjected to uniform load, the stress resultants are independent of the transverse shear stiffness, and hence identical to those given by the ordinary plate theory. The deflection is equal to that of a rigid-shear plate plus an additional deflection due to shear strains in the core. This shear deflection is inversely proportional to the shear stiffness. Graphically, these are shown in Fig.5.5 and 5.6, where the finite element results are obtained with a 4 x 4 idealization of a quadrant of the plate.

The finite element solutions are in good agreement with the theoretical values for all aspect ratios and shearing rigidities considered. As can be seen in Fig. 5.5, the additional deflection due to transverse shear may be well over 100%. In a square plate, this increase in deflection is found to be 180% for a shear parameter $Sa^2/D = 10$. The increase is 220% for a 2 x 1 plate of the same shear stiffness.

Although deflection in a simply supported sandwich plate is substantially increased because of the transverse shear deformations, the stresses remain unchanged. The maximum moments plotted in Fig. 5.6 are valid for all shear rigidities, the moments found by finite element method show very little variation over a wide range of the shearing stiffnesses used; in most cases the variation is within 1% of

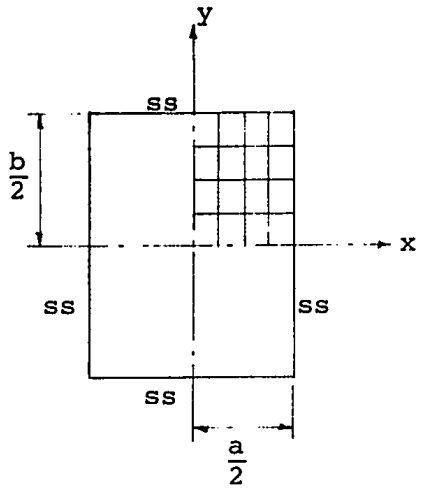

$q = 1\ lb/in^2$

$a = 120$ in

$t = 0.025$ in

$h = 1.975$ in

$E = 10^7$ psi

$\nu = 0.3$

b and G_c vary

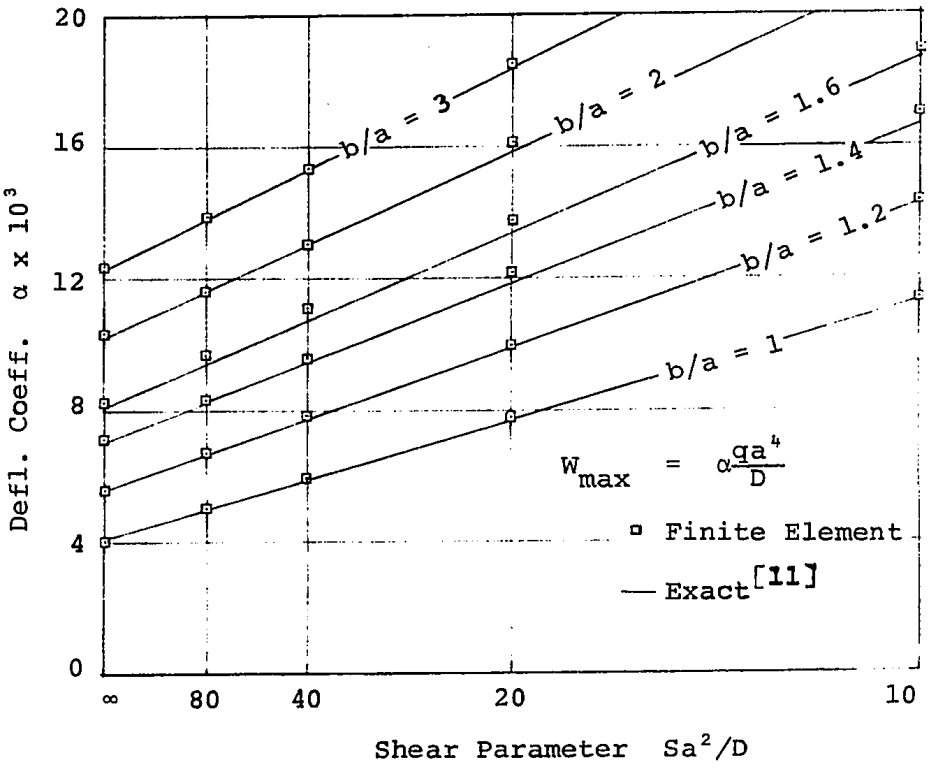

FIG. 5.5 INFLUENCE OF TRANSVERSE SHEARS ON THE MAXIMUM DEFLECTION OF SIMPLY-SUPPORTED PLATES SUBJECTED TO UNIFORM LOAD

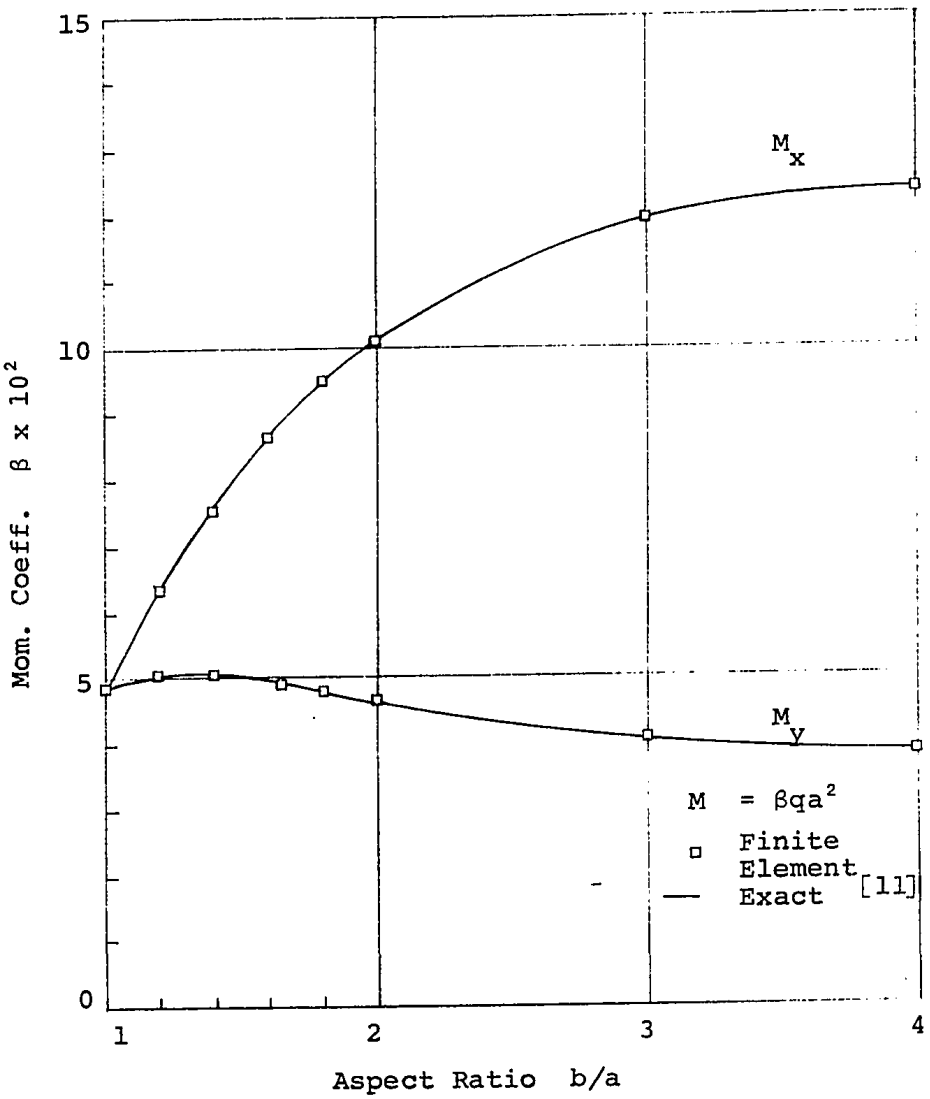

FIG. 5.6 MAXIMUM MOMENTS FOR ALL SHEAR STIFFNESSES. SIMPLY SUPPORTED PLATE, UNIFORM LOAD

the theoretical values.

Figs. 5.7 and 5.8 show similar graphs for the case of clamped plates. Theoretical results are not available for comparison except when the plate has rigid shear and results from classical thin-plate theory are used. Additional deflection due to transverse shear deformation is again inversely proportional to the shear rigidity. The influence of transverse shear on the deflection of clamped plates is much more pronounced than in the case of simply-supported plates; for example, the additional deflection at the center of a square plate is 700% in a clamped plate but only 180% in simply supported plates (shear parameter Sa^2/D equal to 10 in both cases).

Unlike the case of simply-supported plate, stresses in clamped plate are reduced due to shear deformation, the relieving effect is not great,as can be seen in Fig. 5.8. The reduction in the maximum negative moment is approximately 20% for plates having a shear parameter of 10. The variation of the maximum moment in the longer span (i.e. M_y) is rather peculiar and unexpected. For plates having low aspect ratio the reduction of M_y is monotonic (see Fig. 5.9) but not so when the aspect ratio is greater or equal to 1.6.

5.3 CONVERGENCE OF THE SOLUTIONS OBTAINED BY THE RIGHT-ANGLED TRIANGULAR SANDWICH PLATE ELEMENT

To study the convergence characteristics of the right-

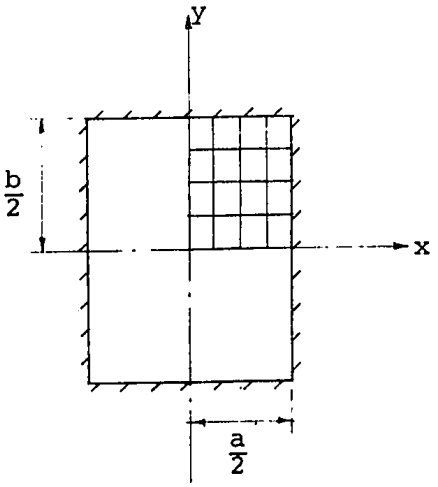

$q = 1\ lb/in^2$

$a = 120$ in

$t = 0.025$ in

$h = 1.975$ in

$E = 10^7$ psi

$\nu = 0.3$

G_c and b vary

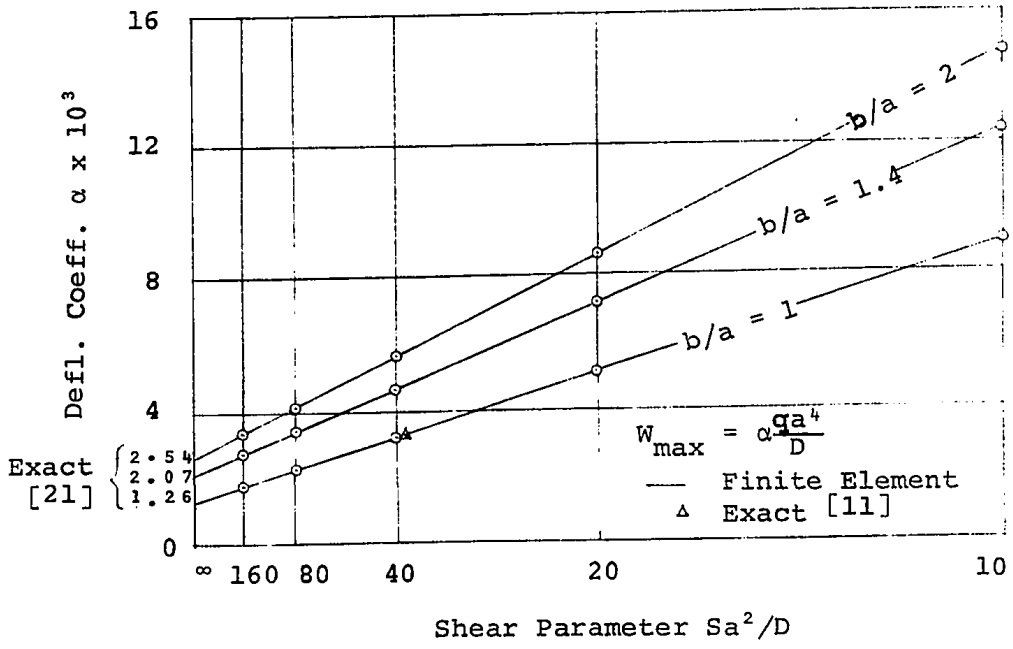

FIG. 5.7 INFLUENCE OF TRANSVERSE SHEARS ON THE DEFLECTION OF CLAMPED PLATES SUBJECTED TO UNIFORM LOAD

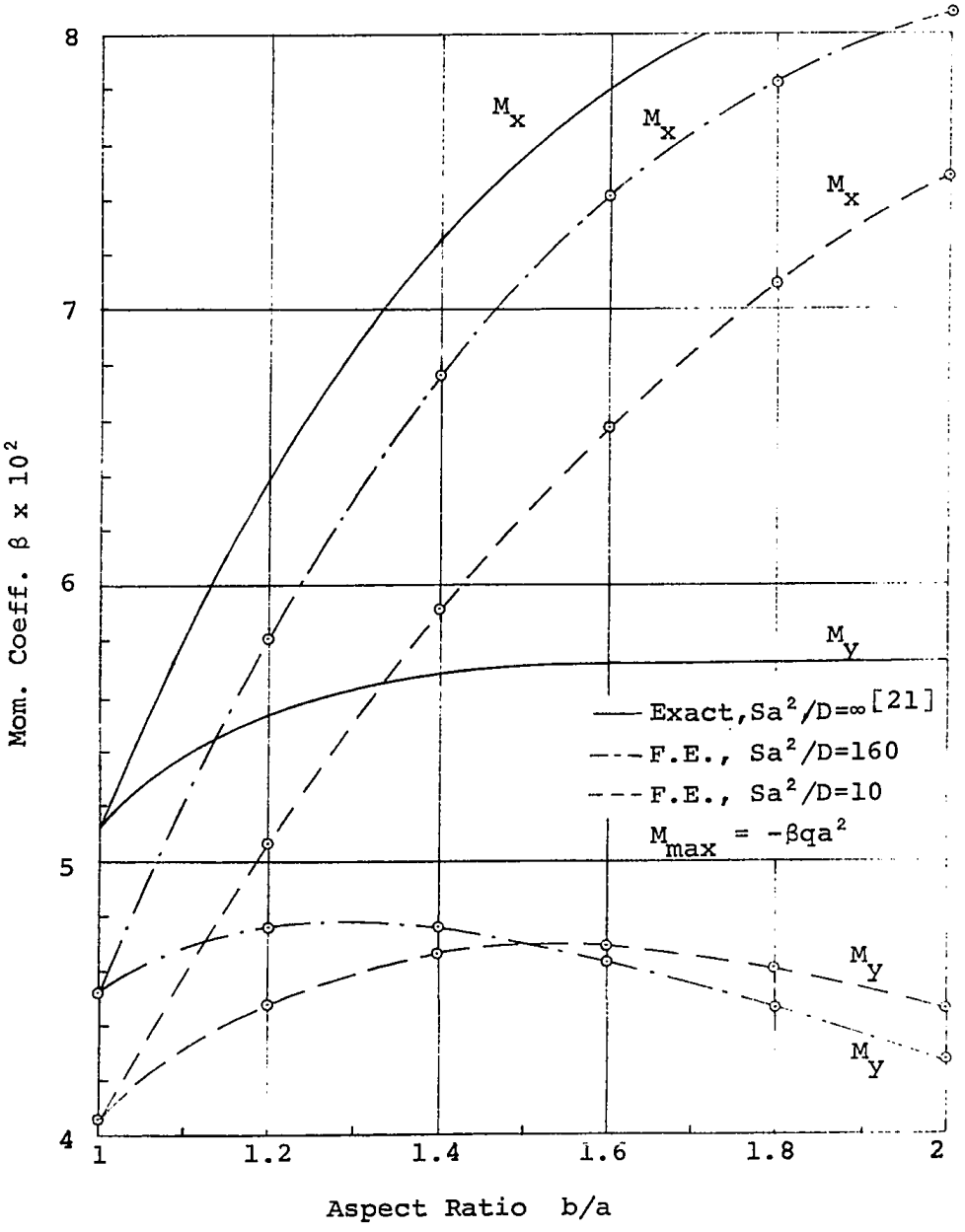

FIG. 5.8 INFLUENCE OF TRANSVERSE SHEARS ON THE MAXIMUM STRESSES IN CLAMPED PLATE SUBJECTED TO UNIFORM LOAD

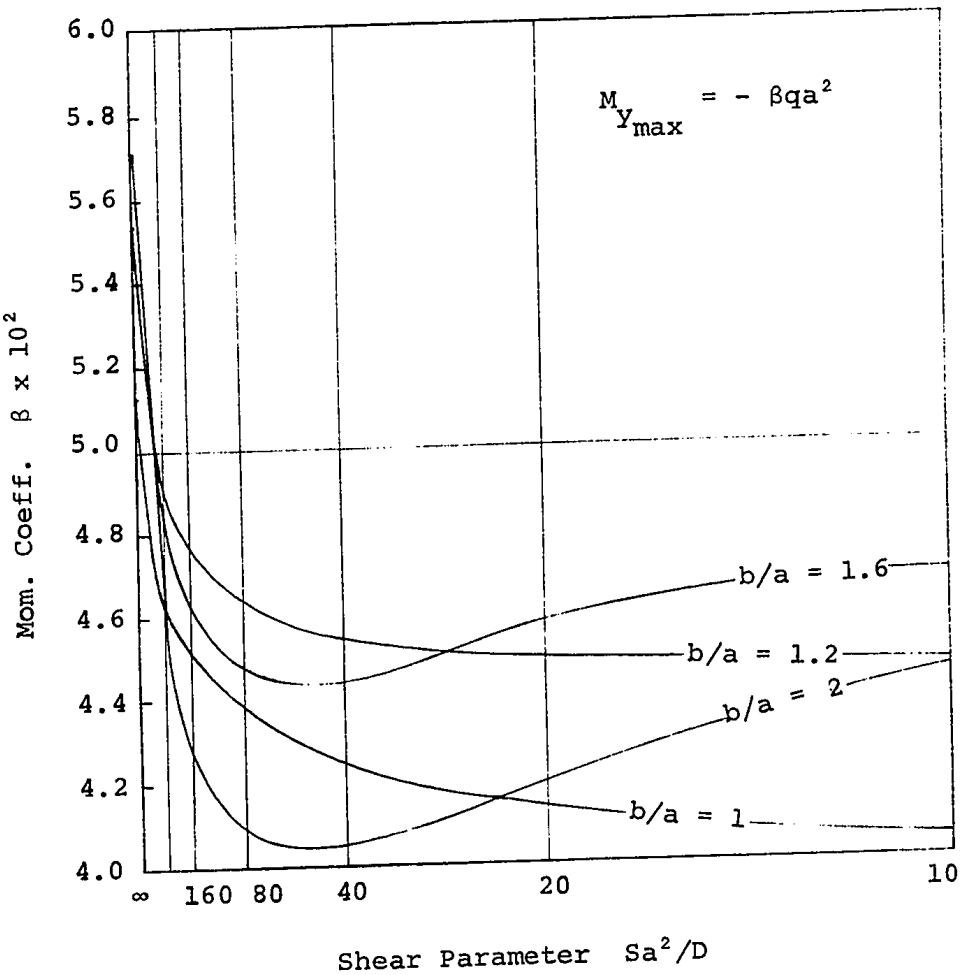

FIG. 5.9 INFLUENCE OF TRANSVERSE SHEAR ON MAXIMUM MOMENT M_y IN CLAMPED PLATE - UNIFORM PRESSURE

angled triangular elements the two square plates used previously for the rectangular element are analyzed. The finite element idealizations for the plates are shown in Fig. 5.10, in which the numbers of square units per half span are 1, 2, 4 and 6. The number of triangular elements used is twice the corresponding number of square elements, although the total number of degrees of freedom remains the same.

Numerical values of the maximum deflection and moments obtained by using four different mesh sizes are given in Table 5.3 for the simply supported plate, and in Table 5.4 for the clamped plate. The results appear to converge to the exact solutions, although the calculated deflections oscillate about the exact value. It is interesting to compare these results with those obtained by using the rectangular elements (Tables 5.1 and 5.2); the deflection seems to converge slightly faster in the triangular element case, whereas the stresses converge at a much slower rate.

5.4 ANALYSIS OF ORTHOTROPIC SANDWICH PLATES

The problems discussed so far, are for plates having both isotropic facings and isotropic cores. The overall orthotropy of a sandwich plate is usually due to the orthotropic properties of the materials used for the faces or the core, or both. However, in many applications the orthotropy derives solely from the geometry of construction of the core.

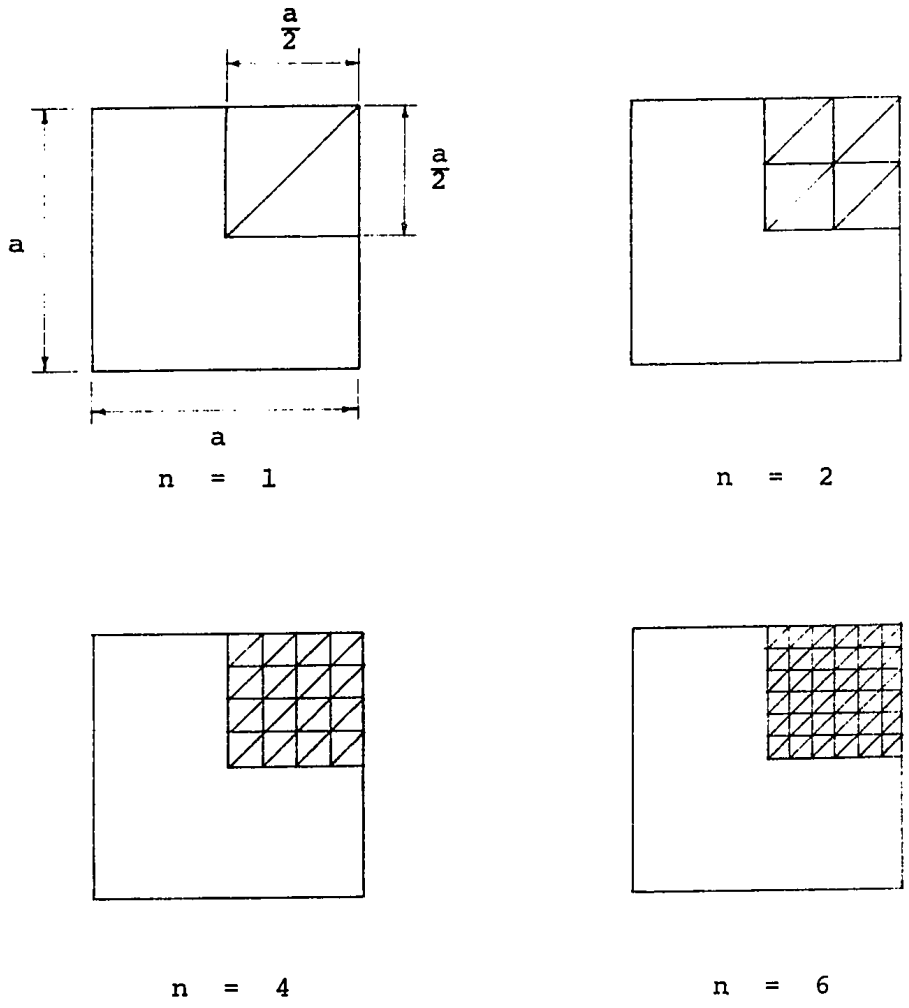

FIG. 5.10 IDEALIZATION OF A SQUARE PLATE USING TRIANGULAR ELEMENTS

TABLE 5.3

SQUARE SIMPLY-SUPPORTED ISOTROPIC SANDWICH PLATE.SIMILAR FACES, UNIFORM LOAD

$Sa^2/D = 10 \qquad \nu = 0.3$

Mesh Size, n	Deflection at Center		Moments at Center	
	F.E.	% Error	F.E.	% Error
1	1.059	-8.6	1.86	-61
2	1.143	0.0	3.78	-21
4	1.165	2.0	4.56	-4.8
6	1.166	2.2	4.69	-2.1
Exact[11]	1.141	-	4.79	-
Multi-plier	$10^{-2}q\frac{a^4}{D}$		$10^{-2}qa^2$	

TABLE 5.4

SQUARE CLAMPED ISOTROPIC SANDWICH PLATE SIMILAR FACES, UNIFORM LOAD

$Sa^2/D = 4\pi^2 \qquad \nu = 0.3$

Mesh Size, n	Deflection at Center		Maximum Negative Moments	
	F.E.	% Error	F.E.	% Error
1	2.64	-4.9	1.29	-65
2	3.26	-0.3	2.84	-31
4	3.27	0.6	3.36	-18
6	3.28	0.9	3.75	-8.5
Exact[11]	3.25	-	4.10	-
Multi-plier	$10^{-3}qa^4/D$		$10^{-2}\ qa^2$	

To-date, there exists very few published results for bending of orthotropic sandwich plates. Raville [32] has obtained a series solution for simply-supported plates having isotropic facings and orthotropic core subjected to uniform loading. Basu and Dawson [33] and Folie [34] have used numerical methods to solve the general governing equations of orthotropic sandwich plates. Numerical results for square clamped plates under uniform pressure are given in the paper by Folie.

In Table 5.5 a selection of Raville's results are compared to those obtained by the finite element method using an 8 x 8 rectangular mesh to solve a quadrant of the plate. For the finite element solutions, the plate properties are assumed as follows:

Plate dimensions in x,y directions 24" x 32"
Core and facing thicknesses 2.0" and 0.001"
Facing material properties $E = 10^7$ psi, $\nu = 0.3$
Core shear modulus $G_{yz} = 114$ psi; and
$G_{xz}/G_{yz} = 0.4, 1.0, 2.5$.

There is good agreement between the two sets of results for the deflection and moments, but shear forces calculated by the finite element method are generally 10% too low. Inspection of Table 5.5 shows that the transverse shear stiffness has a great influence on the load distribution in the plate. When the shearing rigidities are the same in both

TABLE 5.5

SIMPLY-SUPPORTED ORTHOTROPIC SANDWICH PLATE UNDER UNIFORM LOAD

$D_x = D_y = D$, $b/a = 4/3$, $\nu = 0.3$, $S_y a^2 D = \pi^2/1.648$

Maximum Value	$S_x = 2.5\ S_y$		$S_x = S_y$		$S_x = 0.4\ S_y$	
	F.E.	Raville	F.E.	Raville	F.E.	Raville
$\frac{wD}{qa^4}$ (a)	0.0154	0.0147	0.0220	0.0209	0.0347	0.0325
$\frac{M_x}{qa^2}$ (a)	0.0854	0.0842	0.0718	0.0713	0.0459	0.0473
$\frac{M_y}{qa^2}$ (a)	0.0370	0.0375	0.0506	0.0502	0.0766	0.0745
$\frac{Q_x}{qa}$ (b)	0.396	0.425	0.0372	0.401	0.315	0.349
$\frac{Q_y}{qa}$ (c)	0.270	0.302	0.0320	0.358	0.400	0.434

(a) at plate center; (b) at middle of short edge; (c) at middle of long edge

directions, the shorter span carries a greater share of the load as can be expected. For this particular plate the maximum moment in the short span is 1.4 times that in the long direction; if the shearing rigidity in the short span is reduced to 40% of its original value, the maximum moment in this span is now equal to only 60% of the maximum value in the long direction.

A series of graphs are presented in Appendix C showing the maximum deflections and stresses in square orthotropic sandwich plates subjected to uniform loading. Two edge conditions are considered: simply-supported and clamped. Because of the scarcity of published results, these graphs should be of value to the designers.

CHAPTER VI

APPLICATION TO THE ANALYSIS OF FOLDED SANDWICH PLATES

6.1 INTRODUCTION

In the previous Chapter, various problems of bending of flat sandwich plates have been considered; in this Chapter examples of the application of the finite element method to problems of sandwich folded plates are described. The results of the analysis of two sandwich folded plates will be compared to experimental data taken from Ref. [37]

Since the stresses in folded plates are caused by bending and membrane actions, the complete element stiffness matrix which includes both types of action must be used. Along the intersection of the panels which make up the folded plate, continuity of displacements and normal slopes should be maintained; these compatibility requirements are satisfied completely by the elements developed in Chapter III. Furthermore, since the elements possess only geometrical degrees of freedom such as displacements and rotations, no difficulties arise due to the transformation of the generalized forces and displacements along the junctions. Several assumptions adopted by most existing theories of folded plates are not necessary in finite element methods; there would be no difficulty in taking into account the flexibility of the diaphragms, as well as other features such as material orthotropy, variable thickness, cut-outs, etc.

6.2 9.5 FOOT FOLDED PLATE-COMPARISON BETWEEN FINITE ELEMENT SOLUTIONS AND EXPERIMENTAL RESULTS

The first of the two folded plates to be considered is shown in Fig. 6.1. It consists of six similar sandwich panels rigidly connected by means of aluminum channels, which were welded together at four inch intervals. These channels were not used at the two outside longitudinal ridges, hence these ridges are free to deform. The panels were made up with 0.025 in thick aluminum facings bonded to one inch thick honeycomb core. Details of the connections and test procedure are fully reported in Ref. [37].

For the finite element analysis, rectangular elements and beam elements are used to idealize the panels and the reinforcing channels respectively. One half of the plate is divided into a rectangular mesh of 18 x 6, the first number refers to the number of transverse subdivisions and the second to the number of longitudinal subdivisions from diaphragm to midspan.

Figs.6.2 to 6.5 show the results obtained for the folded plate subjected to uniform line loads of 24 lb/ft at ridges 2 to 6 inclusive. A study of the results indicates that the displacements obtained from the finite element solution agree remarkably well with the experimental data. Whereas, the stresses are overestimated by the finite element method, the greatest differences are found at the inner ridges. Stresses in the top facing are generally higher than

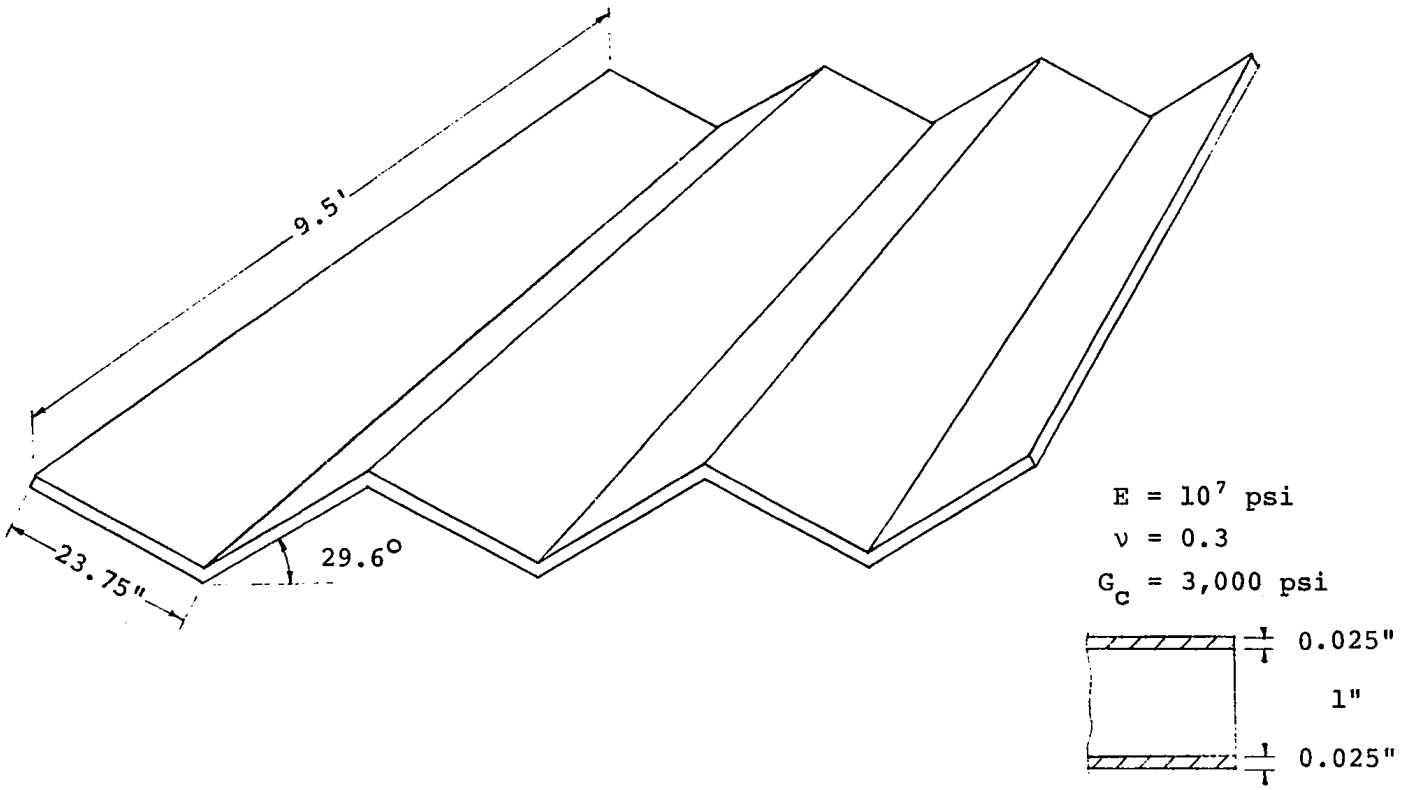

FIG. 6.1 THE 9.5 FOOT FOLDED SANDWICH PLATE.
ALUMINUM FACINGS, PAPER HONEYCOMB CORE

those in the bottom, the difference in magnitude indicates the influence of the slab action of the plates; for this example, the contribution by bending stresses to the total stresses is less than 12%. The longitudinal stresses, as well as the deflection vary linearly over the width of the plates, as can be expected since the plate length-to-width ratio of 4.25 is high.

Fig. 6.5 shows the deflection of the folded plate loaded uniformly at ridge 3; since the loading was not symmetrical, torsional effects were present. Again, the finite element solutions compare favorably with the experimental results. Stresses are not shown for this case because they were not reported in Ref. [37].

6.3 19-FOOT FOLDED PLATE-COMPARISON BETWEEN FINITE ELEMENT SOLUTIONS AND EXPERIMENTAL RESULTS

This sandwich folded plate has similar geometry to the previous one (Fig. 6.6). The core was made of polystyrene foam, which has much lower shear rigidity than honeycomb core. The panels were connected by the same type of channel sections, which were also used to stiffen the longitudinal outside edges.

Because the plate length-to-width ratio of this folded plate is more than twice that of the previous one, longitudinal stresses and deflections are expected to vary even more linearly over the plate width. Consequently, a coarse mesh of 6 x 10 was thought to be sufficient for the

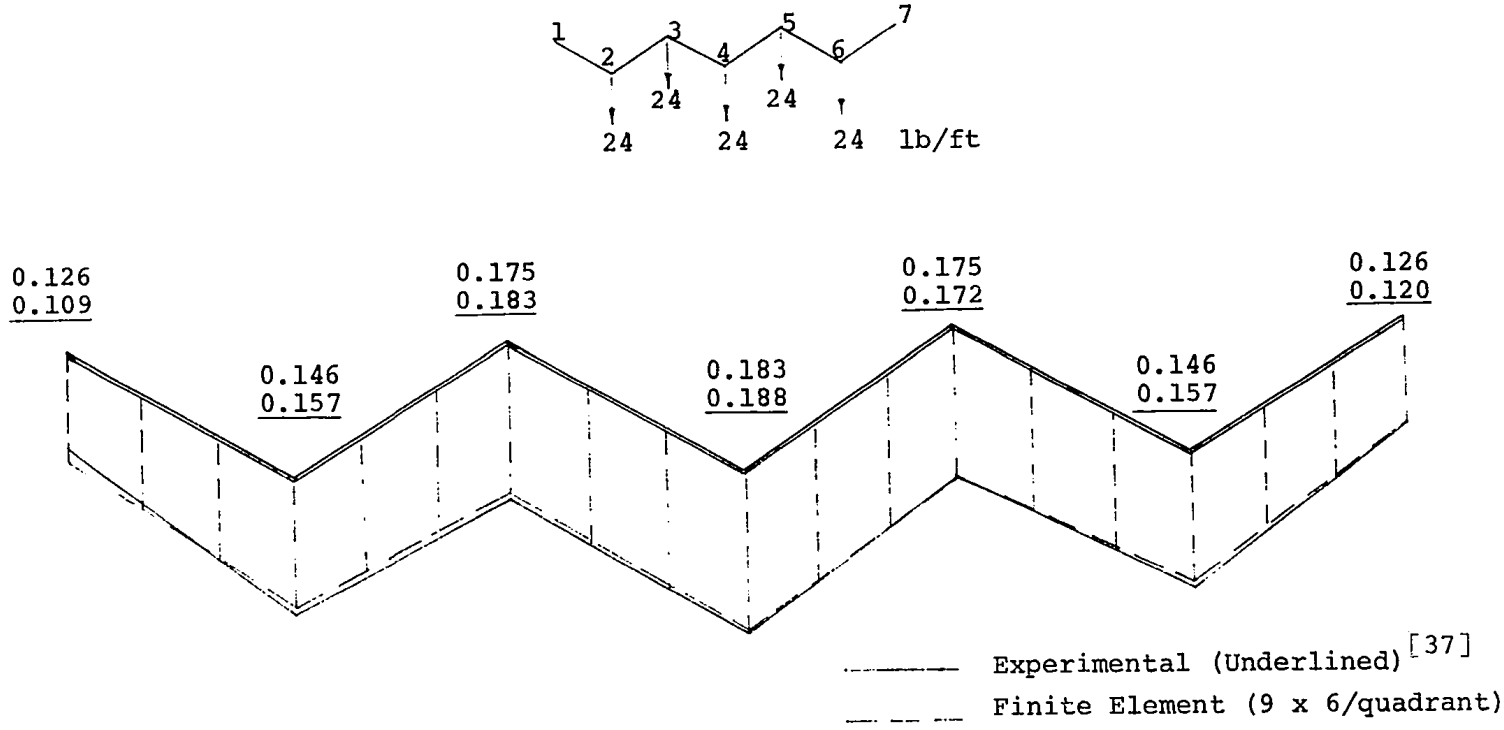

FIG. 6.2 DEFLECTION (INCHES) AT MID-SPAN OF 9.5 FOOT FOLDED PLATE. RIDGES 2,3,4,5,6 LOADED UNIFORMLY WITH 24 LB/FT

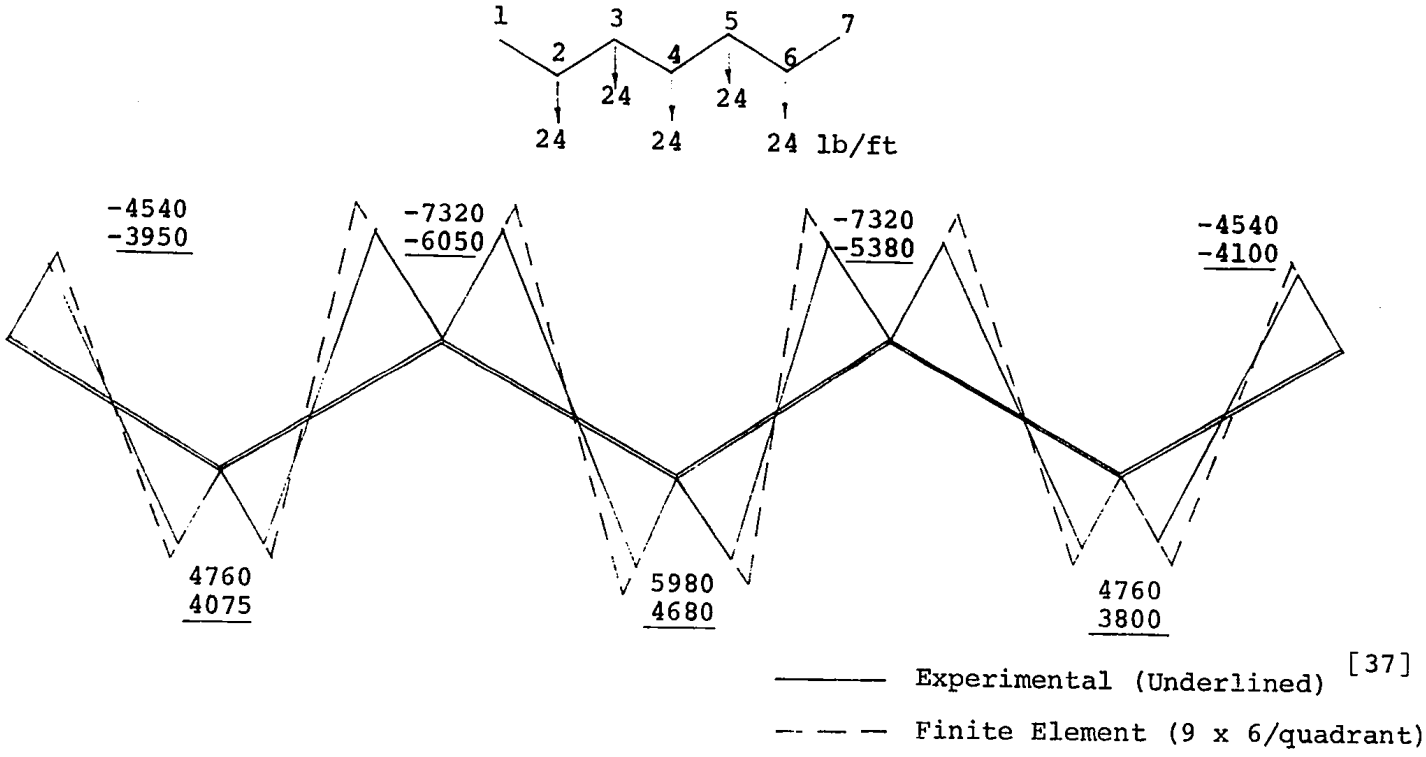

FIG. 6.3 LONGITUDINAL STRESSES (PSI) IN TOP FACING AT MID-SPAN SECTION OF THE 9.5 FOOT FOLDED PLATE

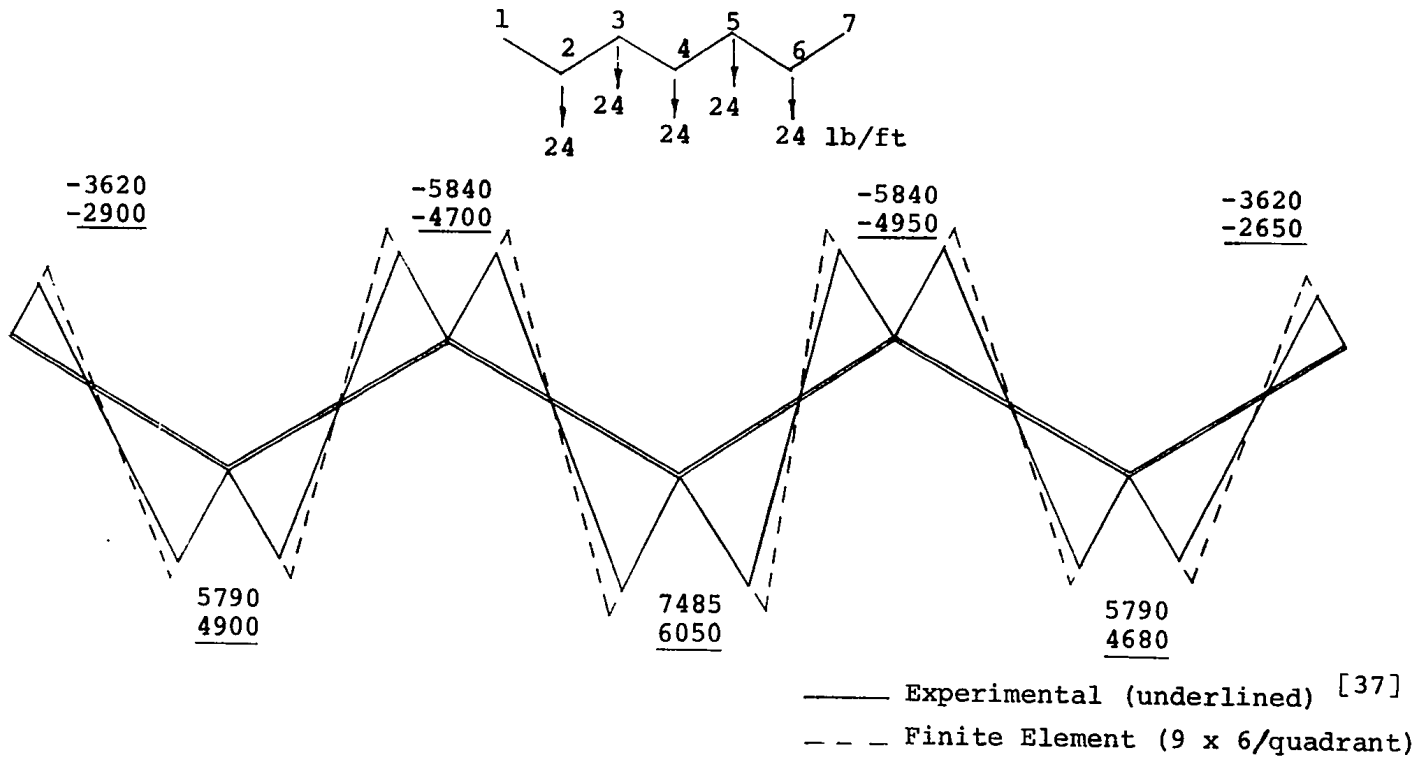

FIG. 6.4 LONGITUDINAL STRESSES (PSI) IN BOTTOM FACING AT MID-SPAN SECTION OF THE 9.5 FOOT FOLDED PLATE

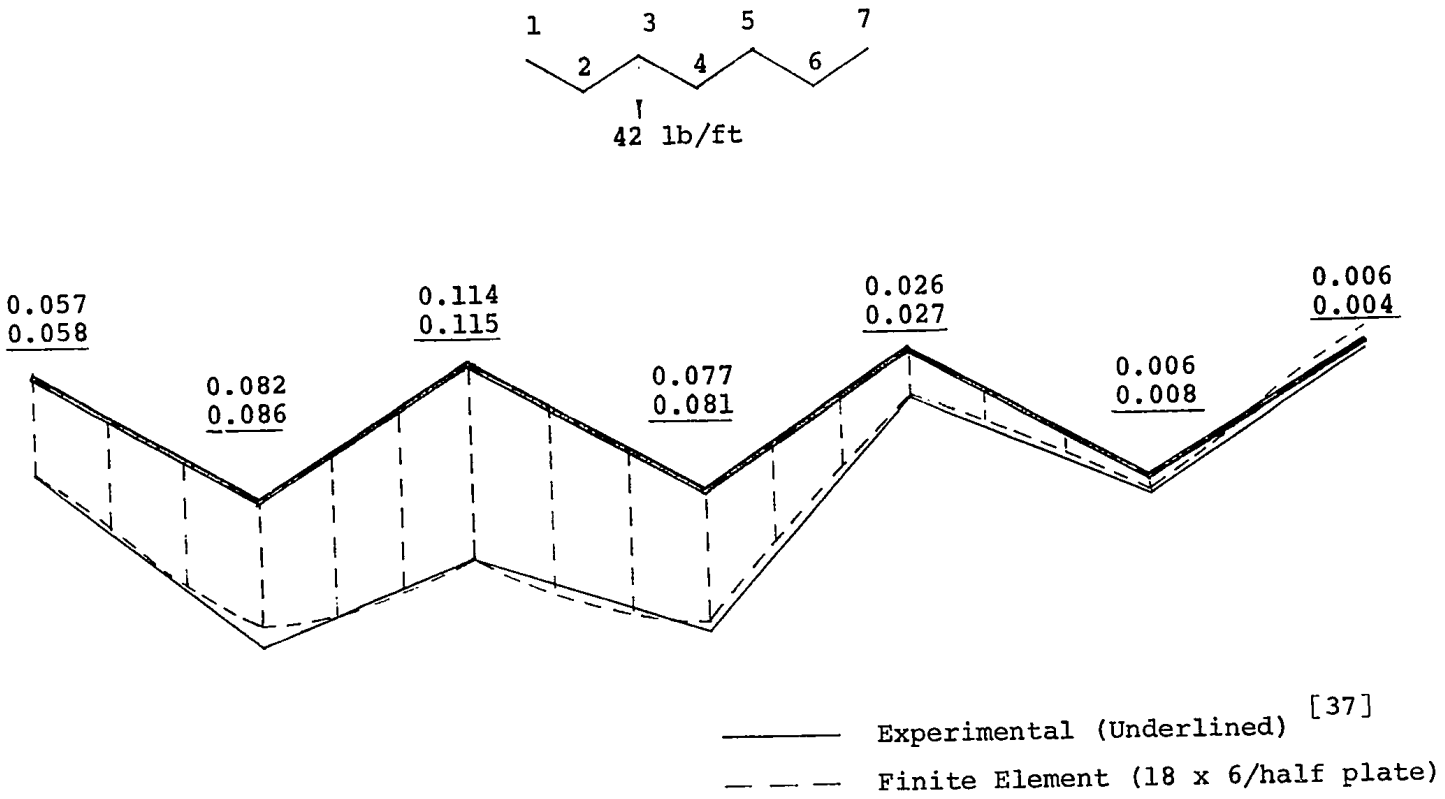

FIG. 6.5 DEFLECTION (INCHES) AT MID-SPAN OF 9.5 FOOT FOLDED PLATE. RIDGE 3 UNIFORMLY LOADED WITH 42 LB/FT

whole structure.

Figs.6.7 to 6.9 show the results obtained for the case of uniform surface pressure acting over the entire plate. Good agreement between finite element solutions and experimental results are observed for both displacements and stresses.

The deflections along the mid-span section of the folded plate are plotted in Fig. 6.10, the plate in this case was supported by a column placed on ridge 3 at 2 ft away from the mid-span. Reaction on the column was measured by a load cell and equal to 1,800 lbs.[37] This load is considered as external forces in the finite element analysis in order to eliminate the effect of column deformation, which is in fact, negligible as indicated by the theoretical results. The percentage difference between the two sets of displacements varies from 27% at one outside edge to 8% at another. The effect of the column is to reduce the stresses and deflections in the adjacent panels; however, at the immediate vicinity of the column high stress concentration would undoubtedly occur. This effect could be further studied by finite element analysis, however, this was not done because of the lack of experimental data for comparison.

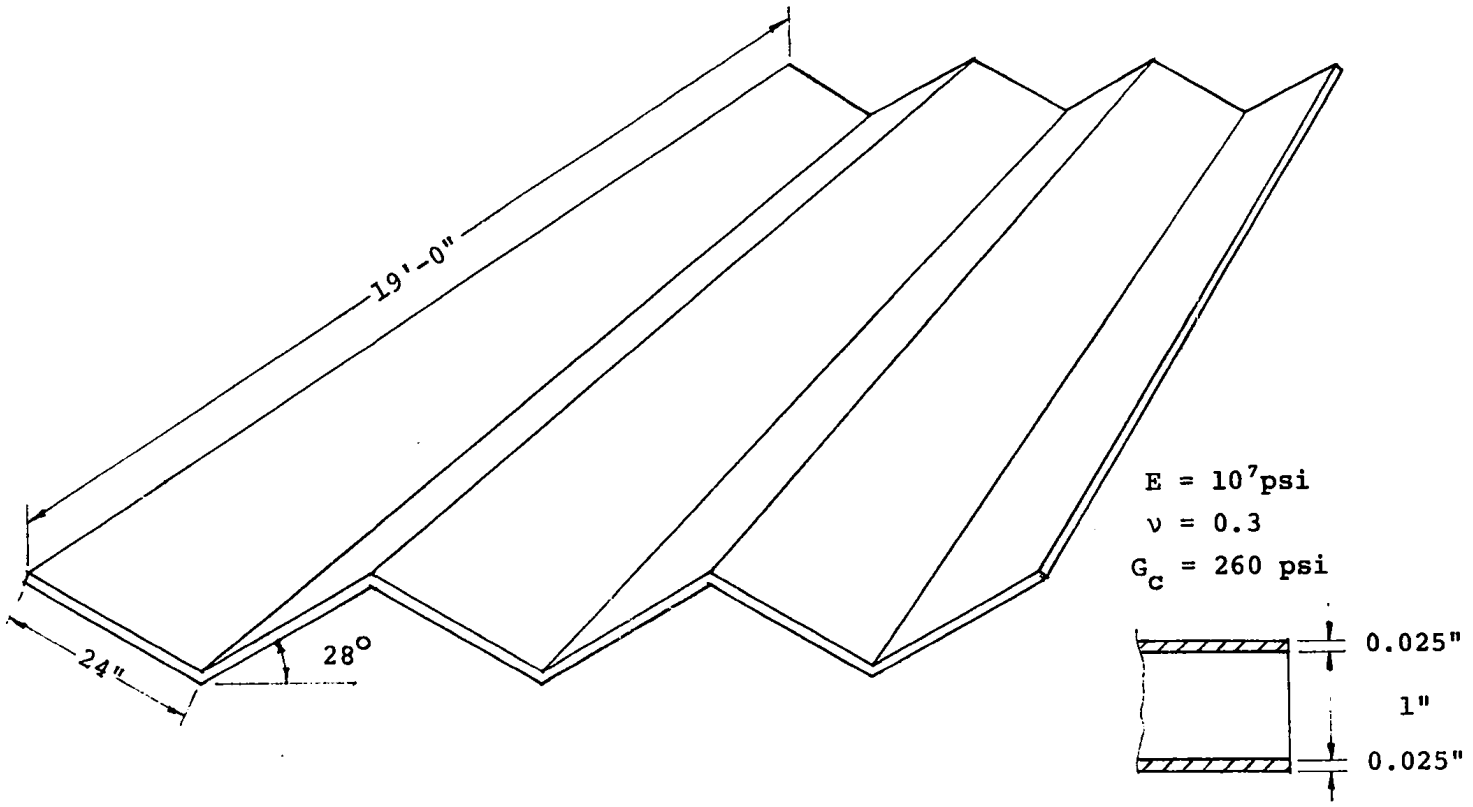

FIG. 6.6 THE 19 FOOT FOLDED SANDWICH PLATE.
ALUMINUM FACINGS, POLYSTYRENE CORE

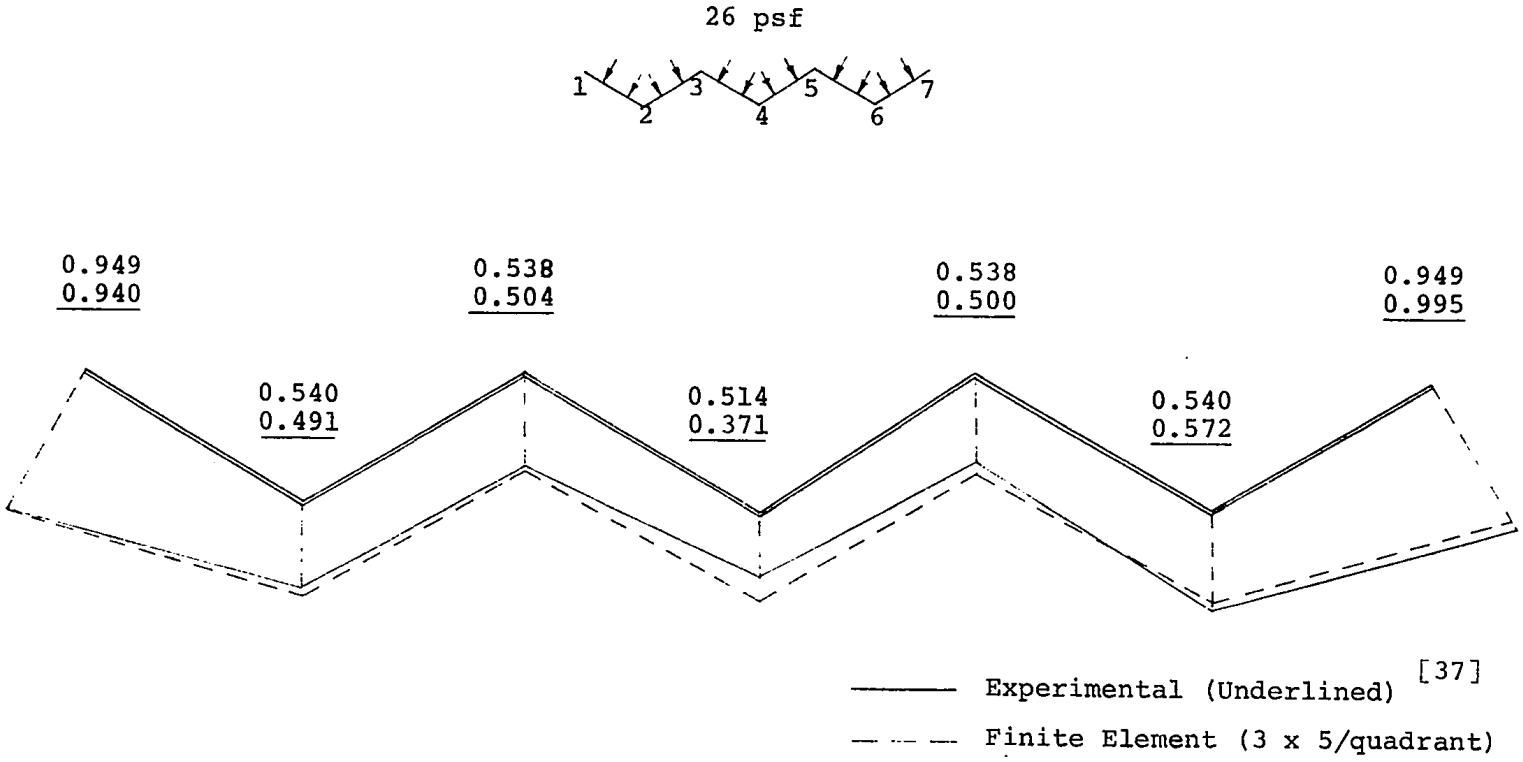

FIG. 6.7 DEFLECTION (INCHES) AT MID-SPAN OF THE 19 FOOT FOLDED PLATE. UNIFORM PRESSURE 26 PSF

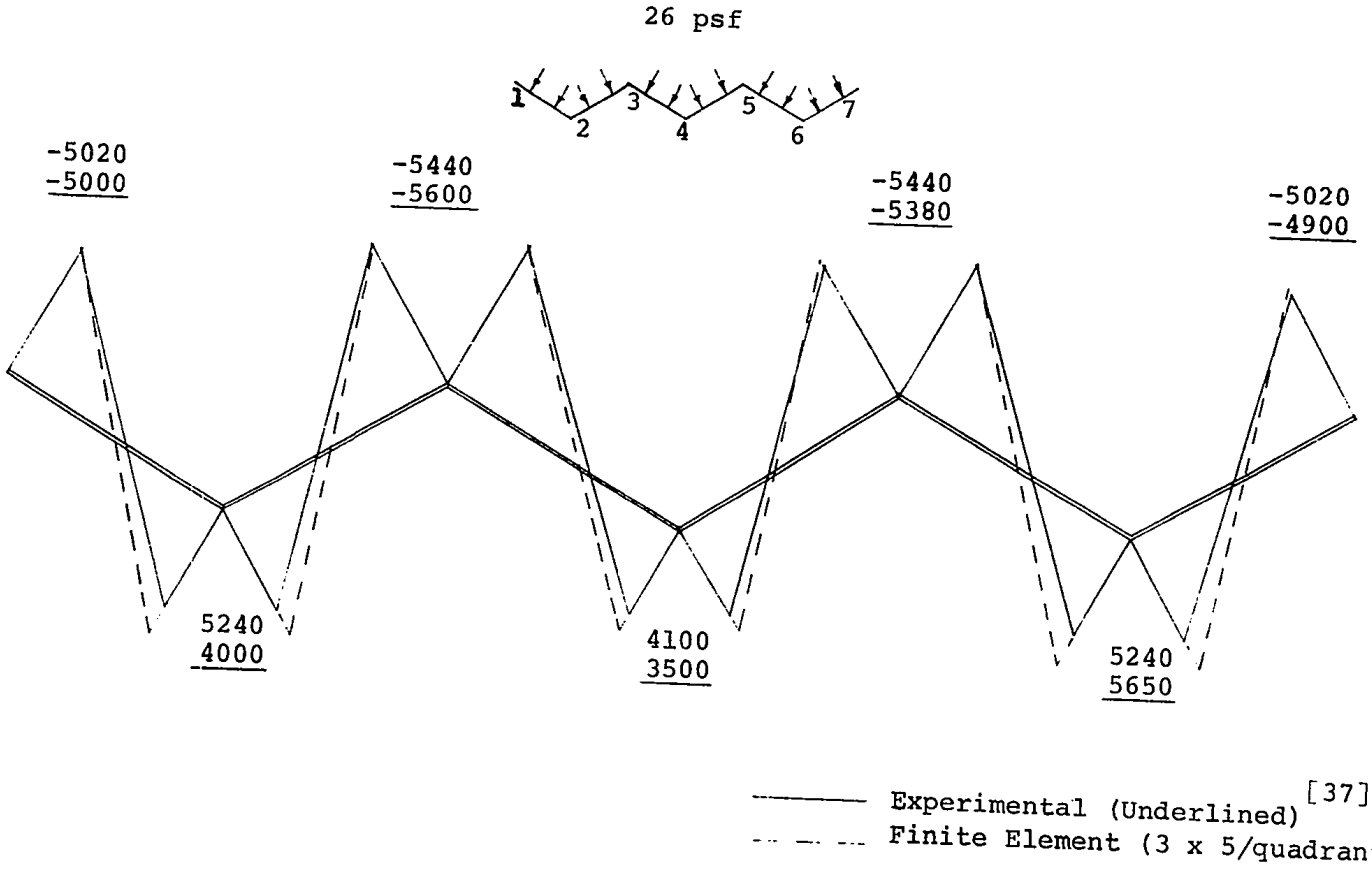

FIG. 6.8 LONGITUDINAL STRESSES (PSI) IN TOP FACING AT MIDSPAN SECTION OF THE 19 FOOT FOLDED PLATE

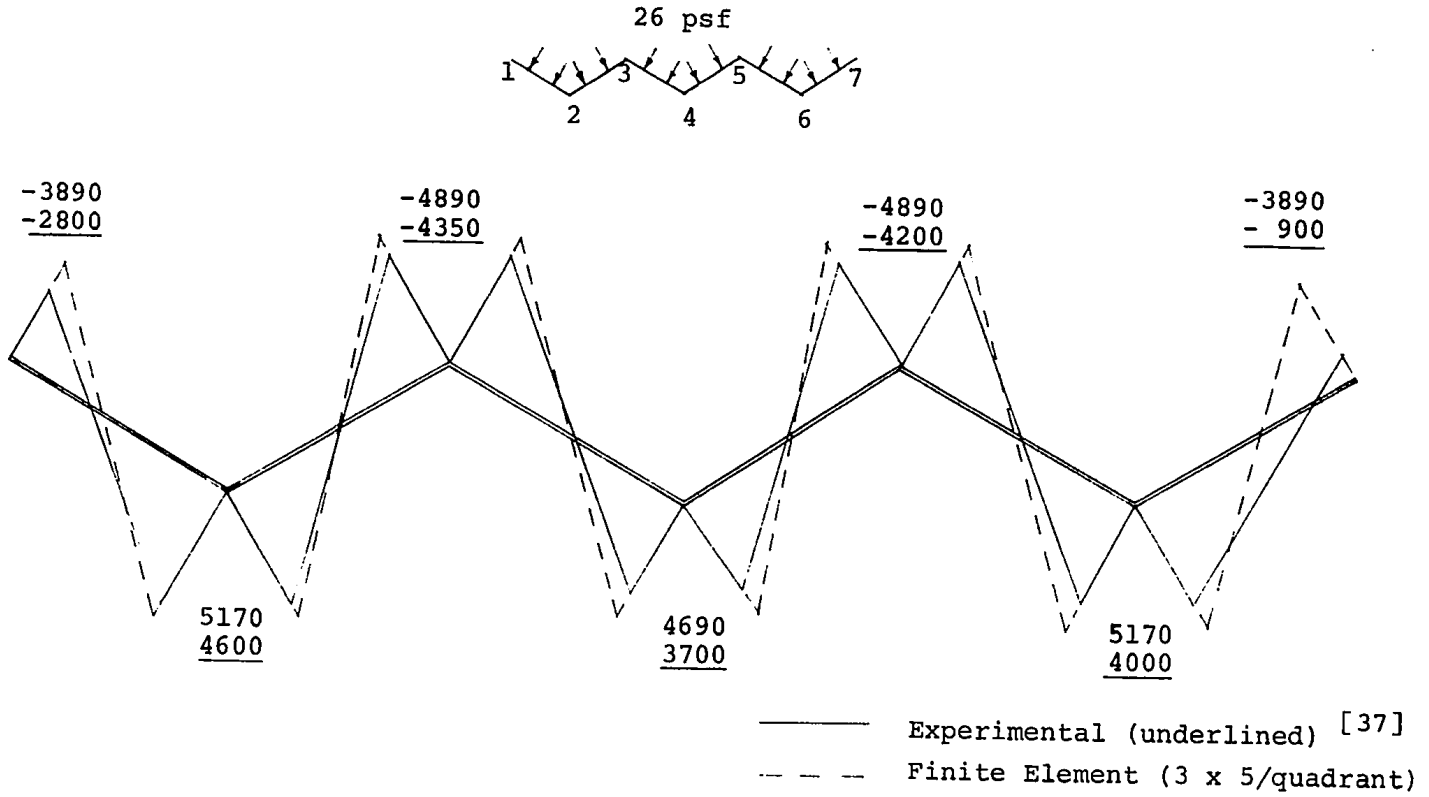

FIG. 6.9 LONGITUDINAL STRESSES (PSI) IN BOTTOM FACING AT MIDSPAN SECTION OF THE 19 FOOT FOLDED PLATE

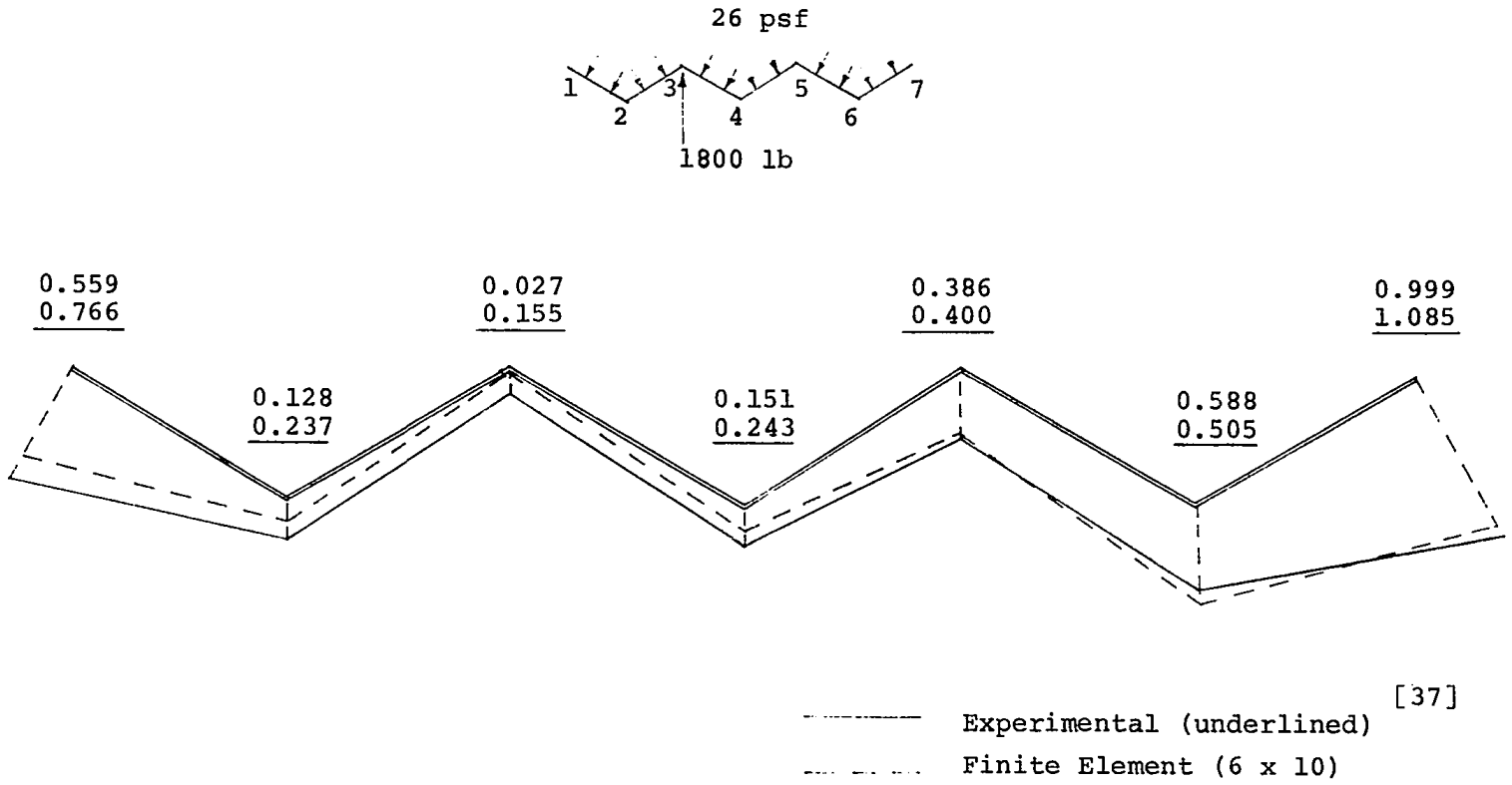

FIG. 6.10 DEFLECTION (INCHES) AT MIDSPAN OF THE 19 FOOT FOLDED PLATE. INTERIOR COLUMN-SUPPORT (AT RIDGE 3) PLACED 2 FT AWAY FROM MIDSPAN

CHAPTER VII

APPLICATIONS TO THE ANALYSIS OF PANELIZED BUILDINGS MADE UP OF SANDWICH PANELS

7.1 INTRODUCTION

In the previous Chapter application of the finite element technique to the analysis of folded sandwich plates was presented, the panels of the test-structures were used as roofing components to carry relatively light load over a large span. However, sandwich panels can also be used in complete assembly of a building, construction of many such structures has been reported. [39]

In frameless panelized buildings, the panels serve as main load-carrying elements. Dead and live loads are carried by bending of the floor-panels to the load-bearing wall-panels and resisted by column action. Wind load is transferred by bending of the transverse walls and by diaphram action of the floors to the walls parallel to the wind direction and resisted by shear-wall action. Thus, in this type of structure the wall and floor panels distribute and resist all loads, three-dimensional rigidity is achieved without the use of bracing or framing system.

In this Chapter, the finite element technique is applied to the analysis of a sandwich panelized building. The results are compared to experimental data obtained from tests of a four-storey half-scale model.

7.2 DESCRIPTION OF THE TEST MODEL

A half-scale panelized building model is being built and tested by the System Building Group at Sir George Williams University. When fully constructed, it will consist of four storeys and six room units in floor plan.

Fig. 7.1 shows a perspective view of the model at its fifth stage of assembly. The walls and floors are made up of sandwich panels, openings were introduced in the walls to represent door spaces. Two different panel sizes (Fig. 7.2a) are used, one of 2 ft x 6 ft for the floors and the other of 2 ft x 4 ft for the walls, thus a floor consists of three panels joined together.

Each panel is made up of 2 in thick polystyrene foamed core (shear modulus G_c = 1200 psi) sandwiched between two aluminum faces of 0.025 in thickness. The panel edges are reinforced with wooden frame (Figs. 7.2 b and 7.2 c) to prevent possible premature crushing or delamination. This wooden frame also facilitates the connection between the panels.

Panel-to-panel connections are effected using specially designed aluminum extrusions. Fig. 7.3a shows the connection between two floor panels, and Fig. 7.3 b shows a cross-section of the extrusion in the connection of the wall and floor panels. Steel staples (spaced at 3/4 in center-to-center) are used to attach the panel frame to the flanges of

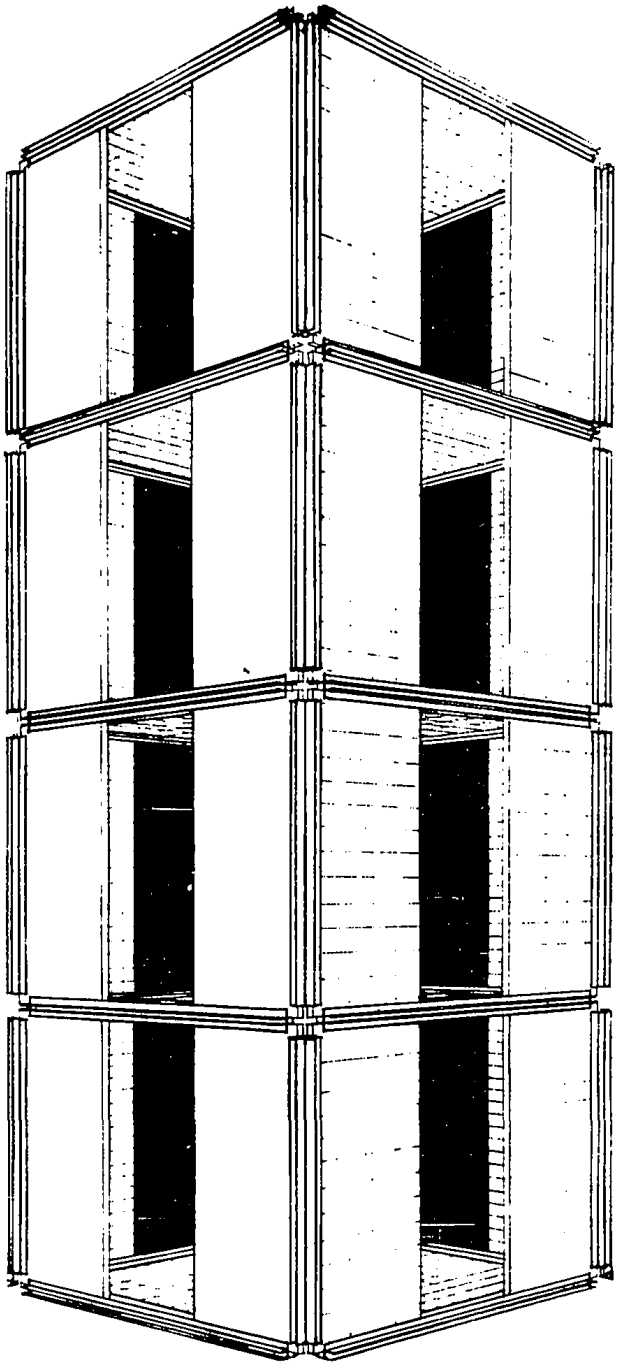

FIG. 7.1 PERSPECTIVE VIEW OF PANELIZED BUILDING MODEL.6 FT 4 IN SQUARE FLOOR, 16 FT 11 IN HIGH

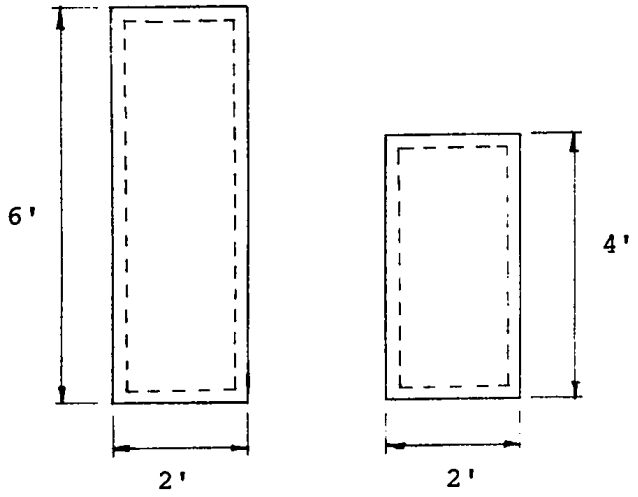

FIG. 7.2a TYPICAL PANEL SIZES

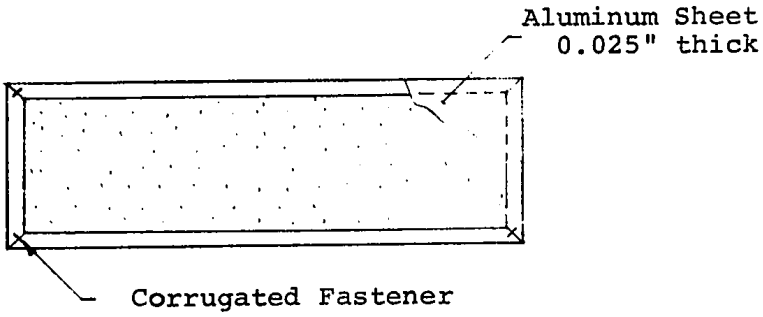

FIG. 7.2b TYPICAL PANEL FRAME

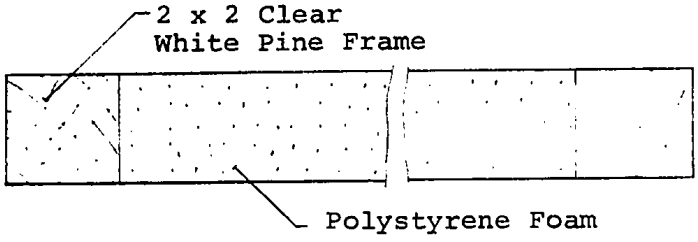

FIG. 7.2c TYPICAL PANEL SECTION

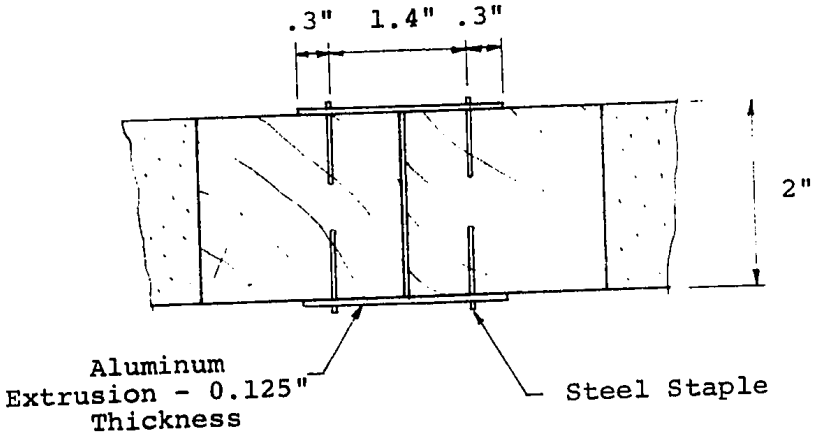

FIG. 7.3a CONNECTION OF FLOOR PANELS

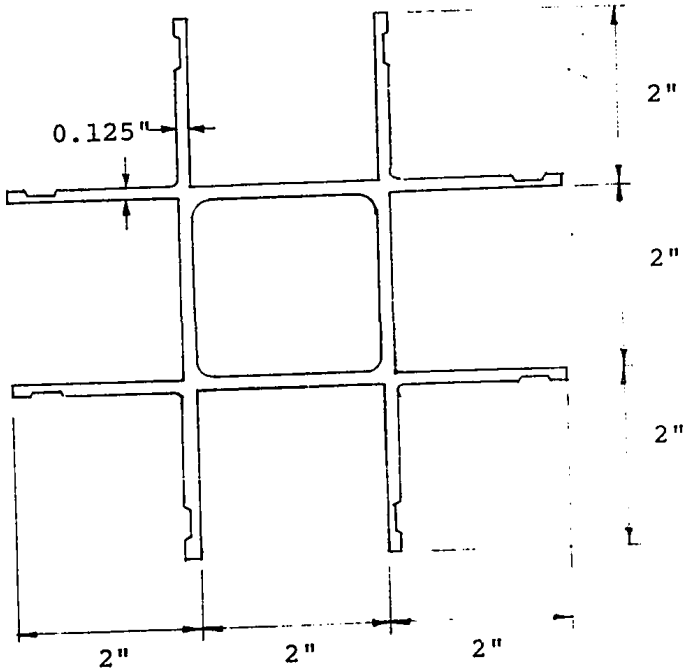

FIG. 7.3b CONNECTION OF WALL PANELS

the extrusions.

The model was subjected to vertical and horizontal loads simulating gravity and wind load, respectively. Strains and displacements were recorded at various points in each stage of loading or unloading. Full description of the design details, experimental procedure and the data-acquisition system can be found in a series of reports issued by the System Building Center at Sir George Williams University.[40,41,42]

7.3 FINITE ELEMENT ANALYSIS OF THE MODEL AND COMPARISON OF THE RESULTS

To represent the full structural action of the wall and floor panels of the building, a three-dimensional assemblage of finite elements is used for the analysis. Both in-plane and bending components of forces and displacements are considered, the element stiffness matrix is obtained by superimposing the membrane and bending parts as explained in Chapter IV.

Since the structure is symmetric and the applied loadings can be split up into symmetric and antisymmetric components, only one quarter of the complete structure is analysed. Fig. 7.4 shows the idealized model for one quarter of a typical storey of the structure, the panels are represented by rectangular sandwich elements and the connecting beams by line elements of equivalent stiffnesses (indicated by heavy lines in Fig. 7.4).

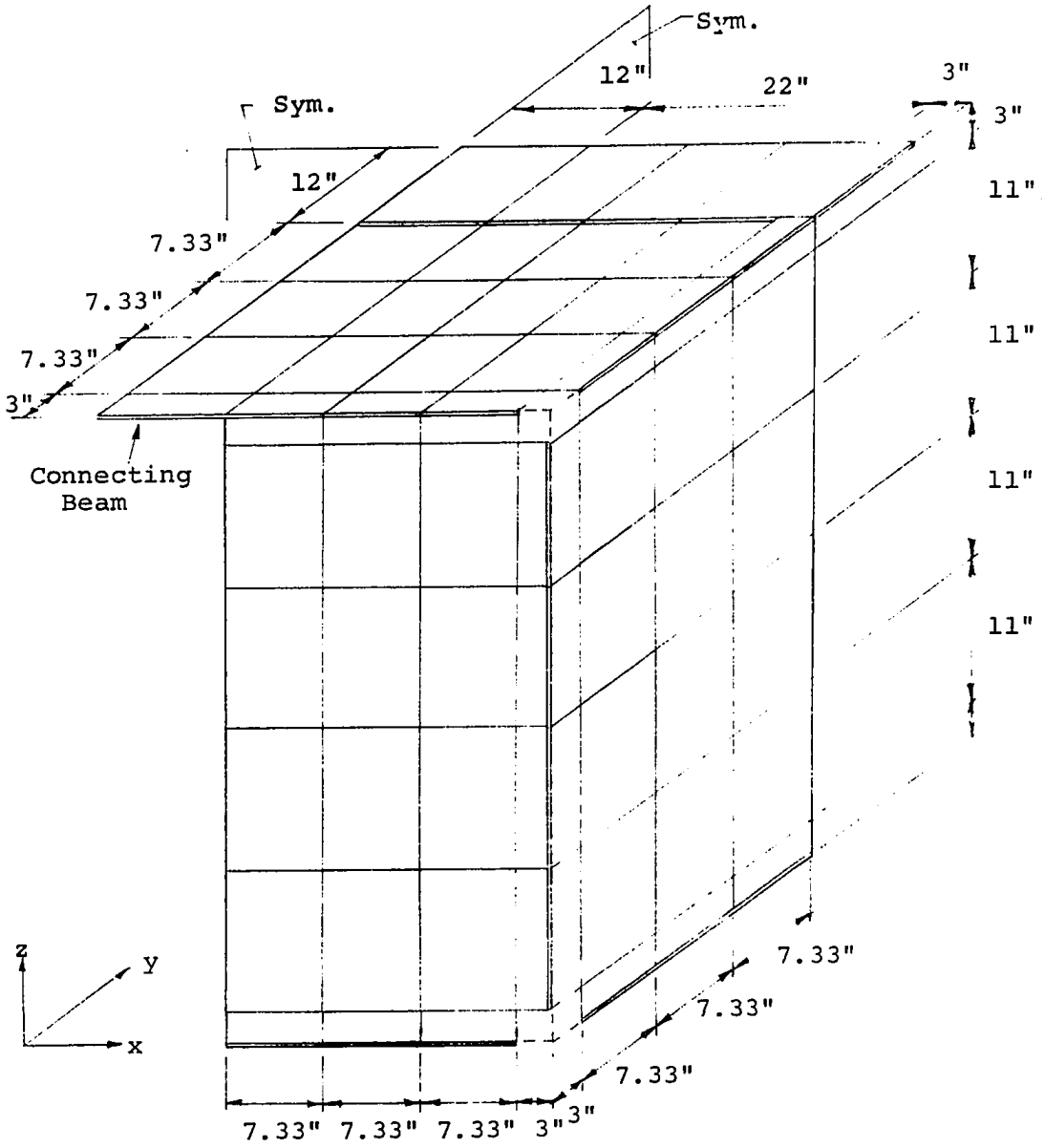

FIG. 7.4 FINITE ELEMENT IDEALIZATION FOR ONE QUADRANT OF A TYPICAL STOREY OF THE PANELIZED BUILDING

The structure is analyzed for the case of uniform horizontal load applied at the top floor level, discussion and comparison of the results in this Chapter are for this type of loading only. Because the attachment of the wall-panels to the foundation frame is by means of steel staples, the structure is assumed to be hinged at the base.

The load-deflection curves at each floor level is plotted in Fig. 7.5, which shows both experimental and finite element values. Inspection of the curves indicates that there are large discrepancies between the two sets of results. The maximum deflection, which occurs at the top floor level, as found by the finite element analysis is only half of the measured deflection. At lower floor levels the difference becomes larger since the actual deflection varies linearly through the height of the building whereas, the theoretical deflection decreases at an increasing rate.

A peculiarity in the behavior of the model structure can be seen in Fig. 7.5, where the load-deflection curves show that as the load increases, the deflection also increases but at a lower rate. And it is interesting to note that the slopes of the load-deflection curves at the initial stage of unloading match those of the theoretical curves. This indicates that the structure becomes stiffer when the deformation or the applied loading reaches a certain stage. This behavior may be attributed to the nature of the panel connections, where some joint-slippage must have occurred

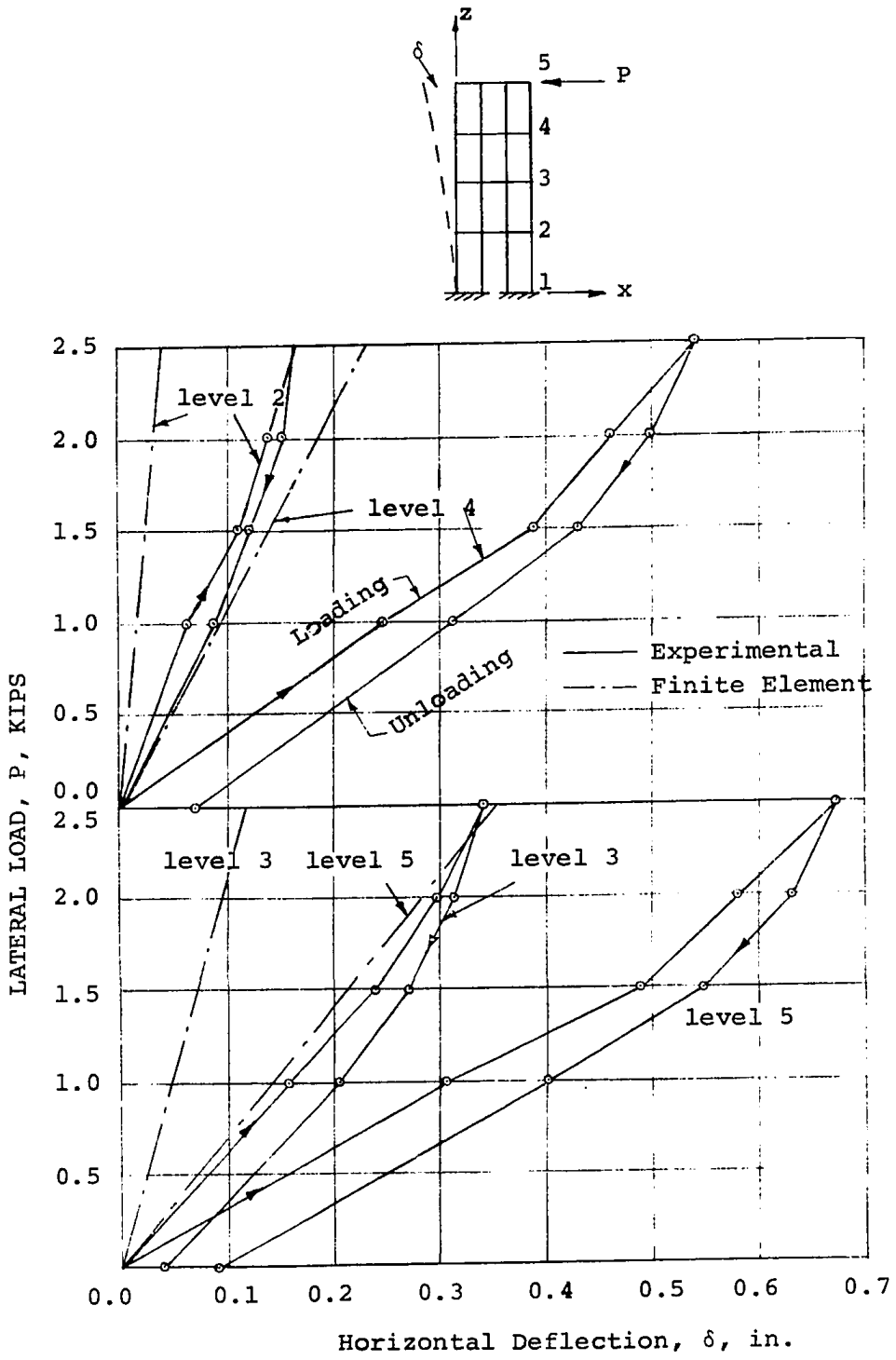

FIG. 7.5 HORIZONTAL DEFLECTION AT FLOOR LEVELS

before the connections became effective.

To verify the above conjecture a shear-wall analysis of the model omitting the floors and the cross-walls is performed, the resulting deflections are much higher than the experimental values. This illustrates that in the initial stage of loading because of joint-slips the floors and the cross-walls had only partial restraint on the rest of the structure. In fact, during the test it was observed that the staples which attached the tension side wall-panels to the foundation-frame were loosened and the panel corners were raised up by an amount equal to 3/16 in. The extent of the influence of joint-slippage is not fully understood and further tests are to be carried out to obtain more information. Consequently, it would seem that at present, no definite conclusion can be reached regarding the comparison of the deflection. However, comparison of the stresses is still possible since equilibrium of the structure must be maintained regardless of the amount of joint slippage.

Figures 7.6 to 7.9 show the distribution of the longitudinal strains in the panels at various levels of the building model, the plotted values are for a particular lateral loading of 2,500 lbs applied uniformly at the top. Generally, the measured strains are less than the predicted values, however they are of the same order of magnitude. Discrepancies between the two sets of results may be due to several reasons:

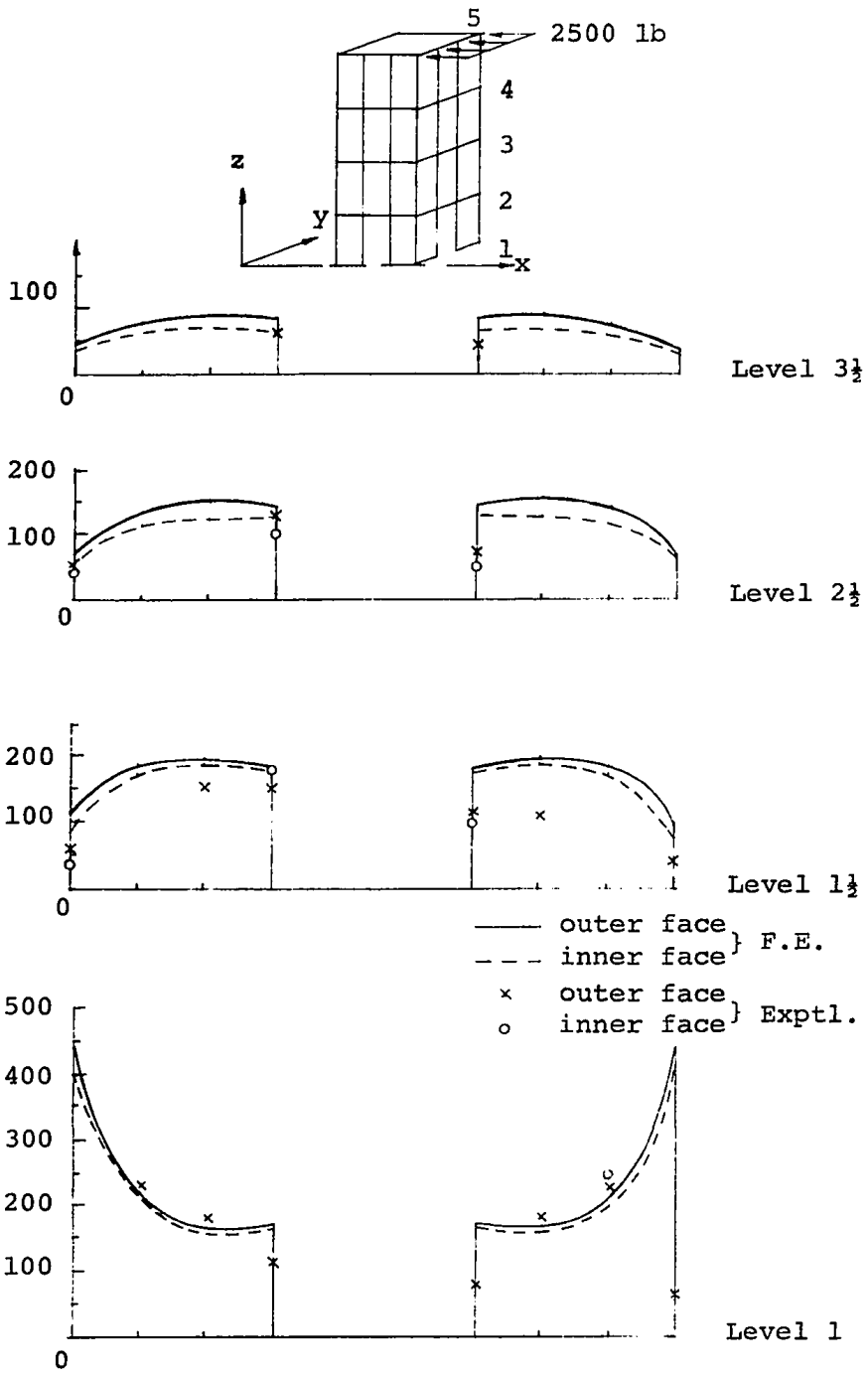

FIG. 7.6 DISTRIBUTION OF LONGITUDINAL STRAINS (MICRO IN/IN) IN PANELS FACING POSITIVE X-DIRECTION

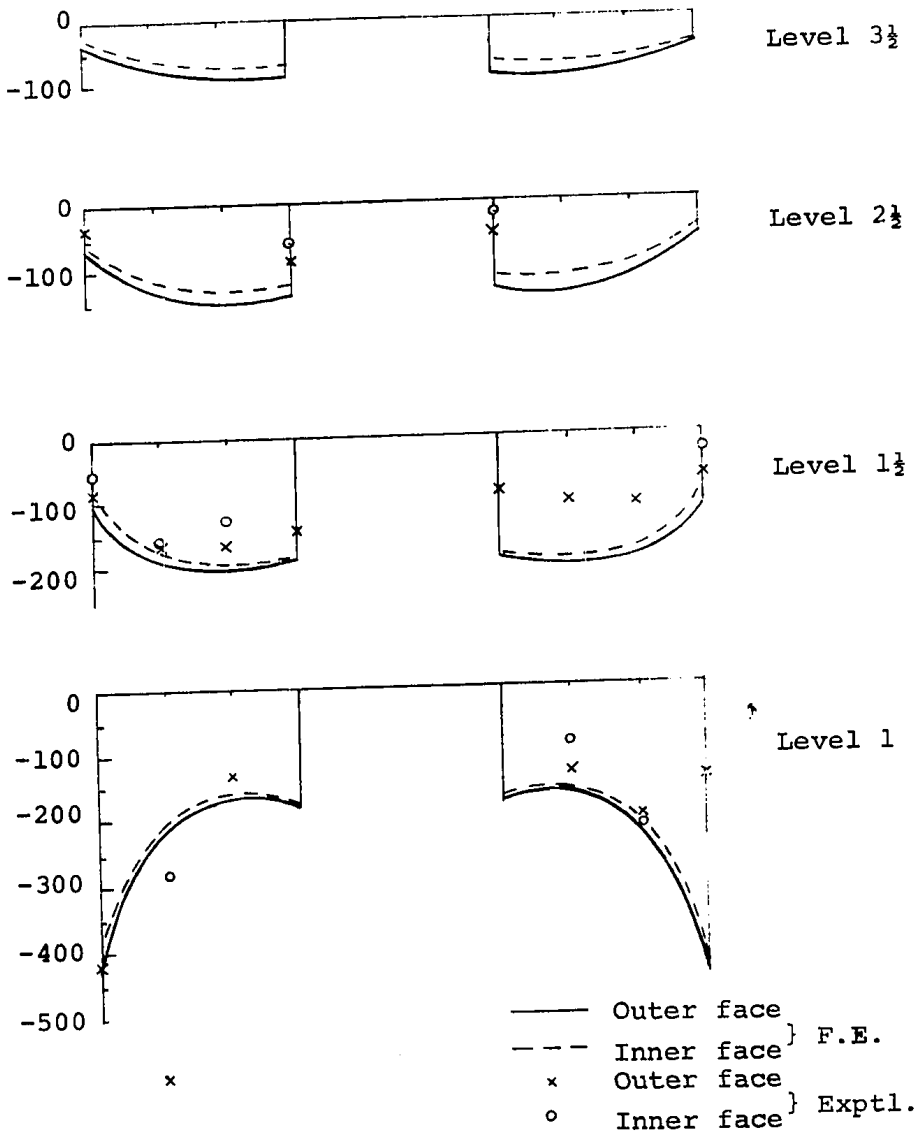

FIG. 7.7 DISTRIBUTION OF LONGITUDINAL STRAINS (MICRO IN/IN) IN PANELS FACING NEGATIVE X-DIRECTION

- experimental and instrumental errors.
- separation of the facing and the core at gage locations.
- stress concentration and effects of the connecting extrusions and the wooden frame.

In the panels perpendicular to the load direction, the longitudinal strain distribution is approximately uniform over the panel width (Figures 7.6, 7.7) except at the base portion. These panels are subjected to bending, however the bending effect is not great, as manifested by the narrow difference between the strains in the outer and inner faces. The bending effect virtually diminishes in the panels parallel to the load direction, longitudinal strain distribution in these shear-panels is practically linear (see Figures 7.8, 7.9) over the panel width at all sections.

As a further check on the effect of the bending stiffness of the panels, a membrane analysis of the same structure is carried out. The results show that the displacements and the stresses are increased approximately 8% and 5% respectively, as compared to the results of the full membrane-bending analysis.

One advantage of the membrane analysis is that only three equations of equilibrium equations are set up at a node whereas six equations are required in the full analysis. This allows considerable saving in computer time and storage.

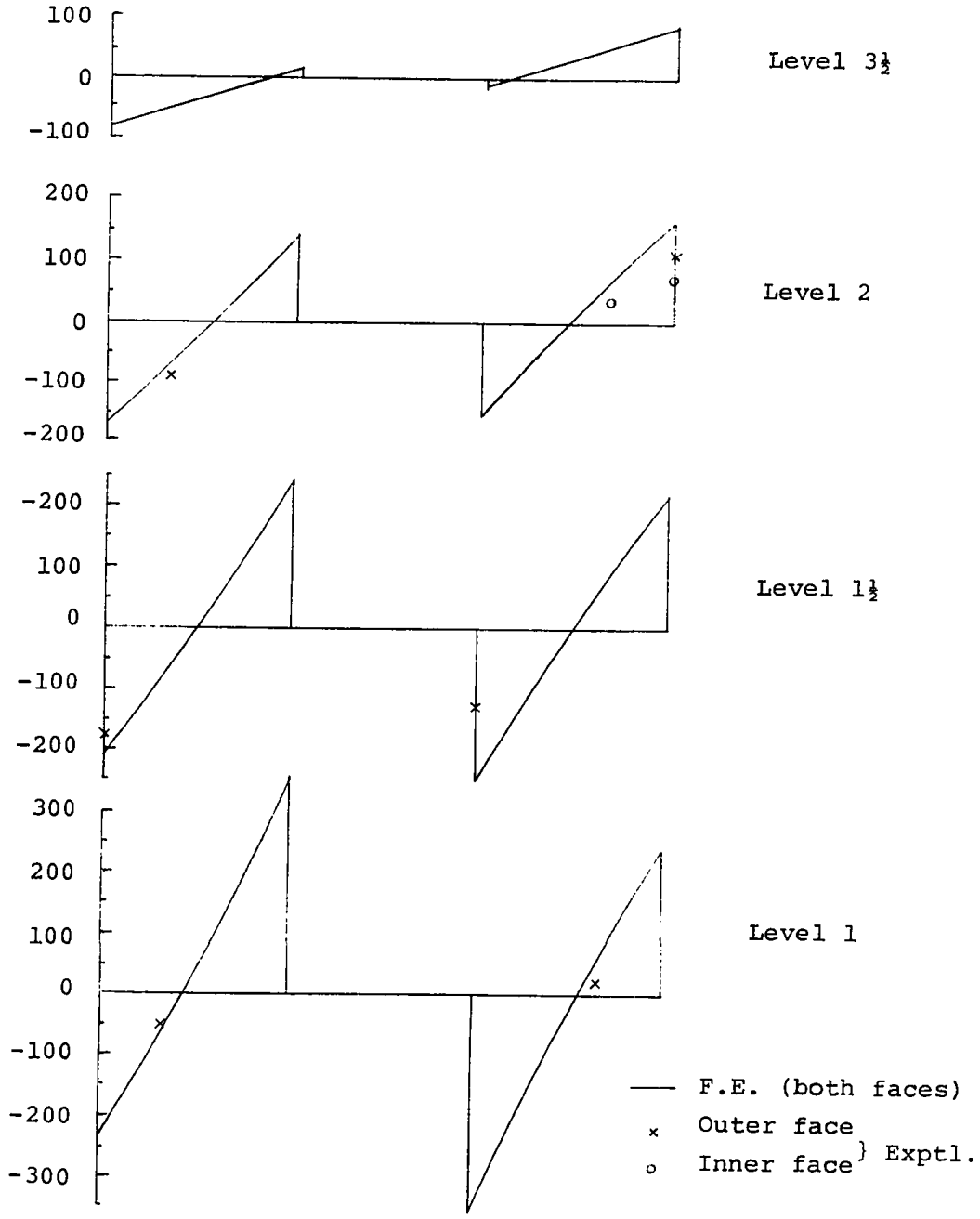

FIG. 7.8 DISTRIBUTION OF LONGITUDINAL STRAINS (MICRO IN/IN) IN PANELS FACING POSITIVE Y-DIRECTION

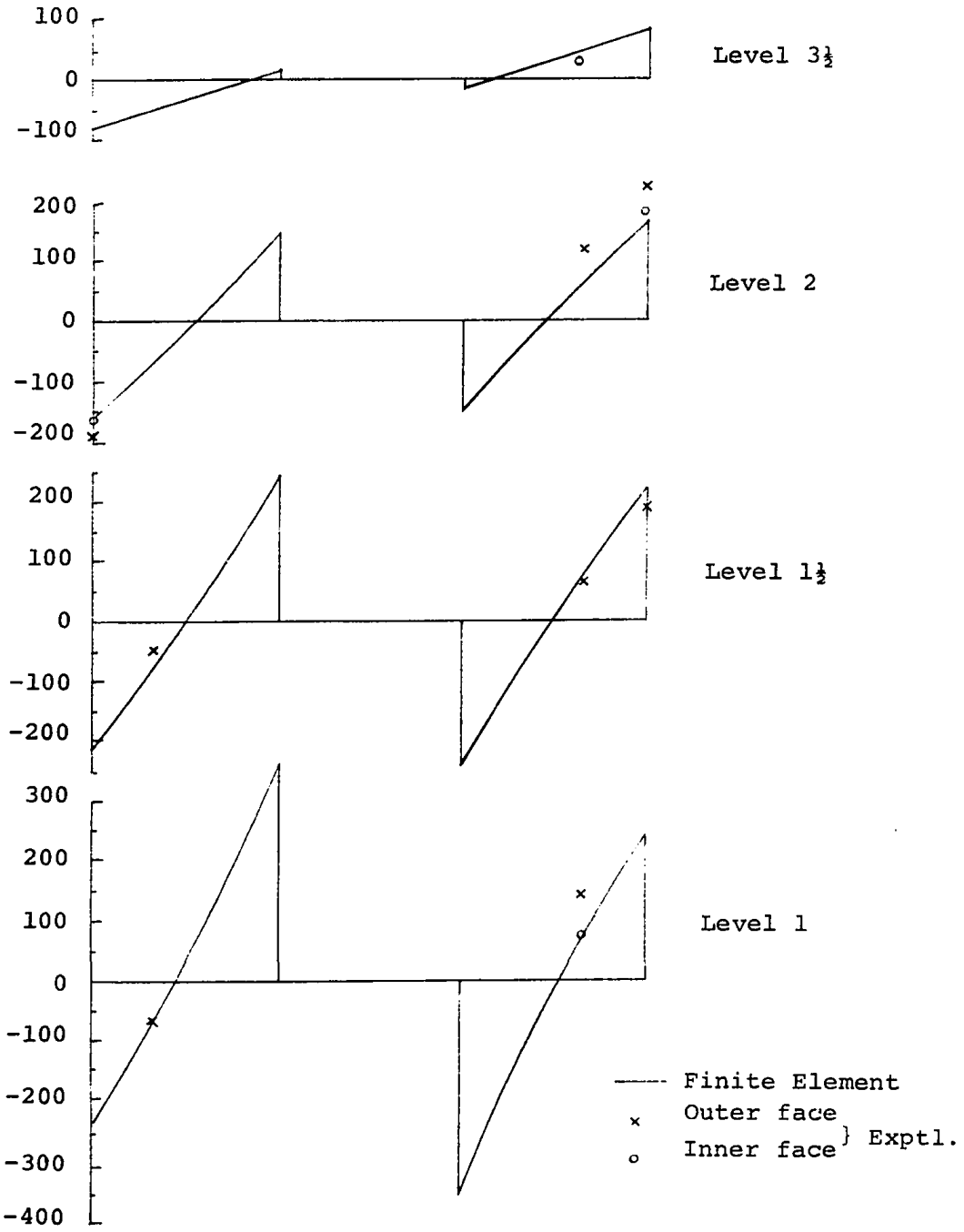

FIG. 7.9 DISTRIBUTION OF LONGITUDINAL STRAINS (MICRO IN/IN) IN PANELS FACING NEGATIVE Y-DIRECTION

CHAPTER VIII

SUMMARY AND CONCLUSIONS

The finite element technique has been extended for applications to two and three-dimensional sandwich plate-structures. Stiffness matrices for bending and membrane actions of sandwich elements having rectangular and right-angled triangular shapes were derived by using the assumed stress distribution approach. The proposed elements are applicable to sandwich construction with both orthotropic core and facings. The latter may be of different materials and thickness. A large capacity computer program capable of handling any type of plate structures was developed to effect the solutions.

One feature of the present elements is the ability of approximating a rather complex distribution of stresses in the material-layers while full compatibility of displacements and slopes is maintained at the element boundaries; this compatibility still exists even when elements meet at an angle such as along the fold-lines of a folded plate structure. Another feature is that the transverse shear deformation, which characterizes all sandwich constructions, is taken into account without introducing any degrees of freedom other than the deflection and edge rotations. Having only these geometrical degrees of freedom, the elements can be used for structures of arbitrary shape.

Application of these elements to flat sandwich plate problems leads to the following conclusions:

1. The deflection and stresses obtained with the rectangular and triangular elements converge rapidly to the "exact" values as the mesh is refined. Results given by the rectangular elements are generally better than those given by the triangular ones for a given mesh size.

2. For common types of sandwich construction subjected to transverse loading, the transverse shear deformation increases significantly the deflection of the plates. The influence of the core shear stiffness on the stresses depends on the type of edge supports. In clamped plates the effect is to reduce the magnitude of the stresses, whereas in simply-supported isotropic plates no change in stresses occurs.

3. The solutions obtained for rectangular orthotropic sandwich plates are in good agreement with the available analytical solutions. The degree of orthotropy has a great influence on the stress distribution in the plate regardless of the type of edge supports.

Applications of the method to the analysis of two folded sandwich plate structures and one four-storey sandwich panelized building lead to further conclusions.

4. Comparison of the F.E. results to experimental data shows encouraging agreement. The predicted stresses are generally on the safe side.

5. The connections between panels can greatly affect the behavior of the structure; if they are not sufficiently rigid, excessive deformation may result even at low level of loading.

6. Although only results for one particular panelized building are given, it seems that for lateral load analysis the membrane solutions are not much different from the full membrane-bending solutions.

REFERENCES

REFERENCES

[1] Williams, D. et al, "Flat Sandwich Panels Under Compressive End Loads", Roy. Aircr. Est., Rept. AD3174,(1941).

[2] Leggett, D.M.A., and Hopkins, H.G., "Sandwich Panels and Cylinders Under Compressive End Loads", Aeronaut. Res. Council, Rept. and Mem. No. 2262, (1949).

[3] Hopkins, H.G., and Pearson, S., "The Behavior of Flat Sandwich Panels Under Uniform Transverse Loading", Roy. Aircr. Est., Rept. SME 3277, (1944).

[4] March, H.W., "Buckling Under Compressive End Load", U.S. Forest Prod. Lab., Rept. No. 1583, (1948).

[5] Ericksen, W.S., and March, H.W., "Compressive Buckling of Sandwich Panels Having Facings of Unequal Thickness", U.S. Forest Prod. Lab., Rept. No. 1583-B, (1950).

[6] Libov, C., and Batdorf, S.A., "A General Small-Deflection Theory for Flat Sandwich Plates", NACA Rept. No. 899, (1948).

[7] Reissner, E., "On Bending of Elastic Plates", Quar. Appl. Math., Vol. 5, pp.55-68, (1947).

[8] Goodier, J.N., and Hsu, C.S., "Nonsinusoidal Buckling Modes of Sandwich Plates", J. Aero. Sci., Vol. 21, (1954).

[9] Eringen, A.C., "Bending and Buckling of Rectangular Sandwich Plates", Proc. 1st U.S. Nat. Congr. Appl. Mech. (ASME, New York, N.Y.), p.381, (1952).

[10] Hoff, N.J., "Bending and Buckling of Rectangular Sandwich Plates", NACA TN 2225, (1950).

[11] Plantema, F.J., Sandwich Construction (The Bending and Buckling of Sandwich Beams, Plates and Shells), John Wiley and Sons, N.Y., (1966).

[12] Allen, H.G., Analysis and Design of Structural Sandwich Panels, Pergamon Press, (1969).

[13] Monforton, G.R., and Schmit, L.A., Jr., "Finite Element Analysis of Sandwich Plates and Cylindrical Shells With Laminated Faces", Proc. 2nd Conference on Matrix Methods in Structural Mechanics, Wright-Patterson AFB, Ohio, pp.573-616, (1968).

[14] Abel, J.F., and Popov, E.P., "Static and Dynamic Finite Element Analysis of Sandwich Structures", Proc. 2nd Conference on Matrix Methods in Structural Mechanics, Wright-Patterson AFB, Ohio, pp.213-245, (1968).

[15] Yu, Y.Y., "A New Theory of Elastic Sandwich Plates, One-Dimensional Case", J. Appl. Mech., Vol. 26, pp. 653-662, (1959).

[16] Pryor, C.W., and Barker, R.M., "A Finite Element Analysis Including Transverse Shear Effects for Applications to Laminated Plates", AIAA Journal, Vol. 9, No. 5, pp. 790-801, (1971).

[17] Lundgren, H.R., and Salama, A.E., "Buckling of Multilayer Plates by Finite Element", J. of Eng. Mech. Div., Vol. 97, pp.477-493, (1971).

[18] Pian, T.H.H., "Derivation of Element Stiffness Matrices by Assumed Stress Distributions", AIAA Journal, Vol. 2, pp.1333-1336, (1964).

[19] Pian, T.H.H., and Tong, P., "Rationalization in Deriving Element Stiffness Matrix by Assumed Stress Approach", Proc. of 2nd Conference on Matrix Methods in Structural Mechanics, Wright-Patterson, AFB, Ohio, pp. 441-469, (1968).

[20] Ueng, C.E.S., and Lin, Y.J., "On Bending of Orthotropic Sandwich Plates", AIAA Journal, Vol. 4, pp.2241-2242, (Dec. 1966).

[21] Timoshenko, S., and Woinowsky-Krieger, S., Theory of Plates and Shells, McGraw-Hill Book Co., New York, N.Y., (1959).

[22] Pian, T.H.H., "Element Stiffness-Matrices for Boundary Compatibility and for Prescribed Boundary Stresses", Proc. Conf. Matrix Meth. Struc. Mech., Wright-Patterson AFB, pp.455-477, (1965).

[23] Severn, R.T., and Taylor, P.R., "The Finite Element Method for Flexure of Slabs When Stress Distributions are Assumed", Proc. Instn. Civ. Engrs., Vol. 34, pp. 153-170, (1966).

[24] Allwood, R.J., and Cornes, G.M.M., "A Polygonal Finite Element for Plate Bending Problems Using the Assumed Stress Approach", In. J. Num. Meth. Eng. Vol. 1, pp.135-149, (1969).

[25] Zienkiewicz, O.C., and Cheung, Y.K., "Finite Element Method of Analysis for Arch Dam Shells and Comparison with Finite Difference Procedures", International Symposium on Theory of Arch Dams, Southampton University, (1964).

[26] Mehrotra, B.L. et al., "Analysis of Three Dimensional Thin-Walled Structures", J. of Struct. Div., Vol. ,pp.2863-2872, (Dec. 1969).

[27] Zienkiewicz, O.C. et al., "Three-Dimensional Analysis of Buildings Composed of Floor and Wall Panels", Proc. Instn. Civil. Engrs., Vol. 49, pp.319-332, (1971).

[28] Rockey, K.C., and Evans, H.R., "A Finite Element Solution for Folded Plate Structures", International Conference on Space Structures, University of Surrey, (1966).

[29] Mufty, A.A., and Harris, P.J., "Further Developments in the Use of Linear Displacement Functions in the Finite Element Analysis of Orthotropic Plates and Shells", Transactions of the Eng. Inst. of Can. Vol. 14, (Jan. 1971).

[30] Zienkiewicz, O.C., The Finite Element Method in Engineering Science, McGraw-Hill, London, (1971).

[31] Pin, Tong and Pian, T.H.H., "A Variational Principle and the Convergence of a Finite Element Method Based on Assumed Stress Distribution", Int. J. Solids Structures, Vol. 5, pp. 463-472, (1969).

[32] Raville, M.E., "Deflection and Stresses in a Uniformily Loaded, Simply-Supported Rectangular Sandwich Plate", FPL Report 1847, (Dec. 1955).

[33] Basu, A.K., and Dawson, J.M., "Orthotropic Sandwich Plates, Proc. Instn. Civ. Engrs., Suppl., pp.87-115, (1970).

[34] Folie, G.M., "Bending of Clamped Orthotropic Sandwich Plates", J. Eng. Mech. Div. ASCE, Vol. pp.243-265, (June, 1970).

[35] Cook, R.D., "On Certain Approximations in Sandwich Plate Analysis", J. of Appl. Mech., Vol. pp.39-44, (March, 1966).

[36] Cheng, S., "A Formula for the Torsional Stiffness of Rectangular Sandwich Plates", J. of Appl. Mech. Vol. 28, pp.307-310, (June, 1961).

[37] Fazio, P.P., and Kennedy, J.B., "Experimental and Theoretical Study of Aluminum Sandwich Elements and in Particular Aluminum Folded Sandwich Plate Structures", Final Report, Department of Civil Engineering, Sir George Williams University, (June, 1968).

[38] Ahmed, K.M., "Static and Dynamic Analysis of Sandwich Structures by the Method of Finite Element", Journal of Sound and Vibration, V.18, pp.75-91, (Jan. 1971).

[39] Gubenko, A.B. "Building Structures With Plastics", Proc. of Conference on Plastics in Building Structures, Pergammon Press, pp.299-308, (1965).

[40] Fazio, P.P., and Mikler, J., "Modular Panelized Building, Final Design and Experimental Set-Up of a Half-Scale Four-Storey Panelized Building Model", Report No. SBC-09, Department of Civil Engineering, Sir George Williams University,(July, 1970).

[41] Fazio, P.P., and Palusamy, S., "Panelized Building Model, Acquisition and Coding of Experimental Data", Report No. SBC-19, CE-72-3, Department of Civil Engineering, Sir George Williams University, (March, 1972).

[42] Fazio, P.P., and Palusamy, S., "Data Acquisition System for Large-Scale Structural Testing", Report No. SBC-18, CE71-10, Department of Civil Engineering, Sir George Williams University, (November, 1971).

APPENDIX A

MATRICES USED IN THE DERIVATION OF THE STIFFNESS MATRICES FOR THE RECTANGULAR SANDWICH ELEMENT

APPENDIX A

MATRICES USED IN THE DERIVATION OF THE STIFFNESS MATRICES FOR THE RECTANGULAR SANDWICH ELEMENT

$$
\begin{bmatrix}
1-\bar{x} & 0 & 0 & \bar{x} & 0 & 0 & 0 & 0 & 0 & 0 & 0 & 0 \\
0 & 1-\bar{x} & 0 & 0 & \bar{x} & 0 & 0 & 0 & 0 & 0 & 0 & 0 \\
0 & 0 & 1-\bar{x} & 0 & 0 & \bar{x} & 0 & 0 & 0 & 0 & 0 & 0 \\
0 & 0 & 0 & 0 & 0 & 0 & 1-\bar{x} & 0 & \bar{x} & 0 & 0 & 0 \\
0 & 0 & 0 & 0 & 0 & 0 & 0 & 1-\bar{x} & 0 & \bar{x} & 0 & 0 \\
0 & 0 & 0 & 0 & 0 & 0 & 0 & 0 & 1-\bar{x} & 0 & \bar{x} & 0 \\
1-\bar{y} & 0 & 0 & 0 & 0 & 0 & \bar{y} & 0 & 0 & 0 & 0 & 0 \\
0 & 1-\bar{y} & 0 & 0 & 0 & 0 & 0 & \bar{y} & 0 & 0 & 0 & 0 \\
0 & 0 & 1-\bar{y} & 0 & 0 & 0 & 0 & 0 & \bar{y} & 0 & 0 & 0 \\
0 & 0 & 0 & 1-\bar{y} & 0 & 0 & 0 & 0 & 0 & \bar{y} & 0 & 0 \\
0 & 0 & 0 & 0 & 1-\bar{y} & 0 & 0 & 0 & 0 & 0 & \bar{y} & 0 \\
0 & 0 & 0 & 0 & 0 & 1-\bar{y} & 0 & 0 & 0 & 0 & 0 & \bar{y}
\end{bmatrix}
$$

MATRIX $[L]_b$ in $\{u\} = [L]\{q\}$ (3.20)

$$
\begin{bmatrix}
0 & 0 & 0 & 0 & 0 & 0 & -1 & -\bar{x} & 0 & -\bar{x}^2 & 0 & 0 & 0 & 0 & 0 & 0 & 0 \\
0 & 0 & 0 & 0 & 0 & 0 & 0 & 0 & 0 & 0 & 0 & 0 & -1 & -\bar{x} & 0 & -\bar{x}^2 & 0 \\
0 & 0 & 0 & 0 & 0 & 0 & 0 & 0 & -\frac{1}{b} & 0 & -\frac{\bar{x}}{b} & 0 & 0 & -\frac{1}{a} & 0 & -\frac{2\bar{x}}{a} & 0 \\
0 & 0 & 0 & 0 & 0 & 0 & 1 & \bar{x} & 1 & \bar{x}^2 & \bar{x} & 1 & 0 & 0 & 0 & 0 & 0 \\
0 & 0 & 0 & -\frac{b\bar{x}}{a} & 0 & 0 & 0 & 0 & 0 & 0 & 0 & -\frac{a\bar{x}}{b} & 1 & \bar{x} & 1 & \bar{x}^2 & 1 \\
0 & 0 & 0 & -\frac{b}{a^2} & 0 & 0 & 0 & 0 & \frac{1}{b} & 0 & \frac{\bar{x}}{b} & \frac{1}{b} & 0 & \frac{1}{a} & 0 & 2\frac{\bar{x}}{a} & 0 \\
0 & 0 & 0 & 0 & 0 & 0 & 0 & 0 & 0 & 0 & 0 & 0 & -1 & 0 & -\bar{y} & 0 & -\bar{y}^2 \\
-1 & 0 & -\bar{y} & 0 & 0 & -\bar{y}^2 & 0 & 0 & 0 & 0 & 0 & 0 & 0 & 0 & 0 & 0 & 0 \\
0 & -\frac{1}{a} & 0 & 0 & -\frac{\bar{y}}{a} & 0 & 0 & 0 & 0 & 0 & 0 & 0 & 0 & 0 & -\frac{1}{b} & 0 & -\frac{2\bar{y}}{b} \\
0 & 0 & 0 & -\frac{b\bar{y}}{a} & 0 & 0 & 0 & 0 & 0 & 0 & 0 & -\frac{a\bar{y}}{b} & 1 & 1 & \bar{y} & 1 & \bar{y}^2 \\
1 & 1 & \bar{y} & 1 & \bar{y} & \bar{y}^2 & 0 & 0 & 0 & 0 & 0 & 0 & 0 & 0 & 0 & 0 & 0 \\
0 & \frac{1}{a} & 0 & \frac{1}{a} & \frac{\bar{y}}{a} & 0 & 0 & 0 & 0 & 0 & 0 & -\frac{a}{b^2} & 0 & 0 & \frac{1}{b} & 0 & \frac{2\bar{y}}{b}
\end{bmatrix}
$$

MATRIX $[R]_b$ in $\{S\} = [R]\ \{\beta\}$ (3.20a)

$$\begin{bmatrix} 1-\bar{x} & 0 & \bar{x} & 0 & 0 & 0 & 0 & 0 \\ 0 & 1-\bar{x} & 0 & \bar{x} & 0 & 0 & 0 & 0 \\ 0 & 0 & 1-\bar{y} & 0 & 0 & 0 & \bar{y} & 0 \\ 0 & 0 & 0 & 1-\bar{y} & 0 & 0 & 0 & \bar{y} \\ 0 & 0 & 0 & 0 & 1-\bar{x} & 0 & \bar{x} & 0 \\ 0 & 0 & 0 & 0 & 0 & 1-\bar{x} & 0 & \bar{x} \\ 1-\bar{y} & 0 & 0 & 0 & \bar{y} & 0 & 0 & 0 \\ 0 & 1-\bar{y} & 0 & 0 & 0 & \bar{y} & 0 & 0 \end{bmatrix}$$

MATRIX $[L]_m$ in $\{u\} = [L]\{q\}$ (3.26)

$$t \begin{bmatrix} 0 & 0 & 0 & 0 & 0 & 0 & 0 & 0 & \frac{a\bar{x}}{b} & 0 & \frac{a\bar{x}^2}{2b} & -1 \\ 0 & 0 & 0 & 0 & 0 & 0 & -1 & -\bar{x} & 0 & -\bar{x}^2 & 0 & 0 \\ 1 & 1 & \bar{y} & 1 & \bar{y} & \bar{y}^2 & 0 & 0 & 0 & 0 & 0 & 0 \\ 0 & -\frac{b\bar{y}}{a} & 0 & -\frac{2b\bar{y}}{a} & -\frac{b\bar{y}^2}{2a} & 0 & 0 & 0 & -\frac{a}{b} & 0 & -\frac{a}{2b} & 1 \\ 0 & -\frac{b}{a} & 0 & -\frac{2b\bar{x}}{a} & -\frac{b}{2a} & 0 & 0 & 0 & -\frac{a\bar{x}}{b} & 0 & -\frac{a\bar{x}^2}{2b} & 1 \\ 0 & 0 & 0 & \frac{b^2}{a^2} & 0 & 0 & 1 & \bar{x} & 1 & \bar{x}^2 & \bar{x} & 0 \\ -1 & 0 & -\bar{y} & 0 & 0 & -\bar{y}^2 & 0 & 0 & 0 & 0 & 0 & 0 \\ 0 & \frac{b\bar{y}}{a} & 0 & 0 & \frac{b\bar{y}^2}{a} & 0 & 0 & 0 & 0 & 0 & 0 & -1 \end{bmatrix}$$

MATRIX $[R]_m$ in $\{S\} = [R]\{\beta\}$ (3.27)

APPENDIX B

MATRICES USED IN DERIVATION OF THE STIFFNESS MATRICES FOR RIGHT-ANGLED TRIANGULAR SANDWICH ELEMENT

$$
\begin{bmatrix}
\overset{1}{-sc} & \overset{2}{-sc\bar{x}} & \overset{3}{-sc\bar{x}} & \overset{4}{(\frac{s^3}{c}-2sc)\bar{x}^2} & \overset{5}{-sc\bar{x}^2} & \overset{6}{-sc\bar{x}^2} & \overset{7}{sc} & \overset{8}{sc\bar{x}} & \overset{9}{sc\bar{x}} & \overset{10}{sc\bar{x}^2} & \overset{11}{sc\bar{x}^2} & \overset{12}{\frac{c}{s}(2-3c^2)\bar{x}^2} & \overset{13}{d} & \overset{14}{d\bar{x}} & \overset{15}{d\bar{x}} & \overset{16}{d\bar{x}} & \overset{17}{d\bar{x}} \\
s^2 & s^2\bar{x} & s^2\bar{x} & 3s^2\bar{x}^2 & s^2\bar{x}^2 & s^2\bar{x}^2 & c^2 & c^2\bar{x} & c^2\bar{x} & c^2\bar{x}^2 & c^2\bar{x}^2 & 3c^2\bar{x}^2 & -2cs & -2cs\bar{x} & -2cs\bar{x} & -2cs\bar{x} & -2cs\bar{x}^2 \\
0 & -\frac{s}{a} & 0 & -2\frac{s\bar{x}}{a} & -\frac{s\bar{x}}{a} & 0 & 0 & 0 & \frac{c}{b} & 0 & \frac{c\bar{x}}{b} & 2\frac{c\bar{x}}{b} & 0 & \frac{c}{a} & -\frac{s}{b} & 2c\frac{\bar{x}}{a} & -2\frac{s\bar{x}}{b} \\
0 & 0 & 0 & -\frac{b}{a}y & 0 & 0 & 0 & 0 & 0 & 0 & 0 & -\frac{a}{b}\bar{y} & 1 & 1 & \bar{y} & 1 & \bar{y}^2 \\
1 & 1 & \bar{y} & 1 & \bar{y} & \bar{y}^2 & 0 & 0 & 0 & 0 & 0 & 0 & 0 & 0 & 0 & 0 & 0 \\
0 & \frac{1}{a} & 0 & \frac{1}{a} & \frac{\bar{y}}{a} & 0 & 0 & 0 & 0 & 0 & 0 & -\frac{a}{b^2} & 0 & 0 & \frac{1}{b} & 0 & 2\frac{\bar{y}}{b} \\
0 & 0 & 0 & 0 & 0 & 0 & -1 & -\bar{x} & 0 & -\bar{x}^2 & 0 & 0 & 0 & 0 & 0 & 0 & 0 \\
0 & 0 & 0 & 0 & 0 & 0 & 0 & 0 & 0 & 0 & 0 & 0 & -1 & -\bar{x} & 0 & -\bar{x}^2 & 0 \\
0 & 0 & 0 & 0 & 0 & 0 & 0 & 0 & -\frac{1}{b} & 0 & -\frac{\bar{x}}{b} & 0 & 0 & -\frac{1}{a} & 0 & -2\frac{\bar{x}}{a} & 0
\end{bmatrix}
$$

$c = \cos\theta$

$s = \sin\theta$

$d = c^2 - s^2$

MATRIX $[R]_b$ in $\{S\} = [R]\{\beta\}$ (3.30)

$$\begin{bmatrix}
s(1-\bar{x}) & c(1-\bar{x}) & 0 & s\bar{x} & c\bar{x} & 0 & 0 & 0 & 0 \\
c(1-\bar{x}) & -s(1-\bar{x}) & 0 & c\bar{x} & -s\bar{x} & 0 & 0 & 0 & 0 \\
0 & 0 & 1-\bar{x} & 0 & 0 & \bar{x} & 0 & 0 & 0 \\
0 & 0 & 0 & \bar{y} & 0 & 0 & 1-\bar{y} & 0 & 0 \\
0 & 0 & 0 & 0 & \bar{y} & 0 & 0 & 1-\bar{y} & 0 \\
0 & 0 & 0 & 0 & 0 & \bar{y} & 0 & 0 & 1-\bar{y} \\
1-\bar{x} & 0 & 0 & 0 & 0 & 0 & \bar{x} & 0 & 0 \\
0 & 1-\bar{x} & 0 & 0 & 0 & 0 & 0 & \bar{x} & 0 \\
0 & 0 & 1-\bar{x} & 0 & 0 & 0 & 0 & 0 & \bar{x}
\end{bmatrix}$$

$$\text{MATRIX } [L]_b \text{ in } \{u\} = [L]\{q\} \qquad (3.31)$$

$$t\begin{bmatrix}
s^2 & 3s^2\bar{x} & s^2\bar{x} & 6s^2\bar{x}^2 & 2s^2\bar{x}^2 & s^2\bar{x}^2 & c^2 & c^2\bar{x} & 3c^2\bar{x} & c^2\bar{x}^2 & 2c^2\bar{x}^2 & -2sc \\
-sc & (-2sc+\frac{s^3}{c})\bar{x} & -sc\bar{x} & 3(\frac{s^3}{c}-sc)\bar{x}^2 & \frac{1}{2}(\frac{s^3}{c}-3sc)\bar{x}^2 & -sc\bar{x}^2 & sc & sc\bar{x} & (2cs-\frac{c^3}{s})\bar{x} & sc\bar{x}^2 & \frac{1}{2}(3cs-\frac{c^3}{s})\bar{x}^2 & (c^2-s^2) \\
1 & 1 & \bar{y} & 1 & \bar{y} & \bar{y}^2 & 0 & 0 & -\frac{a}{b} & 0 & 0 & 0 \\
0 & -\frac{b\bar{y}}{a^2} & 0 & -\frac{2b\bar{y}}{a^2} & -\frac{b\bar{y}^2}{2a} & 0 & 0 & 0 & \frac{a\bar{x}}{b} & 0 & -\frac{a}{2b} & 1 \\
0 & 0 & 0 & 0 & 0 & 0 & 0 & 0 & 0 & 0 & \frac{a\bar{x}^2}{2b} & -1 \\
0 & 0 & 0 & 0 & 0 & 0 & -1 & -\bar{x} & 0 & -\bar{x}^2 & 0 & 0
\end{bmatrix}$$

$s = \sin\theta$

$c = \cos\theta$

MATRIX $[R]_m$ in eq. $\{S\} = [R]\{\beta\}$ (3.34)

$$\begin{bmatrix} -s(1-\bar{x}) & c(1-\bar{x}) & -s\bar{x} & c\bar{x} & 0 & 0 \\ c(1-\bar{x}) & s(1-\bar{x}) & c\bar{x} & s\bar{x} & 0 & 0 \\ 0 & 0 & \bar{y} & 0 & (1-\bar{y}) & 0 \\ 0 & 0 & 0 & \bar{y} & 0 & (1-\bar{y}) \\ (1-\bar{x}) & 0 & 0 & 0 & \bar{x} & 0 \\ 0 & (1-\bar{x}) & 0 & 0 & 0 & \bar{x} \end{bmatrix}$$

MATRIX $[L]_m$ in $\{u\} = [L]\{q\}$ (3.35)

APPENDIX C

DESIGN CHARTS FOR SQUARE ORTHOTROPIC SANDWICH PLATES

APPENDIX C

DESIGN CHARTS FOR SQUARE ORTHOTROPIC SANDWICH PLATES

Coefficients for maximum deflection and stresses in square orthotropic sandwich plates subjected to uniform transverse loading are shown in Figs. C.1 to C.7. Two cases of boundary conditions are considered:

1. Simply supported edges
2. Clamped edges

To obtain the actual values for maximum deflection and stresses, the following relations are used:

$$w_{max} = \alpha q a^4/D$$
$$M_{max} = \beta q a^2$$
$$Q_{max} = \gamma q a$$

The coefficients α, β, γ are obtained by finite element analysis using an 8 x 8 mesh idealization of one quadrant of the plate.

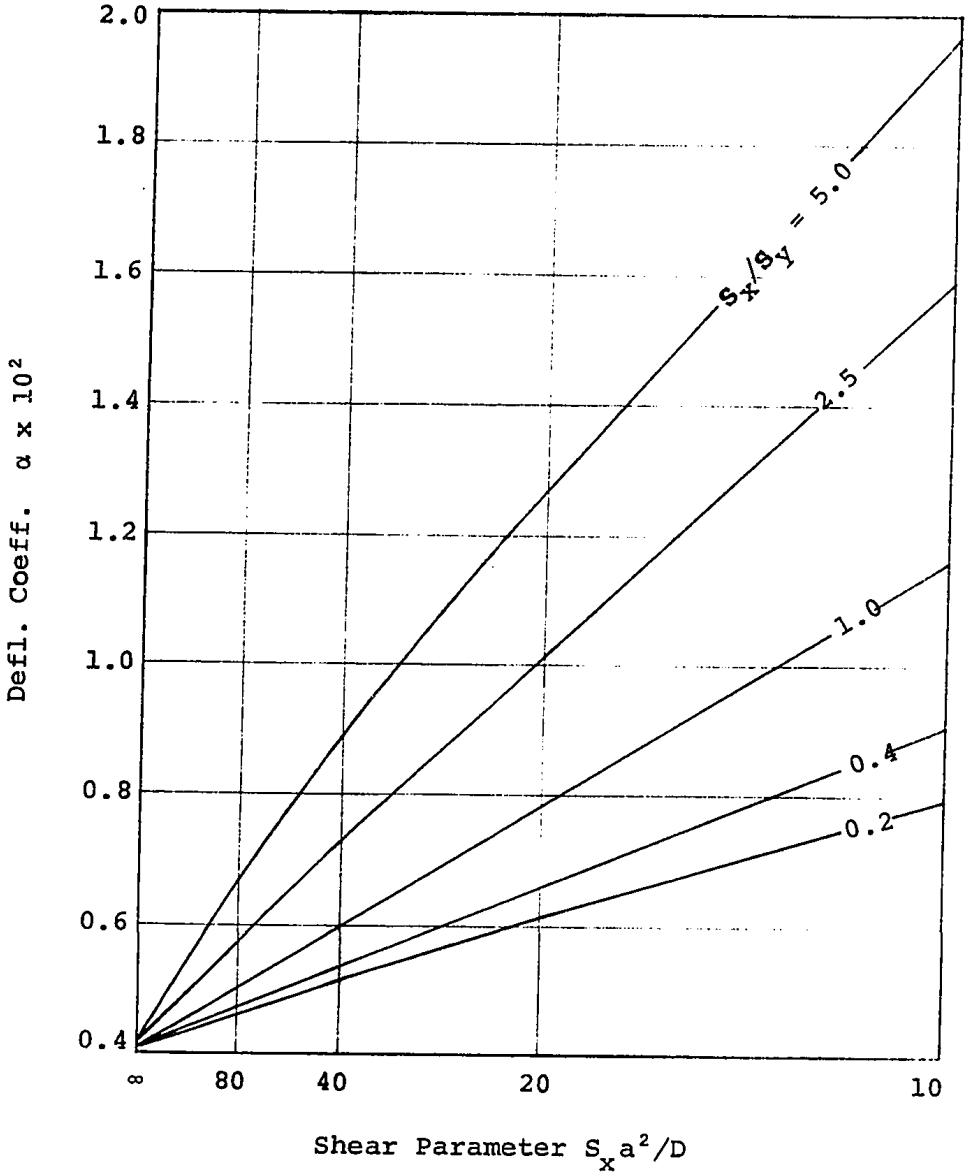

FIG. C.1 MAXIMUM DEFLECTION IN SIMPLY-SUPPORTED SQUARE ORTHOTROPIC SANDWICH PLATE

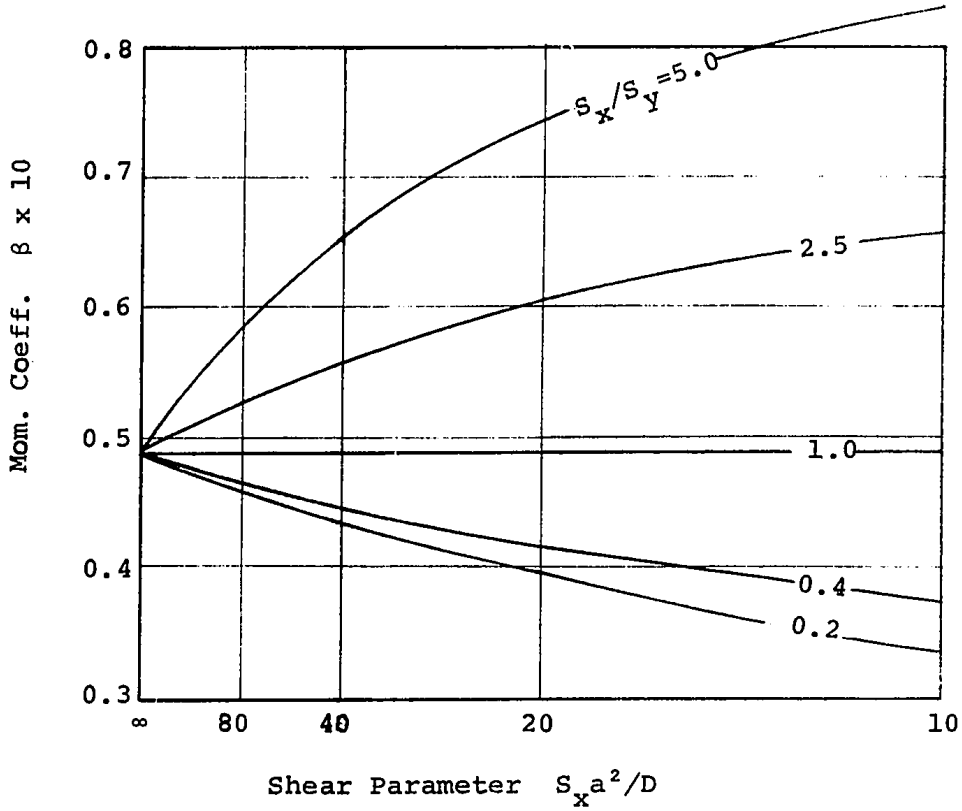

FIG. C.2 MOMENT IN X-DIRECTION AT CENTER OF SQUARE SIMPLY-SUPPORTED ORTHOTROPIC SANDWICH PLATE

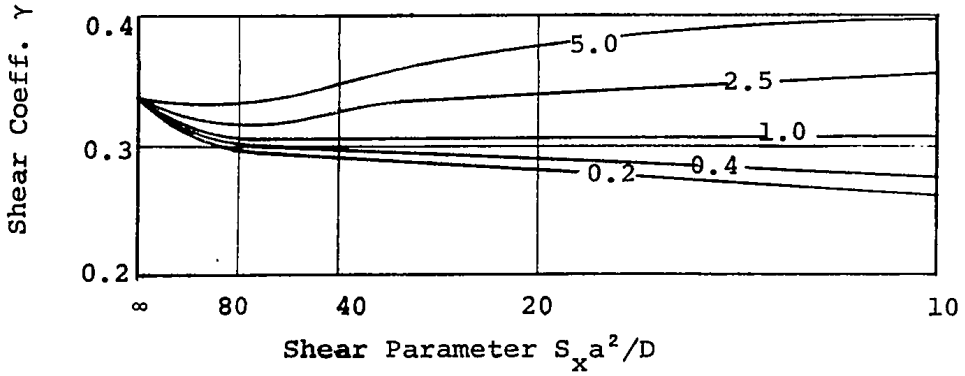

FIG. C.3 MAXIMUM TRANSVERSE SHEAR FORCE IN X-DIRECTION. SQUARE SIMPLY-SUPPORTED ORTHOTROPIC SANDWICH PLATE

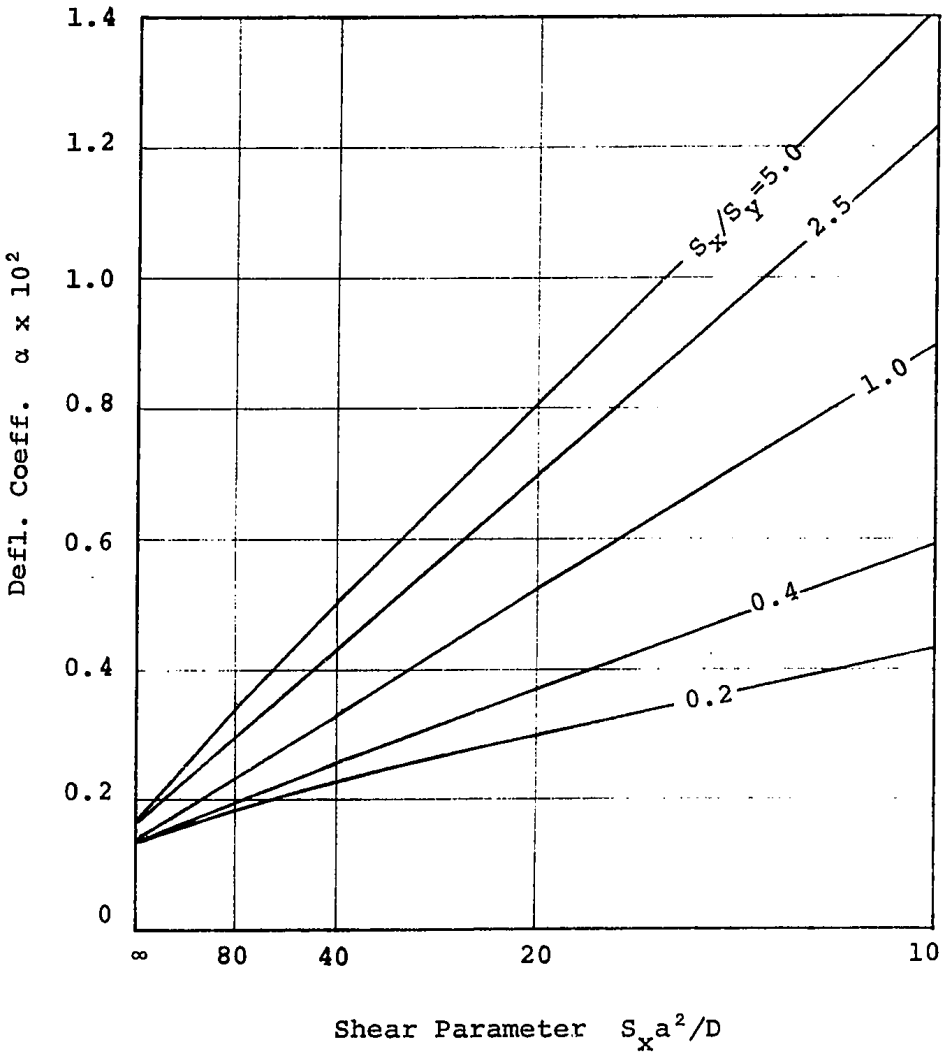

FIG.C.4 MAXIMUM DEFLECTION IN CLAMPED SQUARE ORTHOTROPIC SANDWICH PLATE

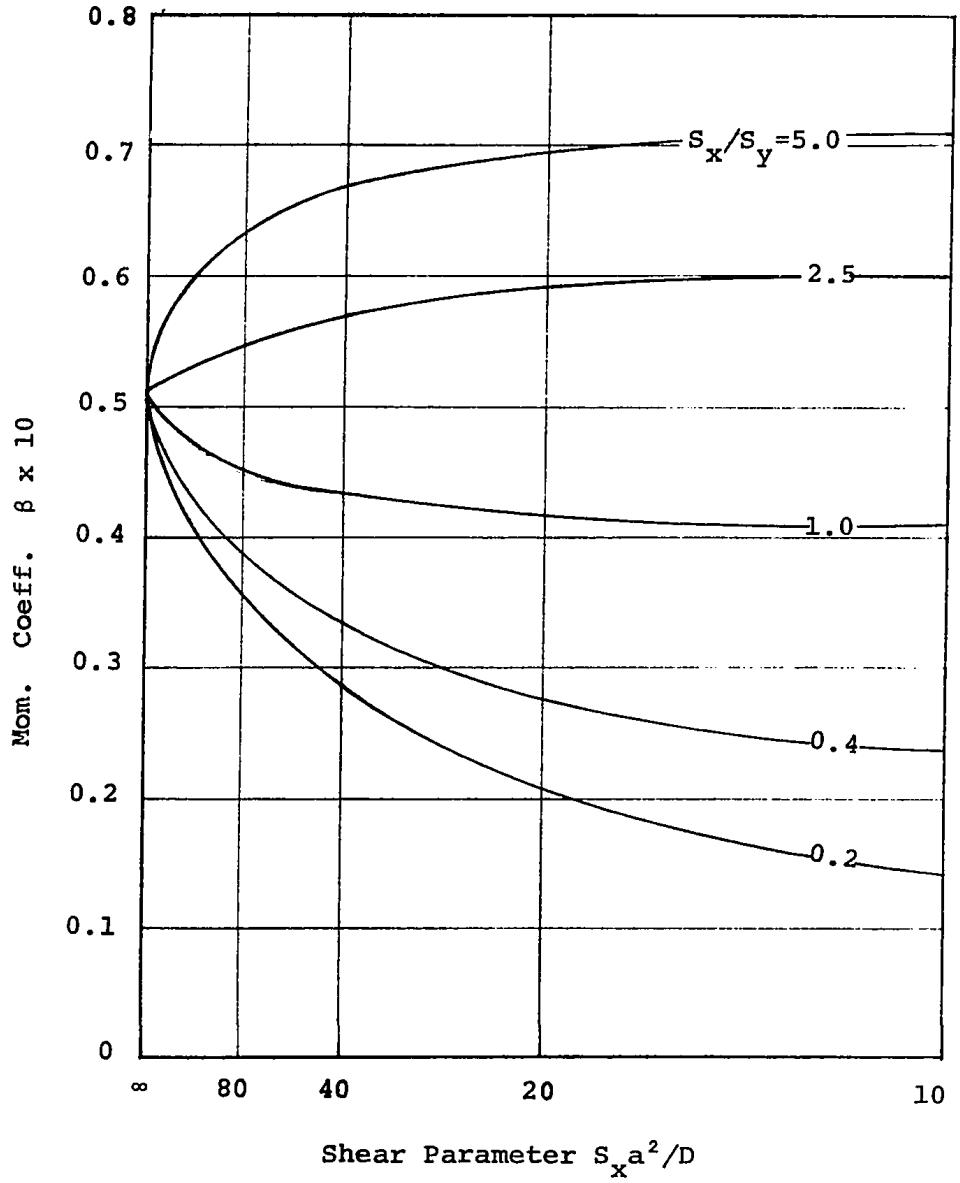

FIG. C.5 MAXIMUM BENDING MOMENT IN X-DIRECTION FOR CLAMPED SQUARE ORTHOTROPIC SANDWICH PLATE

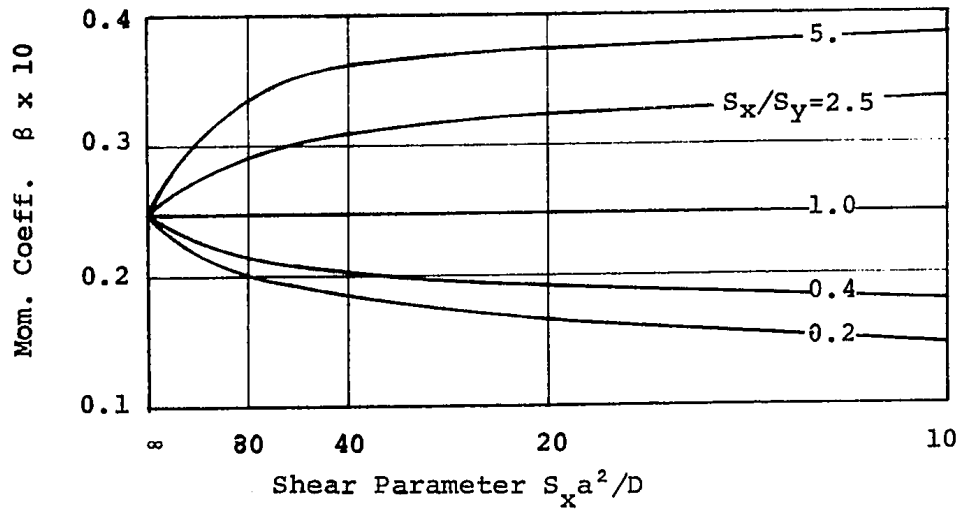

FIG.C.6 MOMENT IN X-DIRECTION AT CENTER OF SQUARE CLAMPED ORTHOTROPIC SANDWICH PLATE

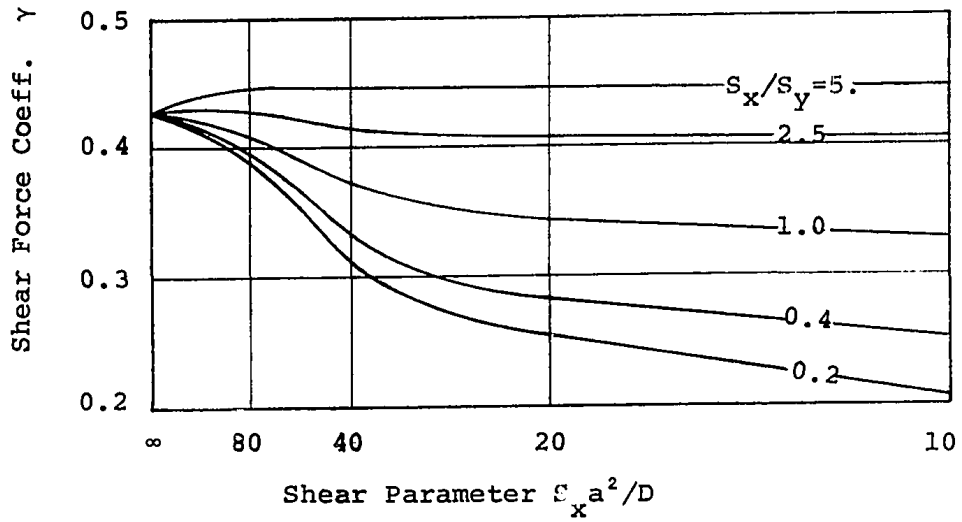

FIG. C.7 MAXIMUM TRANSVERSE SHEAR FORCE IN X-DIRECTION FOR SQUARE CLAMPED ORTHOTROPIC SANDWICH PLATE